PmrAB-regulated LPS Phosphoethanolamine Modifications Have Multiple Roles in *Citrobacter rodentium*

Charles Viau

Department of Microbiology and Immunology

McGill University, Montreal

A thesis submitted to McGill University in partial fulfillment of the requirements of the degree of Doctor of Philosophy

ABSTRACT

Gram-negative bacteria have the ability to modify their lipopolysaccharide (LPS) in response to changing environmental conditions. The principal regulator of LPS modifications in the *Enterobacteriaceae* is the PmrA-PmrB (PmrAB) two-component system, which is activated by micromolar concentrations of Fe^{3+} and Al^{3+} and mildly acidic pH. PmrAB mediates the transcription of *pmrC* and *cptA*, encoding phosphoethanolamine (pEtN) transferases that catalyze the addition of pEtN to the 1- and 4'-phosphoryl groups of the lipid A moiety and to the phosphoryl group of heptose-I of the core moiety of LPS, respectively. The first objective was to determine if PmrC- and CptA-mediated pEtN modifications play a role in maintaining outer membrane integrity in *C. rodentium* under PmrAB-inducing conditions. To assess the role of pEtN modifications in outer membrane integrity, *C. rodentium* Δ*pmrAB*, Δ*pmrC*, Δ*cptA* and Δ*pmrC*Δ*cptA* strains were generated. The Δ*pmrC*, Δ*pmrC*Δ*cptA* and Δ*pmrAB* demonstrated increased susceptibility to hydrophobic antibiotics, whereas only the Δ*pmrC*Δ*cptA* and Δ*pmrAB* strains displayed a loss of OM integrity under PmrAB-inducing conditions. The second objective was to determine the mechanism by which PmrC- and CptA-mediated pEtN modifications maintain outer membrane integrity under PmrAB-inducing conditions. Whole-cell lysate LPS extractions performed on Δ*waaL* strains grown in the presence of micromolar concentrations of iron demonstrated that the Δ*waaL*Δ*pmrC*Δ*cptA* strain accumulates free lipid A, which is a measure of a defect in LPS turnover. Using sucrose density gradient centrifugation, it was shown that the Δ*waaL*Δ*pmrC*Δ*cptA* strain accumulated LPS throughout its cell envelope in the presence of micromolar iron, whereas the Δ*waaL* strain had most of its LPS in the fractions corresponding to the outer membrane, suggesting that pEtN modifications are involved in the transfer of LPS from the IM to the OM. The third objective was to determine whether the response to iron results in the formation of OM vesicles (OMVs). It was determined that OM vesiculation does occur in the

presence of 50 to 100 μM $FeSO_4$, confirmed by the presence of CroP, an OM protease. In addition, the isolated OMVs were shown to be more bactericidal against the Δ*waaL*Δ*pmrC*Δ*cptA* strain than the Δ*waaL* strain, suggesting that PmrC and CptA are involved in conferring protection against these OMVs.

RÉSUMÉ

Les bactéries à Gram négatif peuvent modifier la couche externe de lipopolysaccharide (LPS) pour s'adapter au changement des conditions environnementales. Le principal régulateur des modifications du LPS chez les entérobactéries est le système à deux composants PmrA-PmrB (PmrAB), qui est activé par des concentrations de Fe^{3+} et d'Al^{3+} de l'ordre du micromolaire, ainsi que par un pH acide. PmrAB induit la transcription des gènes *pmrC* et *cptA*, qui codent pour des transférases de phosphoéthanolamine (pEtN) et catalysent l'addition de pEtN aux groupes 1-, 4'-phosphoryl du lipide A et au groupe phosphoryl du résidu heptose-I du noyau. Le premier objectif est de déterminer si les modifications du LPS induites par PmrC et CptA jouent un rôle dans le maintien l'intégrité de la membrane externe chez *C. rodentium*, dans des conditions qui activent PmrAB. Pour ce faire, les souches de *C. rodentium* Δ*pmrAB*, Δ*pmrC*, Δ*cptA* et Δ*pmrC*Δ*cptA* ont été générées. Les souches Δ*pmrC*, Δ*pmrC*Δ*cptA* et Δ*pmrAB* ont démontré une susceptibilité accrue aux antibiotiques hydrophobes, par contre seules les souches Δ*pmrC*Δ*cptA* et Δ*pmrAB* ont perdu l'intégrité de leur membrane externe. Le deuxième objectif est de déterminer le mécanisme moléculaire par lequel les modifications du LPS induites par PmrC et CptA maintiennent l'intégrité de la membrane externe dans des conditions qui activent PmrAB. Des extractions de LPS ont été réalisées à partir de lysats cellulaires de souches Δ*waaL* produisant un LPS tronqué, afin de pouvoir observer spécifiquement la production de LPS constitué du lipide A et du noyau. Les résultats ont démontré que la souche Δ*waaL*Δ*pmrC*Δ*cptA* accumule du lipide A non lié au noyau. En employant la centrifugation sur gradient de sucrose suivie d'un buvardage de type Western contre le KDO, nous avons montré que la souche Δ*waaL*Δ*pmrC*Δ*cptA* accumule le LPS tout au long de son enveloppe cellulaire, tandis que la souche Δ*waaL* transfert la majorité de son LPS vers la membrane externe. Ceci démontre que les modifications du LPS induites par PmrC et CptA aident au transfert du LPS de la membrane interne vers la membrane externe. Le troisième

objectif est de déterminer si la présence du fer induit la formation de vésicules à la membrane externe. En mesurant la présence de CroP, une protéase de la membrane externe, à la surface de vésicules isolées, nous avons montré que des concentrations de fer de l'ordre de 50 à 100 μM induisent la formation de vésicules. De plus, ces vésicules exercent un effet bactéricide plus important contre la souche Δ*waaL*Δ*pmrC*Δ*cptA* que contre la souche Δ*waaL*, suggérant que PmrC et CptA confèrent aux bactéries *C. rodentium* une protection contre les vésicules produites.

ACKNOWLEDGMENTS

This work was carried out at the Lyman Duff Medical building, at McGill University in the Department of Microbiology and Immunology.

First and foremost, I would to acknowledge my supervisor throughout these five years, Dr. Hervé Le Moual. Thank you for your patience and guidance, which were invaluable to me throughout my Ph. D. I would especially like to thank you for letting me have some freedom in my project, which blossomed very nicely after five years.

Second, I would like to acknowledge Mr. Tom Ringer for our early morning coffee periods. We had many precious conversations over morning coffee together. These morning conversations also included Dr. Greg Matlashewski, whom I would also like to acknowledge, with which we had deep conversations on hockey, more specifically on the Canadiens, which now are a pretty good team. I could always be sure to leave our conversations with a smile. Your friendship was invaluable to me during the stressful periods of my Ph. D.

Third, I would like to acknowledge all of the administrative staff, as you were always friendly and courteous, which made my days sometimes a bit more bareable. Your smiles and laughs will remain in my memories forever.

Fourth, I would like to acknowledge my mom, for being there for me whether during the day, whether with a simple message, or at night, when I was stressed out about something before I went to bed and your words would soothe my conscious. Thank you for being supportive and, most of all, having patience with me.

ABBREVIATIONS

araN	4-amino-4-deoxy-L-arabinose
AMP	Antimicrobial Peptide
AU	Arbitrary Unit
Da	Dalton
EDTA	Ethylenediaminetetraacetic acid
EtBr	Ethidium Bromide
IM	Inner Membrane
KDO	3-Deoxy-D-manno-oct-2-ulosonic acid
LFI	Lethal Factor Inhibitor
LPS	Lipopolysaccharide
MIC	Minimal Inhibitory Concentration
NPN	1-N-phenylnaphthylamine
OM	Outer Membrane
OMV	Outer Membrane Vesicle
pEtN	Phosphoethanolamine
PMB	Polymyxin B
SDS	Sodium dodecyl sulfate

TCS	Two-component system
UndP	Undecaprenyl phosphate
UndPP	Undecaprenyl pyrophosphate

CONTRIBUTIONS TO ORIGINAL SCIENTIFIC KNOWLEDGE

1. We show that PmrC and CptA maintain OM integrity in *C. rodentium*.
2. We demonstrate that PmrC and CptA confer resistance to hydrophobic antibiotics.
3. We show that PmrC and CptA promote lipid A turnover.
4. We demonstrate that lack of PmrC and CptA results in free lipid A accumulation in the presence of iron.
5. We demonstrate that PmrC and CptA promote transfer of LPS to the OM.
6. We show that iron increases Gram-negative bacterial resistance to hydrophobic antibiotics in a concentration-dependent manner.
7. We demonstrate that iron promotes OM vesiculation.
8. We show that PmrC and CptA confer protection against OMVs.

CONTRIBUTION OF AUTHORS

This doctoral thesis was prepared in accordance with the guidelines stated in McGill University's Guidelines for Thesis Preparation. It represents experimental work in the manuscript-based thesis. All studies have been performed in the laboratory of Dr. Hervé Le Moual under his supervision. Detailed contributions of authors are listed below. Authors are designated by their initials.

Chapter 1: Literature Review and Thesis Goals

CV wrote the literature review. HLM provided comments and feedback in editing the chapter.

Chapter 2: Absence of PmrAB-mediated Phosphoethanolamine Modifications of *Citrobacter rodentium* Lipopolysaccharide affects Outer Membrane Integrity

CV and HLM designed the experiments. CV, DKT and JG performed the experiments. CV and VLS generated the mutants. CV and HLM wrote the paper.

Chapter 3: PmrAB-regulated Phosphoethanolamine Modifications Promote Lipopolysaccharide Transfer to the Outer Membrane

CV and HLM designed the experiments. CV performed the experiments. CV and HLM wrote the manuscript.

Chapter 4: PmrAB-regulated Phosphoethanolamine Modifications are involved in Outer Membrane Vesiculation

CV and HLM designed the experiments. CV performed the experiments. CV and HLM wrote the manuscript.

Chapter 5: Conclusions and Future Perspectives

CV wrote the chapter. HLM provided comments and feedback in editing the chapter.

TABLE OF CONTENTS

Chapter 1: Literature Review and Thesis Goals

Chapter 2: Absence of PmrAB-mediated Phosphoethanolamine Modifications of *Citrobacter rodentium* Lipopolysaccharide affects Outer Membrane Integrity

Chapter 3: PmrAB-regulated Phosphoethanolamine Modifications Promote Lipopolysaccharide Transfer to the Outer Membrane

Chapter 4: PmrAB-regulated Phosphoethanolamine Modifications are involved in Outer Membrane Vesiculation

LIST OF FIGURES

Chapter 1

Chapter 2

Chapter 3

Chapter 4

Chapter 5

LIST OF TABLES

Chapter 2

Chapter 3

Chapter 4

Chapter 5

PREFACE TO CHAPTER 1

This thesis tackles the subject of Gram-negative bacterial OM biogenesis. In chapter 1, antibiotic resistance and current antibiotic treatments will be presented. Then, the differences between between Gram-positive and Gram-negative cell walls and the implications for antibiotic resistance will be reviewed. This chapter will then highlight what is known so far on Gram-negative bacterial OM biogenesis exploring such themes as LPS biosynthesis, two-component systems, covalent LPS modifications, iron and OM vesiculation. At the end of this chapter, the thesis goals will be presented.

Chapter 1: Literature Review and Thesis Goals

1.1 The Antibiotic Resistance Issue

Antibiotic resistance is a major issue that is on the rise at the global level. The main causes of antibiotic resistance are the misuse of antibiotics, which selects for resistant strains and leads to their persistence and spread overtime, and the decline of antibiotic discovery programs [1]. As a result of antibiotic resistance, nosocomial infections are the cause of approximately 100,000 deaths and cost more than US$25 billion per year in the USA alone [2]. The most notable example of infections caused by resistant bacterial strains are the ones caused by methicillin-resistant *Staphylococcus aureus* (MRSA) (causing 19,000 deaths/year in the USA and 3 to 4 billion dollars in additional healthcare costs) and infections due to multi-drug resistant Gram-negative bacteria, including *Escherichia coli*, *Acinetobacter*, *Klebsiella*, *Salmonella* and *Pseudomonas* species, which may be virtually untreatable in the near future [1]. Many of the Gram-negative species which pose as multi-drug resistant threats are from the bacterial family called the *Enterobacteriaceae*, which includes such species as *E. coli*, *Salmonella enterica* and *Klebsiella pneumoniae* [3]. *Citrobacter rodentium*, which is part of this family, is a murine pathogen that serves as an infection model for enterohemorrhagic (EHEC) and enteropathogenic (EPEC) *E.coli* infections in humans [4, 5]. EHEC, EPEC and *C. rodentium* all cause the signature attaching and effacing lesions in the gut of their respective hosts [4, 5].

With the worldwide spread of New Delhi Metallo-beta-lactamase-1 (NDM-1) positive Gram-negative bacteria, which have acquired a metallo β-lactamase that cleaves all penicillins, cephalosporins and carbepenems and carry additional factors that provide resistance to aminoglycosides and fluoroquinolones [3], the search for new antibiotics and strategies to combat the issue of Gram-negative multi-drug resistance has begun. As rational drug design has failed in

generating novel druggable targets, researchers are going back to purification of compounds from natural sources to generate novel antibiotics [6, 7]. The treatment of multi-drug resistant infections has even included the use of intravenous colistin, a derivative of the antimicrobial peptide (AMP) polymyxin B, which exhibits nephrotoxicity, although *Acinetobacter baumannii* has already developed resistance to this antimicrobial peptide [8-10]. This reality demonstrates the dire situation of Gram-negative multi-drug resistance and the need for novel solutions to this global issue.

1.2 Antibiotic Resistance Strategies used by Bacteria

Bacteria acquire resistance to antibiotics by accumulating base pair mutations in their genome, leading to selection, or by acquiring extracellular DNA elements through horizontal gene transfer [11]. Horizontal gene transfer includes bacterial conjugation, the process which involves plasmid dissemination from a donor to a recipient strain, DNA transduction, which is the process by which a bacteriophage is incorporated within the bacterial genome and DNA transformation, which is a rarer event, as only a few bacterial species uptake extracellular DNA from their environment [11]. The three major strategies employed by bacteria to evolve antibiotic resistance are: possessing a barrier that restricts access to the antibiotic, encoding enzymes which degrade the antibiotic, and modifying the antibiotic's target so that the antibiotic is rendered ineffective [12]. As examples of these resistance strategies, resistance to macrolides and chloramphenicol is primarily due to a mutation in the 50S ribosomal subunit, which render the antibiotics useless against this target, whereas resistance to penicillins, cephalosporins and carbepenems is mainly due to acquisition of resistance plasmids carrying β-lactamase genes, which inactivate the antibiotics by cleavage of their β-lactam rings [13, 14]. In addition, Gram-negative resistant strains

have demonstrated the ability to alter their outer membrane porin content, which precludes access to within the cell to most β-lactams [14]. Another major resistance mechanism consists of efflux pumps from the single protein Major Facilitator Superfamily that span the inner cell membrane and the Resistance Nodulation Division (RND) family of pumps, which are highly prevalent in Gram-negative bacteria and utilize the proton gradient to actively efflux antibiotics [6]. For example, the opportunistic pathogen *Pseudomonas aeruginosa* possesses the MexAB-OprM system to efflux antibiotics, and its homolog in *E. coli* is the AcrB-TolC system [15]. Interestingly, this efflux pump is upregulated under stress conditions that activate the SoxRS, the superoxide responsive two-component system which responds to oxidative stress in *E. coli* [16].

1.3 Current Strategies to Treat Bacterial Infections

1.3.1 Bactericidal Antibiotics

Bactericidal antibiotics target proteins or cellular components directly involved in bacterial metabolism. These usually kill more than 99.9 % of bacteria [17, 18]. Some examples of such targets are the peptidoglycan layer (β-lactams and glycopeptides), DNA replication (quinolones) and the 30S ribosomal subunit (strictly kanamycin from the aminocyclitol group, which promotes erroneous protein translation) [17]. Disruption of these components results in bacterial cell death through the generation of reactive oxygen species by a general mechanism that depletes cellular NADH, leading to the formation of hydroxyl radicals and activation of the Fenton reaction, which generates radicals by iron oxidation/reduction [17]. This strategy however inherently leads to the selection of resistant strains. To circumvent this issue, the gold standard so far is to modify the antibiotic's scaffold to render them bactericidal again for use in treatment of infections (Fig. 1.0)

[1]. The best known example of classes of antibiotics that have been repeatedly tailored to counter resistance are the β-lactams (penicillins, cephalosporins, and carbepenems) as well as the quinolones (e.g. nalixidic acid) which were further modified (i.e. ciprofloxacin) by, in part, the addition of a fluoride group to the existing scaffold [1]. The classes of penicillins and cephalosporins, which act on penicillin-binding proteins and β-lactamase, respectively, are now in their fourth generation [1]. However, a more recent strategy is to go back to the purification of compounds from natural sources given the need of novel antibiotics to combat the issue of multi-drug resistance, especially from the Gram-negative *Enterobacteriaceae* family [6]. King *et al.* recently showed that aspergillomarasmine A overcomes metallo-β-lactamase (i.e. NDM-1) resistance by rapidly and potently inhibiting this enzyme [19]. When used in combination with meropenem, a carbepenem, it fully restored the activity of this antibiotic against β-lactamase resistant *Enterobacteriaceae*, *Acinetobacter* species and *Pseudomonas aeruginosa in vitro* and successfully treated mice infected with NDM-1 expressing *Klebsiella pneumoniae* [19].

1.3.2 Bacteriostatic Antibiotics

In contrast to the bactericidal strategy, bacteriostatic antibiotics act by stopping bacterial cell growth. The primary antibiotic classes that arrest bacterial cell growth are the macrolides (e.g. erythromycin) and chloramphenicol which target the 50S ribosomal subunit, as well as tetracycline and the aminocyclitol group of antibiotics that target the 30S ribosomal subunit [17]. All of these antibiotics arrest bacterial cell growth by stopping protein translation [17, 18]. The effect of bacteriostatic antibiotics is more pronounced over the time of infection, as the host immune system is better able to control and kill a non-growing pathogenic population [18]. The efficiency of

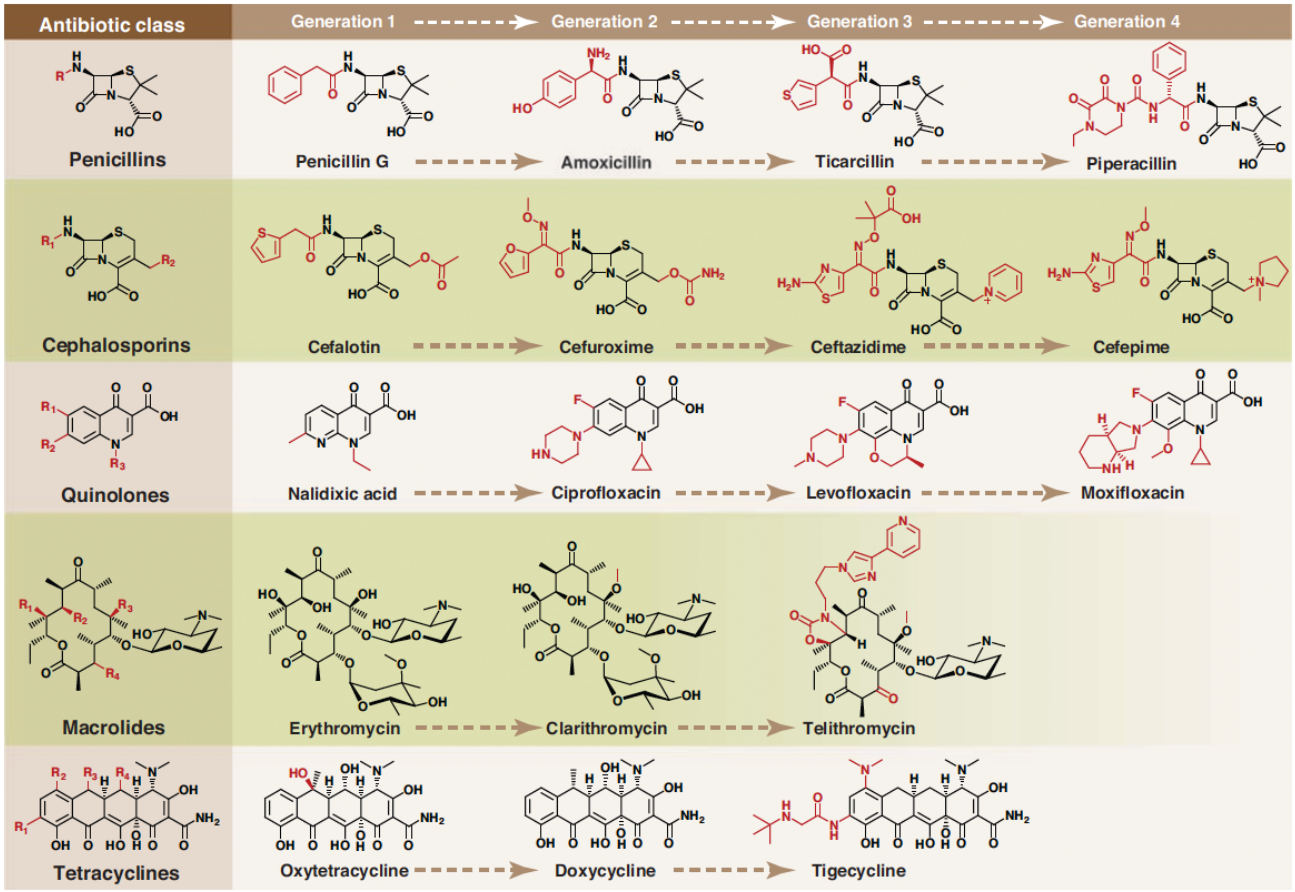

Figure 1.0: The main antibiotic classes used in to treat bacterial infections. The current strategy is to modify existing antibiotic to counter bacterial resistance. [Adapted from Fischbach, M. A. and Walsh, C.T., *Science*, 325, 1089-1093, (2009)].

bacteriostatic antibiotics, as opposed to bactericidal antibiotics, is dependent on the integrity of the host immune system.

1.3.3 Novel Approaches

A more recent strategy to counter antibiotic resistance is to arrest or disarm the pathogens by targeting virulence factors [20]. A virulence factor is defined as a factor involved in promoting the virulence, or ability to cause pathogenesis of a bacterial strain over its avirulent counterpart and need not be essential for bacterial growth [20]. Examples of such therapeutic targets are toxin function, toxin delivery, regulation of virulence gene expression, and bacterial adhesion, all of which are important factors in virulence [20]. Therefore, disarming pathogens of their virulence factors would enable the immune system to better control their growth, or would render them more susceptible to antibiotic therapy. For example, Merck has developed a hydroxamate called LFI, Lethal Factor Inhibitor, that inhibits the lethal factor (LF) component of the anthrax toxin [20]. LF can cleave several host cellular substrates, such as mitochondrial MAP kinase kinases, ultimately leading to cell death [20]. The mechanism of action of LFI is through binding the active site of LF that ultimately offers complete protection from spore infection when administered to mice in combination with ciprofloxacin 66 hours postinfection in a model in which ciprofloxacin alone only offers 50% protection from lethality [20]. Another example of an anti-virulence target is quorum sensing [20]. Quorum sensing is used by bacteria to sense their density by release of diffusible signalling molecules, which alter gene expression when a threshold is reached. This gene regulation includes increased virulence gene expression. In many Gram-negative bacteria, the diffusible signals are acyl-homoserine lactone molecules (AHLs) that are synthesized and recognized by quorum sensing circuits composed of LuxI and LuxR homologs. The LuxI

component synthesizes the AHL component, whereas the LuxR component mediates the transcriptional regulation in response to AHL. Halogenated furanones are suggested to inhibit quorum sensing by increasing LuxR turnover [20]. As a consequence, in *P. aeruginosa*, halogenated furanones inhibit production of exotoxins, repress the expression of quorum sensing regulated genes, and increase the susceptibility of *P. aeruginosa* biofilms to tobramycin *in vitro* [20]. Fortunately, virulence factors are non-essential for cell viability, and as a result, the risk of developing resistance to antimicrobials that target these factors is negligible [20]. A caveat however is that expression of individual virulence factors varies during infection, and hence administration of anti-virulence drugs would have to take this into account, and these drugs would be of narrow spectrum [20].

1.4 Bacterial Species Classification based on Cell Wall Structure

1.4.1 Gram-Positive and Gram-Negative Cell Walls

1.4.1.1 Classification

One way of classifying bacterial species is by the structure of their cell wall. Hans Christian Gram introduced the Gram stain in 1882, which utilizes crystal violet dye to distinguish between Gram-positive and Gram-negative bacteria, based on their ability to retain the dye [21]. Gram-positive bacteria, as the classification implies, are able to retain the dye after the treatment process, whereas Gram-negative are not. Therefore, Gram-positive bacteria stain violet and Gram-positive bacteria stain pink, due to the counter stain which is basic fuschsin [21]. The crystal violet reaction is positive for these bacteria, as their peptidoglycan layer is thick and is able to retain the dye, after treatment [21]. The Gram-positive and Gram-negative cell walls are depicted in Fig. 1.1. In

addition to a thick peptidoglycan layer, the cell wall of Gram-positive bacteria comprises mostly of wall teichoic acids (WTA), which are polyhydric alcohol phosphates linked to the peptidoglycan layer through D-alanine residues. Other molecules that are present in the Gram-positive cell wall are and lipoteichoic acids (LTA) [21, 22]. These molecules differ from WTAs, in that they consist of the same backbone linked to a glycolipid that inserts into the cytoplasmic membrane [21, 22]. Compared to the Gram-positive cell wall, the Gram-negative cell envelope is more complex (Fig. 1.1). The defining feature of the Gram-negative cell is the presence of an additional membrane, the outer membrane (OM). The OM of Gram-negative bacteria appears as a wavy-like membrane structure by electron microscopy [21]. Gram-negative bacteria do comprise a peptidoglycan layer, composed of the same *N*-acetylglucosamine and *N*-acetylmuramic acid crosslinks as in Gram-positive bacteria, but it is much thinner. Between the OM and cytoplasmic membrane, also called inner membrane (IM), is the periplasm. In this space are found many different soluble proteins, which appear as a void by electron microscopy [21].

1.4.2 The Gram-Negative Outer Membrane

The Gram-negative OM is an asymmetric bilayer composed of an inner leaflet of phospholipids and an outer leaflet of lipopolysaccharide [23]. In this asymmetric bilayer, different proteins and lipoproteins are found. For example, there are the general diffusion OM porins (OmpF, OmpC and PhoE), which exist as trimers, that allow water soluble molecules to penetrate within the cell. In addition, there is OmpA, which has a structural role in maintenance of OM integrity and Braun's lipoprotein (Lpp), of which one third of the cell's population anchors the OM to the peptidoglycan layer, is also involved in maintenance of OM integrity [24]. The OM also contains receptors for the uptake of specific nutrients, for example, LamB, which specifically

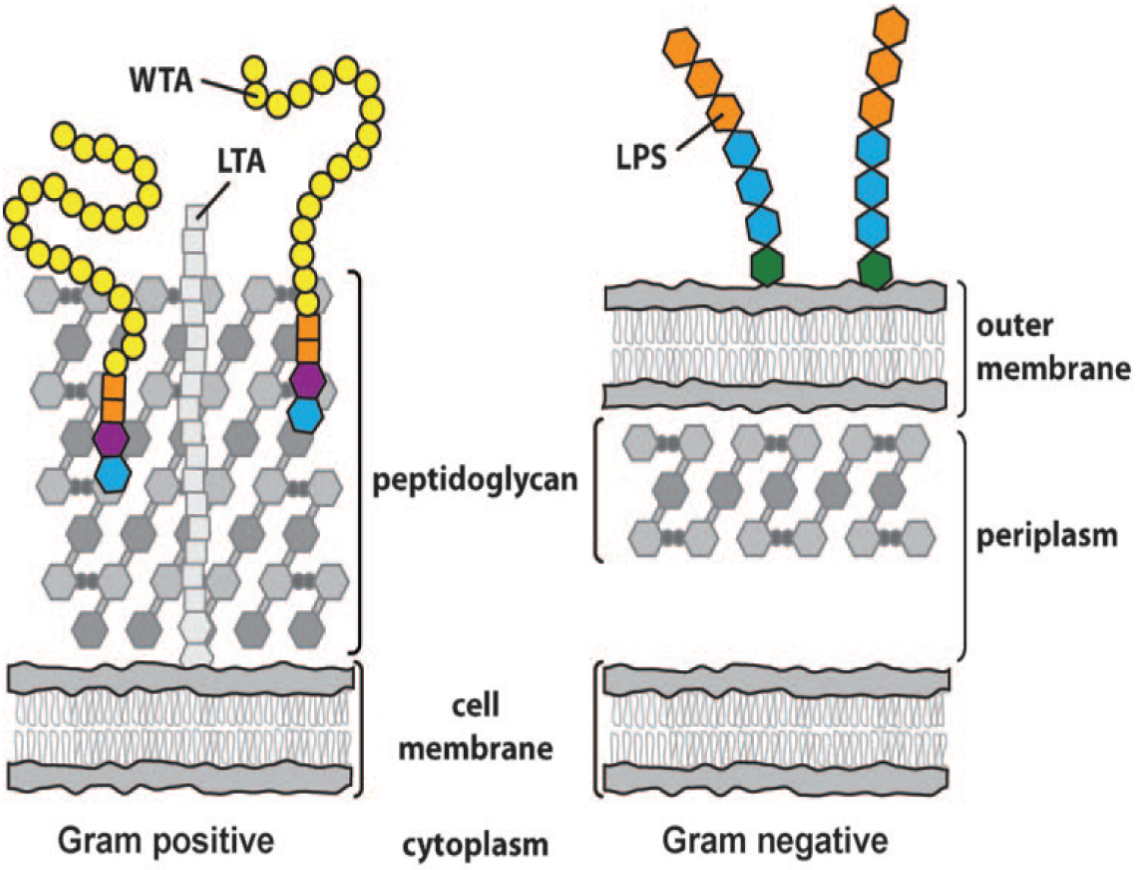

Figure 1.1: The Gram-Positive and Gram-Negative Cell Wall. The defining feature of the Gram-positive cell wall is a thick peptidoglycan layer, whereas the Gram-negative cell wall includes an additional membrane, the outer membrane. WTA: Wall-associated teichoic acid. LTA: lipoteichoic acid. LPS: Lipopolysaccharide. [Adapted from Swoboda, J *et al.*. *Chembiochem*, 11, 35-45, (2010)].

uptakes maltodextrins [24]. There exists also proteins involved in OM and surface appendage biogenesis, for example, Omp85, which is involved in membrane protein insertion as well as proteins involved in protein secretion (type II secretion system), proteases (OmpT) and proteins (LptD) involved in LPS assembly at the OM [24].

1.4.2.1 The Gram-Negative OM and Antibiotic Resistance.

The Gram-negative OM acts as an additional barrier that antibiotics have to cross [24]. Hydrophobic antibiotics have to gain access to the cell interior by direct permeation through the OM LPS layer, as opposed hydrophilic antibiotics diffuse through the channels of the general OM porins, which have a molecular cutoff weight of less than 600 Da [24]. However, the LPS layer of the outer leaflet provides an intrinsic resistance to hydrophobic antibiotics [24]. Therefore, antibiotics such as the macrolides, rifamycins, aminocoumarins, fusidic acid, vancomycin are therefore useless in treating Gram-negative infections, as these bacteria possess an intrinsic resistance to them [24]. Polymyxin B (PMB), an antimicrobial peptide, can be used to sensititize Gram-negative bacteria to hydrophobic antibiotics by disrupting the OM LPS layer, but like colistin, its use is avoided due to nephrotoxicity [24, 25].

1.5 The Gram-Negative Outer Membrane Lipopolysaccharide (LPS) layer

1.5.1 Lipopolysaccharide Structure

The Gram-negative OM is defined by the LPS layer that constitutes the outer leaflet (Fig. 1.2) [26]. LPS is composed of three different moieties, namely lipid A, core oligosaccharide and O-antigen [26].

1.5.1.1 Lipid A

Lipid A is composed of an *N*-acetylglucosamine disaccharide, which is substituted with four to six acyl chains (C_{12} and C_{14}) in the *Enterobacteriaceae* (Fig. 1.2) [26]. Lipid A is synthesized in the cytosol and inner leaflet of the IM via the lipid A biosynthetic pathway, which is catalyzed by nine *lpx* genes (Fig. 1.3)[26]. The *lpx* genes have no mammalian counterparts and therefore represent suitable targets for the development of novel antibiotics [27]. Most notably, LpxC, an *N*-acetylglucosamine deacetylase, is the enzyme responsible for the committed step in lipid A synthesis [26]. The catalytic activity of this enzyme is increased by Fe^{2+}, which replaces the Zn^{2+} ion in its active site [28, 29]. LpxC is a novel antibiotic target that is being studied. CHIR-090 and LpxC-1 are members of a novel class of antibiotics that target LpxC; they have been shown to inhibit LpxC from *E. coli*, *P. aeruginosa* and *Neisseria meningitidis* in the low nanomolar range *in vitro* and to treat *A. baumannii* in a murine model of infection by inhibition of inflammation, respectively [30, 31]. Regulation of LpxC activity is both at the protein and mRNA levels, as it acts as a substrate for the AAA protease FtsH in *E. coli* and has been shown to be regulated by a small RNA found upstream of its coding sequence in *P. aeruginosa* [32, 33]. Resistance to LpxC inhibitors has been attributed to the upregulation of efflux pumps in *P. aeruginosa* and mutations in the *fabZ* gene, involved in the synthesis of the IM carrier required for lipid A synthesis and thus LPS synthesis, in the *Enterobacteriaceae* [33].

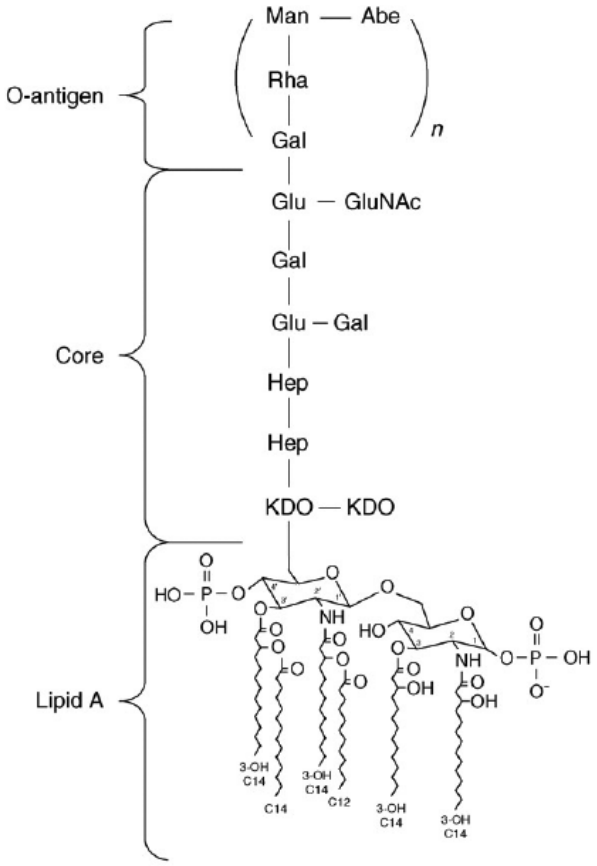

Figure 1.2: *Salmonella enterica* LPS. Lipopolysaccharide consists of three moieties: lipid A, core and O-antigen. Lipid A is the immunogenic portion of LPS, whereas O-antigen is the antigenic portion. [Adapted from Gunn, J.S. *Trends Microbiol*, 16, 284-290, (2008)].

The lipid A moiety serves as the toxic component of LPS, as it binds the Toll Like Receptor 4/MD2 complex on antigen presenting cells and is involved in causing the symptoms of septic shock during the late stages of sepsis [23]. Lipid A is phosphorylated at its 1- and 4' positions, to which covalent modifications are sometimes added, depending on the environment the bacterium finds itself in [23].

Free lipid A (2,3-diacylglucosamine 1-phosphate and lipid IV_a), that is lipid A unligated to KDO, can accumulate in this pathway when certain LPS biosynthesis genes are mutated (Fig. 1.3) [27]. The most notable one is the *msbA* mutant [34]. This mutant is unable to flip the lipid A-KDO_2 across the IM, resulting in the accumulation of this precursor in the inner leaflet of the IM. This local accumulation of lipid A-KDO_2 in the inner leaflet of the IM disrupts the constitutive lipid A pathway, and as the *msbA* gene product is found downstream of LpxC, which is responsible for the committed step in lipid A synthesis, the *msbA* mutant also accumulates free lipid A [34]. Other reported mutants which share the phenotype of free lipid A accumulation are the *waaA* and *lpxK* mutants, which encode the lipid A KDO transferase and 4'-kinase of this pathway, respectively (Fig. 1.3) [35, 36].

1.5.1.2 Core Oligosaccharide

The lipid A moiety of LPS is linked to a hydrophilic moiety, the core oligosaccharide (Fig. 1.2) [23, 26]. The core oligosaccharide is usually separated into the inner and outer cores and it is synthesized by the Waa enzymes found in the inner leaflet of the IM [23, 26]. In the *Enterobacteriaceae,* the inner core is composed of two 3-Deoxy-D-*manno*-oct-2-ulosonic acid (KDO) residues and two *L*- glycero-D-manno-heptopyranose (heptose) saccharides [23, 26]. KDO

is ligated to lipid A via the *waaA* gene product. In contrast to the inner core oligosaccharide, which is relatively conserved throughout Gram-negative bacterial species, the outer core oligosaccharide composition is variable among different Gram-negative bacterial species and therefore is less conserved [26]. Interestingly, WaaA serves as a substrate for the protease FtsH, linking LPS biosynthesis to cell division [37]. Reminiscent of phosphoryl groups present on lipid A, the heptose residues are also phosphorylated, and can be modified depending on the environment [38]. Lack of the phosphoryl groups on the core heptose sugars in *E. coli* leads to an OM defect, which results in increased susceptibility to polymyxin B, novobiocin and SDS, suggesting a role of these phosphoryl groups in maintenance of OM integrity [23]. In *P. aeruginosa*, a *waaP* mutant was shown to display defective LPS biosynthesis, as the strain displayed a truncated form of the core formed of two KDO residues linked to the two heptose residues of the inner core [39]. This was the first report that linked core phosphorylation to LPS biosynthesis, as WaaP phosphorylates the core heptose-I residue. The truncated form of LPS was only found in the IM fractions of the Gram-negative cell envelope, indicating that it was not being transferred to the OM [39]. In a separate report, lack of core phosphorylation also translated into the total loss of *S. enterica* virulence in a mouse model of systemic infection, therefore relating LPS structure to bacterial virulence [40].

1.5.1.3 O-antigen

O-antigen biosynthesis, consisting of a specific number of repeats of a signature oligosaccharide, is determined by the highly polymorphic *rfb* gene cluster and is accomplished through three different pathways: these include the Wzy-dependent, the ABC transporter-dependent and synthase-dependent pathways [23]. All pathways load O-antigen onto the IM acyl

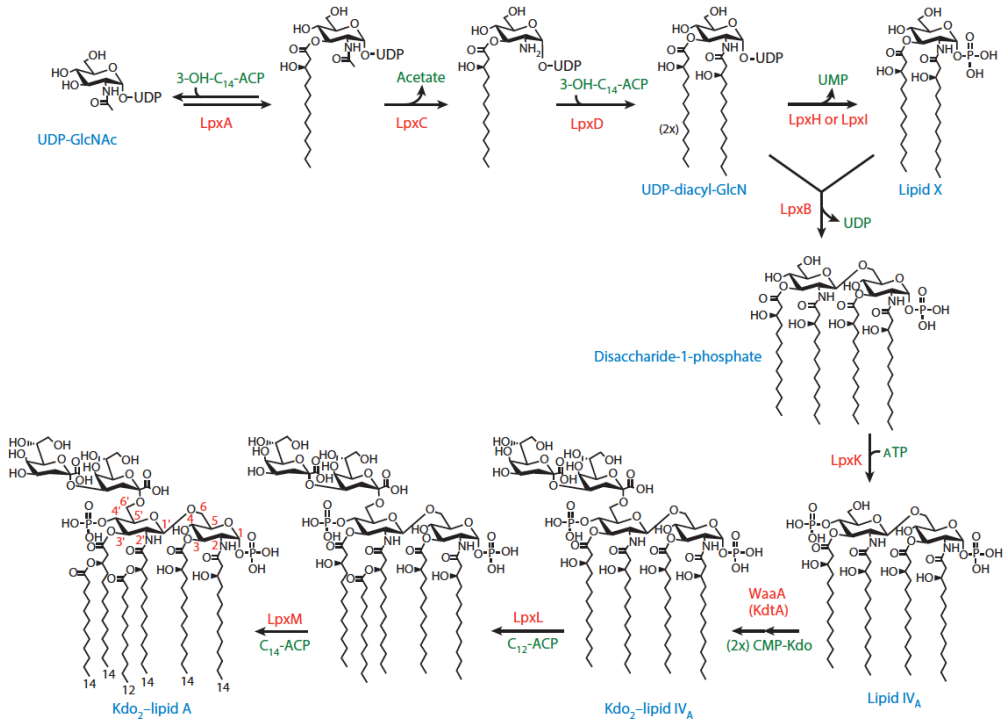

Figure 1.3: The constitutive lipid A pathway. This pathway consists of nine *lpx* genes and *waaA*, whose gene product ligates KDO to the nascent lipid A molecule in the inner leaflet of the IM. [Adapted from Whitfield C. and Trent M.S., *Annu Rev Biochem*, 83, 99-128, (2014)].

lipid carrier undecaprenyl-pyrophosphate, leading to the formation of undecaprenyl-P-O-antigen (Und-P-O-antigen) [23]. The Wzy-dependent pathway is used in *E. coli* and *S. enterica* and involves three proteins: Wzy, Wzx and Wzz. Wzy is the IM polymerase, Wzx is the O-antigen repeat flippase, whereas Wzz is the chain-length regulator, as it name implies, this enzyme regulates the length of the O-antigen chain to be added [23]. Once in the outer leaflet of the IM, facing the periplasm, the O-antigen moiety, taken from Und-P-O-antigen, is then ligated to the nascent lipid A-core chain via the O-antigen ligase, WaaL [23]. O-antigen is the antigenic portion of LPS, to which the host develops antibodies [23]. Some bacterial species do not possess the genes necessary to synthesize O-antigen, and thus their LPS is referred to as rough, whereas species able to cap their LPS with O-antigen are referred to having smooth LPS [23].

1.6 The Lipopolysaccharide Transport (Lpt) Transenvelope Complex and LPS Biosynthesis

A heavily studied system in LPS research is the *lpt* transenvelope complex (Fig. 1.4). This complex shares some similarity to the localization of lipoprotein (*lol*) system, which is used to shuttle lipoproteins to the OM [41]. The *lpt* transenvelope complex is an important area of research as the LPS layer provides an intrinsic barrier to most compounds, including antibiotics, and understanding of this system may lead to potential targets for future antibiotic development. The complex itself consists of seven proteins (LptA, LptB, LptC, LptD, LptE, LptF and LptG), that co-fractionate and co-purify [41]. As the assembly of this transenvelope complex is a regulated process, LPS transport to the OM cannot begin until the proper complex is formed [42].

After ligation of O-antigen to the nascent lipid A-core molecule, the LPS subunit is shuttled to the $LptB_2FG$ ABC transporter, which supplies the energy to the complex to transfer LPS

subunits from the IM to the OM by ATP hydrolysis (Fig. 1.4) [41, 43]. The transporter then delivers the LPS subunit to LptC, which then transfers it to LptA (Fig. 1.4) [41]. LptA has been crystalized as a tetramer, with oligomerization occuring end-to-end, forming a junction between the IM and OM [26, 44]. LptA is known to bind the lipid A portion of LPS as highlighted by its inability to bind mutants that are unable to acylate their lipid with at least four acyl chains [45]. The periplasmic portions of LptC, LptF, LptG, LptD and LptA all share a homologous β-jellyroll domain that is required for transenvelope complex assembly and LPS transport [44, 46, 47]. Once at the OM, the LPS subunit is then shuttled to LptDE OM sorting complex [41]. LptDE forms a heterodimer, and it was shown that the LptE lipoprotein acts as a plug that inserts into the LptD β-barrel [48, 49]. LptE is involved in the proper folding of LptD, as it is required for cysteine bond formation in this protein [50]. Once in the LptD β-barrel, the LPS subunit is then shuttled to the LPS layer of the OM. LptE and LptD have been experimentally shown to interact as a complex at the OM as a dominant-negative mutation of *lptE*, *lptE14*, and its encoded protein, LptE14, was shown to be unable to plug the LptD β-barrel [49]. The LptE14-LptD complex was shown to increase OM permeability to erythromycin, as this hydrophobic antibiotic was able to diffuse through the hydrophobic interior of LptD [49]. A suppressor mutation in the SecB translocation system in combination with the *lptE*14 mutation decreased OM permeability to erythromycin by decreasing the levels of LptD reaching the OM and thereby decreasing the concentration of the LptE14-LptD complex at the OM [49]. Recently, LptE was shown to reverse LPS aggregation *in vitro*, suggesting that this protein is involved in the LPS translocation system and is not only an accessory protein required by LptD for stabilization [51]. In addition, the crystal structure of LptD-LptE OM complex has recently been solved [52]. It revealed a unique two-protein plug- and-barrel architecture with LptE embedded into a 26-stranded β-barrel formed by LptD [52]. It also revealed

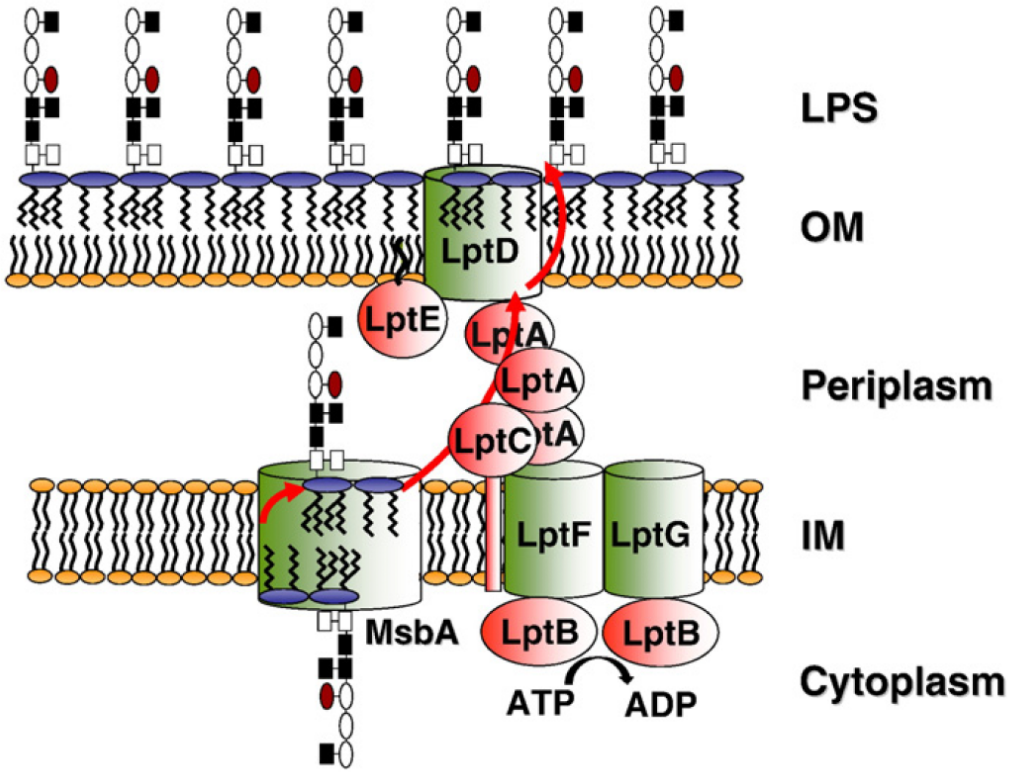

Figure 1.4: The lpt transenvelope complex consisting of seven proteins (LptA-G). This complex forms a junction that delivers LPS from the IM to the OM. [Adapted from Sperandeo, P. *et al.*, *Biochim Biophys Acta*, 1791, 594-602 (2009)].

where LPS could laterally diffuse from the complex, as two prolines distort neighboring β-strands leading to the formation of a potential portal to the OM LPS layer [52]. Interestingly, in an effort to combat Gram-negative multi-drug resistance, a novel class of peptidomimetic antibiotics, which were generated based on the AMP protegrin I, have shown promise in targeting LptD from *P. aeruginosa*, and are now in phase I clinical trials [53, 54]. Their mechanism of action is by inhibiting LPS translocation from the LptD OM barrel to the OM LPS layer [54].

In general, any mutation or depletion in any of the Lpt proteins leads to a lethal phenotype, with an increase in sensitivity to hydrophobic antibiotics, dyes and detergents [55, 56]. Most notably, depletion of any of the following components (i.e. *lptA*, *lptB*, *lptC*, *lptD* or *lptE*) leads to the accumulation of LPS throughout the cell envelope, as demonstrated by sucrose density gradient and distorted cell envelopes as depicted by transmission electron microscopy (Fig. 1.5) [55].

In addition, depletion of any of the *lpt* components leads to the formation of M_{LPS}, which is also observed when *E. coli* is grown under low osmolarity conditions (in 85 mM NaCl), which translates into envelope stress (Fig. 1.6) [57]. M_{LPS} is a modified version of lipid A-core ligated with colanic acid repeats rather than ligated to O-antigen [57].

Colanic acid is a polyanionic heteropolysaccharide containing a repeating unit of *D*-glucose, *L*-fucose, *D*-galactose and *D*-glucoronic acid with *O*-acetyl and *D*-pyruvate side chains and synthesis is governed by the regulator of capsule synthesis (*rcs*) phosphorelay system, which responds to envelope stress, such as the stress posed by low osmolarity conditions [57]. In agreement with this observation, *lptA* and *lptB* are expressed in a σ^E-dependent fashion, σ^E being also involved in the response to envelope stress, highlighting the fact that LPS shuttling to the OM may be promoted under stressful conditions [58].

1.7 Lipopolysaccharide Covalent Modifications

Gram-negative bacteria possess the ability to modify their LPS subunits with covalent modifications depending on environmental conditions [38]. They have developed this ability to adapt to changing environmental conditions, and pathogens seem more apt to do so [38]. Expression of the enzymes responsible for the covalent modifications are regulated by two-component systems in the *Enterobacteriaceae* [38].

1.7.1 Two-Component Systems involved in remodeling LPS with Covalent Modifications

In the *Enterobacteriaceae*, the PhoP-PhoQ (PhoPQ) and PmrA-PmrB (PmrAB) two-component systems are the major regulators of LPS layer remodeling with covalent modifications [59]. PhoPQ is considered the master regulator of virulence in *Salmonella* and other members of the *Enterobacteriaceae*, regulating the expression of more than 200 genes in both *S. enterica* and *E. coli* [60, 61]. Both of these two-component systems are of the EnvZ/OmpR type. EnvZ/OmpR type two-component systems involve a histidine kinase dimer (i.e. PhoQ and PmrB) which autophosphorylates at a histidine residue following activation by a specific environmental signal [59, 62]. The phosphoryl group is then transferred to a cognate response regulator on an aspartic acid residue (i.e. PhoP and PmrA) [62]. PhoQ autophosphorylates in response to micromolar concentrations of Mg^{2+}, acidic pH and antimicrobial peptides (AMPs), whereas PmrB autophosphorylates when exposed to micromolar concentrations of Fe^{3+}, Al^{3+} and mildly acidic pH [63-67]. Transfer of the phosphoryl group to the response regulator promotes its dimerization and increases its affinity for its target gene sequences in the promoter region of the genes it regulates [62]. The consensus sequence for PhoP binding, or "PhoP box" is TGTTTA-5 bps-

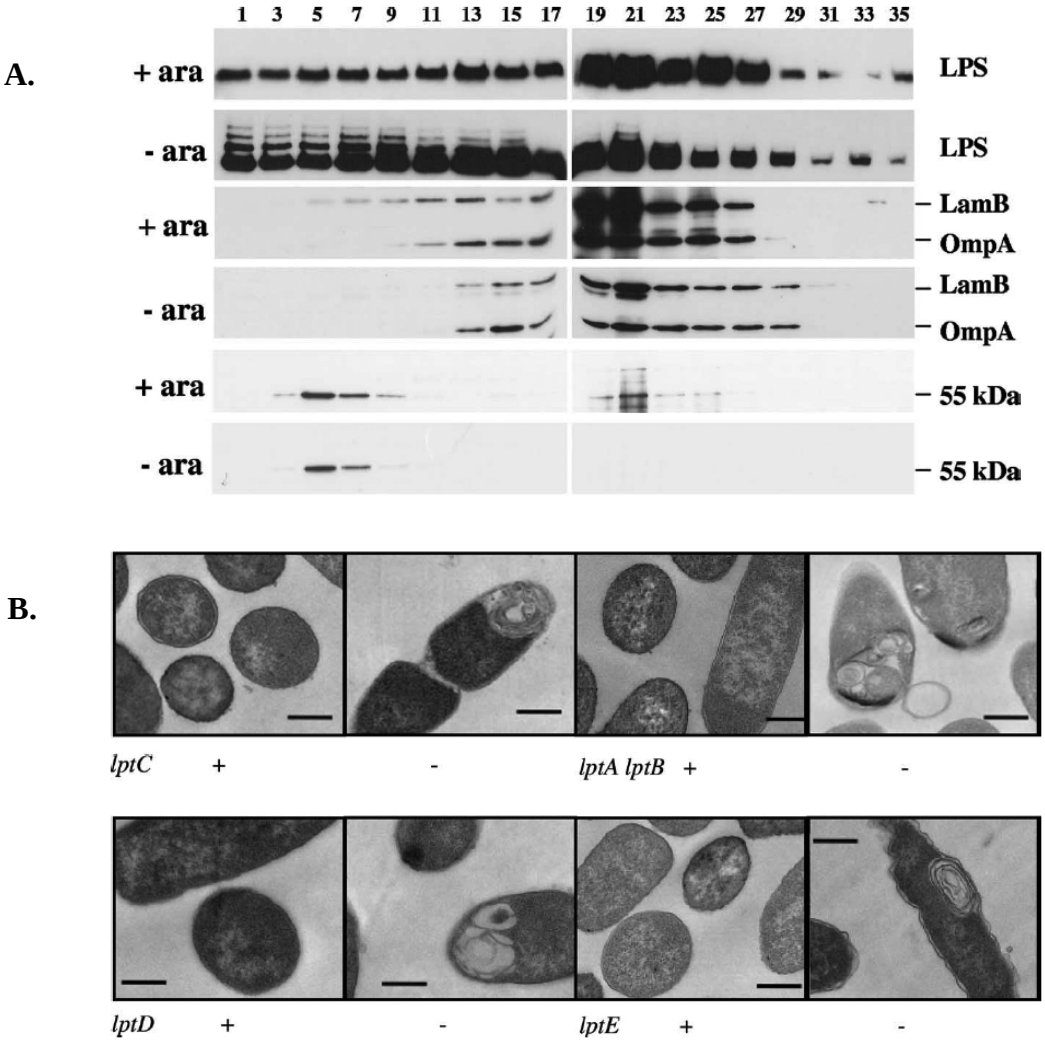

Figure 1.5: Lpt depletion and cell envelope phenotypes. Depletion (-ara) of either LptA, LptB, LptC, LptD or LptE leads to the (A) spread of LPS throughout the cell envelope and (B) anomalous cell envelopes. Notice the anomalous LPS structures in the depleted (-) strains. [Adapted from Sperandeo, P., *et al*., *J Bacteriol*, 190, 4460-4469. (2008)].

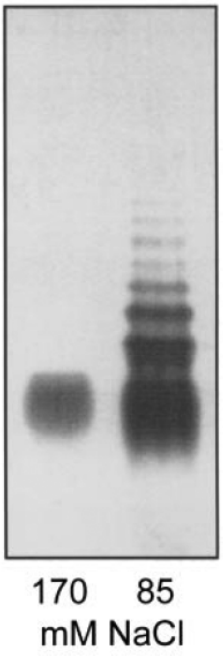

Figure 1.6: Colanic acid repeat addition to LPS under hypoosmotic conditions. Colanic acid repeats are added by WaaL to the core oligosaccharide under hypoosmotic conditions, which is also observed in *lpt*-depleted cells. [Adapted from Meredith, T.C. *et al*., *J Biol Chem*, 282, 7790-7798, (2007)].

where the RNA polymerase σ^{70} element binds, highlighting the role of these response regulators in promoting transcription of their target genes [68-70]. PmrAB is the first example of a signal transduction cascade which responds to ferric iron in bacteria, as Fe^{3+} has been shown to bind the ExxE motif located within the 31-amino acid periplasmic domain of PmrB. Interestingly, Mg^{2+} competes with Fe^{3+} for this binding motif [71]. The same motif can bind Al^{3+}, but only results in 50% of the activation level that is observed for Fe^{3+} [71]. In terms of the contribution to virulence of PmrAB and PhoPQ, both are activated *in vivo* in a mouse model of *Salmonella* infection [72]. *Salmonella pmrA* and/or *pmrB* mutants have been shown to have decreased virulence in both Balb/C mice and chicken macrophage models of infection whereas a *S. enterica phoP* mutant has been shown to be avirulent within murine macrophages, highlighting the importance of the PhoPQ two-component system in virulence for this bacterial species, although this is probably not only due to its role in modifying LPS [73-75]. Mechanistically, it is important to take into consideration that the PmrAB two-component system positively modulates its own expression by promoting transcription of the *pmrCAB* operon, until PmrB exhibits phosphatase activity and dephosphorylates PmrA (Fig. 1.7) [76]. As a result, PmrAB signalling over time in response to iron results in a temporal change in the modification status of LPS, thereby decreasing the level of iron bound to the cell due to shielding of the phosphoryl groups. The same type of regulation is observed for PhoPQ, as PhoP also positively modulate its own expression by upregulating transcription of the *phoPQ* operon initially under PhoPQ-inducing conditions, until PhoQ exhibits phosphatase activity, negatively regulating PhoP-mediated transcription of target genes [77, 78]. This initial surge in *phoPQ* transcription is necessary in promoting *Salmonella* virulence [78].

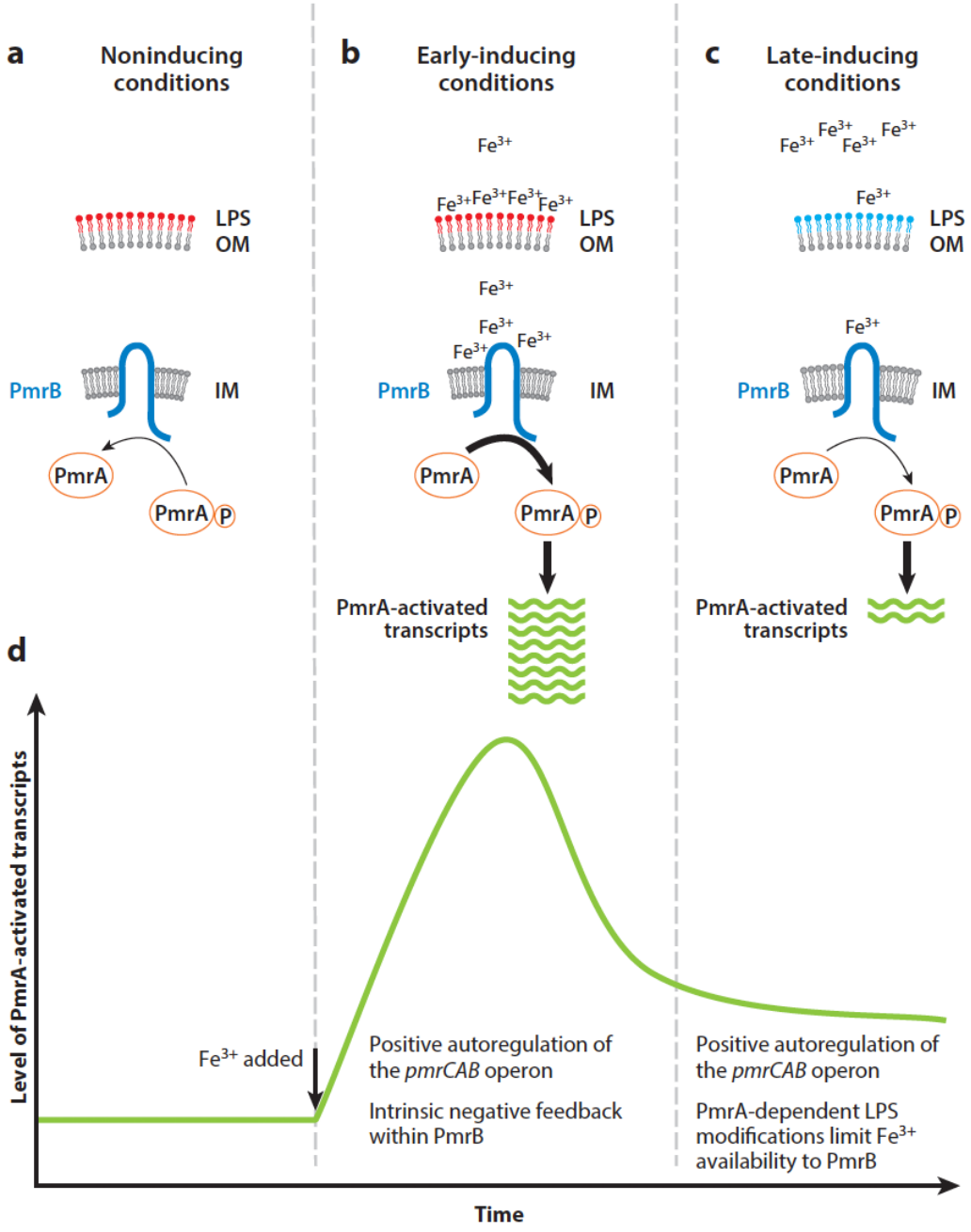

Figure 1.7: The time-dependent effect of PmrAB-mediated transcripts on OM remodeling. The bacterium constantly monitors signals from its environment to modify its LPS layer accordingly. [Adapted from Chen H.D. and Groisman E.A, *Annu Rev Microbiol*, 67, 83-112. (2013)].

1.7.1.1 PmrD Connector protein

In *S. enterica* and *K. pneumoniae*, as opposed to other members of the *Enterobacteriaceae*, the PhoPQ and PmrAB two-component systems are connected by the way of the PmrD protein (Fig. 1.8) [79, 80]. This small 85-amino acid protein binds to and prevents dephosphorylation of the PmrA response regulator, leading to the expression of PmrA-dependent genes in PhoPQ-inducing conditions (i.e. micromolar concentrations of Mg^{2+}) [79]. The *pmrD* gene is present in *E. coli* but is unable to bind PmrA due to allelic differences, whereas the *pmrD* locus is absent from the *Citrobacter rodentium* genome, making it the perfect model to study PmrAB-regulated LPS modifications, independently of PhoPQ [81, 82].

These observations may reflect the different responses that must take place in these species for adaptation and persistence in their environmental niches, which is within macrophages for *S. enterica* and extracellularly for *E. coli* and *C. rodentium* [38].

1.7.2 LPS Modifications governed by Two-Component Systems

PhoP and PmrA govern the transcription of various genes responsible for LPS covalent modifications. PhoP directly regulates the transcription of *pagP*, an OM protein, which catalyzes the addition of a seventh acyl (C16) chain to the lipid A moiety [83]. This modification is thought to increase the hydrophobicity of the LPS layer, rendering AMPs less susceptible to cross the OM, thereby increasing the bacterium's resistance to these host innate immune factors [84]. As for the PmrA-regulated covalent LPS modifications, there are most notably the aminoarabinose (araN) and phosphoethanolamine (pEtN) modifications (Fig. 1.9). The araN modification, which is added to the 4'-phosphoryl group of lipid A is conferred by the *arn* operon (*pmrHFIJKLM* operon or

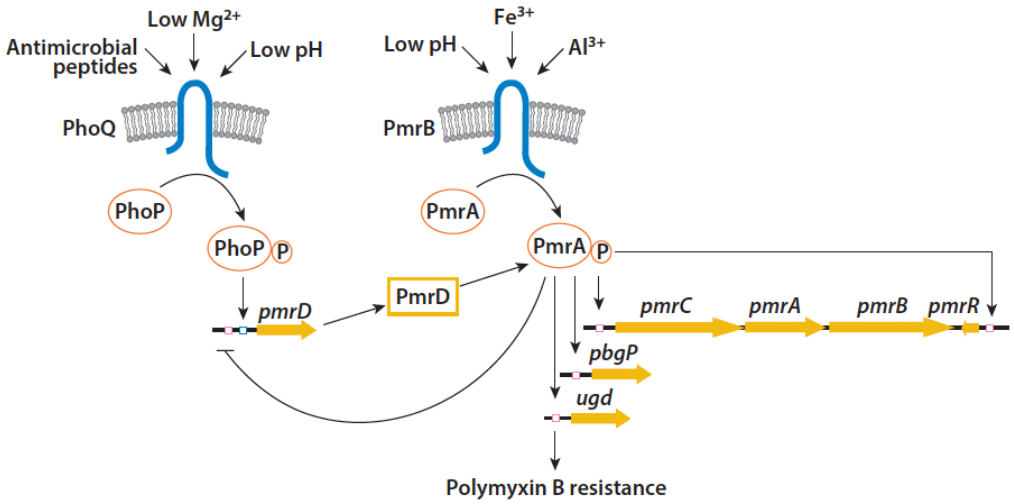

Figure 1.8: PhoPQ and PmrAB crosstalk in *S. enterica*. A PhoP-regulated gene, pmrD gives rise to PmrD, a protein that binds and prevents dephosphorylation of PmrA, leading to expression of PmrA-regulated genes in PhoPQ-inducing conditions. *E.coli* possesses the *pmrD* gene locus, but the gene product is unable to activate PmrA [Adapted from Chen H.D. and Groisman E.A, *Annu Rev Microbiol*, 67, 83-112. (2013)].

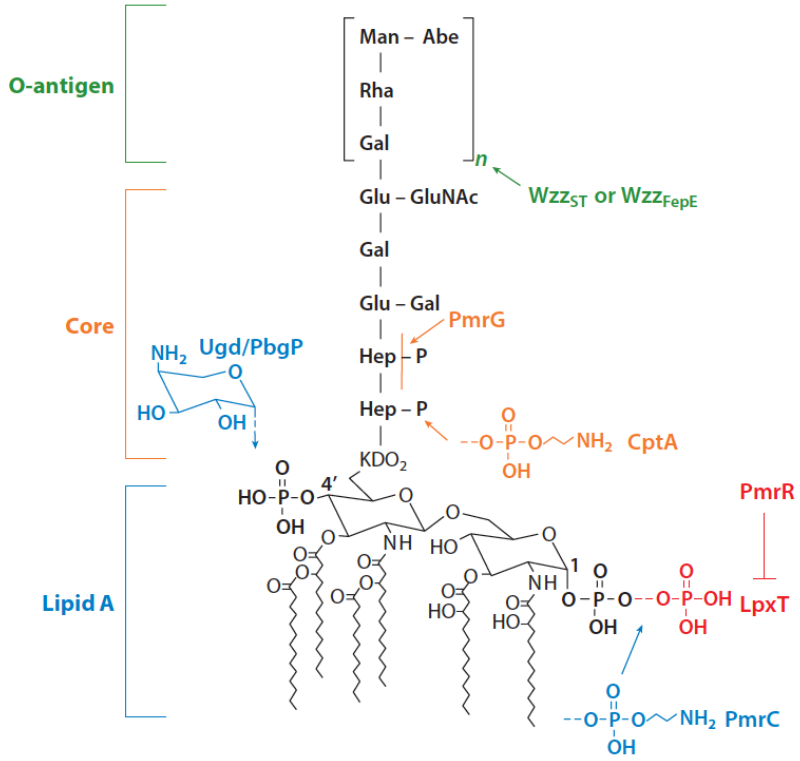

Figure 1.9: PmrAB-regulated LPS Modifications of *S. enterica*. All three moieties of LPS are modified in response to PmrAB induction. [Adapted from Chen H.D. and Groisman E.A, *Annu Rev Microbiol*, 67, 83-112. (2013)].

pbgP) and *ugd*, has been reported to promote resistance to PMB by decreasing the net negative charge of the OM, which is provided most notably by the phosphoryl groups of LPS [85, 86]. In contrast, the pEtN modifications are added at various phosphoryl groups present on the LPS molecule by pEtN transferases. PmrC (EptA, EptC), for which the gene is part of the *pmrCAB* operon, catalyzes the addition of pEtN to the 1- and 4' phosphoryl groups of the lipid A moiety. PmrC, as with the *arn* operon, has also been linked to polymyxin B resistance [87]. CptA (YijP) adds pEtN to the core heptose-I phosphoryl residue, the same phosphoryl group that has been implicated in *Salmonella* virulence, LPS biosynthesis and LPS transfer to the OM [88]. Its implication in resistance to polymyxin B is less clear [88]. It is important to note that neither *S. enterica pmrC* nor *cptA* single mutants show decreased virulence *in vivo*, although a *pmrC cptA* mutant did show a slight decrease in virulence, but less than a 10-fold decrease compared to the wild-type strain, as determined by competitive index experiments [88]. Interestingly, PmrAB also governs the expression of *pmrG*, whose gene product encodes a phosphatase [65]. This phosphatase specifically acts on the core heptose-II phosphoryl group and has been attributed a role in resisting Fe^{3+} toxicity [65]. PmrAB also increases the expression of *wzz* (or *cld*), which encodes the O-antigen chain-length regulator, leading to an increase in O-antigen chain length that results in increased resistance to serum [89, 90]. Interestingly, negative feedback on the PmrAB-regulon is also accomplished through the transcription of a recently described small 30 amino acid peptide called PmrR, for which the ORF is found downstream of the *pmrCAB* operon [76]. PmrR inhibits the activity of another IM protein called LpxT by directly interacting with it. LpxT is an enzyme which constitutively adds a phosphoryl group to the 1-lipid A phosphoryl group, generating lipid A-1-PP and giving the OM an overall negative charge [76, 91]. By inhibiting this enzyme, PmrR allows for the lipid A to be modified by PmrC, rendering the OM less negatively

charged over time and thereby dekcreasing PmrB activation, as Fe^{3+} cannot bind and diffuse through the OM and activate the sensor kinase, leading to decreased PmrA phosphorylation and lesser PmrA-activated transcripts (Fig. 1.7).

Recently, colistin resistance in *K. pneumoniae* and *A. baumannii*, both major Gram-negative multi-drug resistance threats, was decreased by targeting PmrAB with a small molecule inhibitor [92]. In particular, *A. baumannii* has developed resistance to colistin by inactivation of its LPS synthesis genes (*lpxA*, *lpxC* and *lpxD*) or by mutations in *pmrAB*, leading to increased lipid A pEtN addition by PmrC [93]. Compound 1, a 2-aminoimidazole, downregulated the expression of the *pmrCAB* operon by 10-fold in *K. pneumoniae*, resulting in a 1024-fold decrease in the minimal inhibitory concentration of colistin *in vitro* [92]. The same effects of Compound 1 on PmrAB signalling were observed when Compound 1 was tested against a colistin-resistant *A. baumannii*. The mechanism of action by which Compound I increased resistance to colistin was by decreasing the amount of pEtN substitution at the 1-phosphoryl group of lipid A. As PmrAB is not essential for cell viability, resistance was not generated to Compound 1, notably in *A. baumannii*, which is highly mutable [92].

Interestingly, in *Burkholderia cenocepacia*, addition of aminoarabinose to LPS was found to be essential for recognition of LPS by the LPS transport machinery [94]. More specifically, it was shown that LptG, a component of the ABC transporter that drives LPS transfer from the IM to the OM, was shown specifically to interact with the aminoarabinose present in *B. cenocepacia* LPS [94]. Unlike in the *Enterobacteriaceae*, aminoarabinose is added to both the lipid A and core oligosaccharide moieties in *B. cenocepacia*. Strikingly, disruption of this interaction resulted in a lethal phenotype, due to the inability of the mutant to properly shuttle its LPS to the OM, indicating that LPS is indeed essential in this species, as is the case for most Gram-negative species [94]. The

authors specifically mapped the interaction to residue histidine 31 (H31) of LptG, since unmodified LPS was unable to be transferred to the OM, this study revealed that LPS transport evolved with the occurrence of LPS covalent modifications in this species.

1.7.2.1 The *arn* Operon and Polymyxin B Resistance

Aminoarabinose incorporation into LPS requires both the *arn* operon and *ugd* [95]. The *arn* operon encodes both cytoplasmic enzymes as well as IM enzymes and utilizes the IM acyl carrier UndPP (Fig. 1.10), resulting in the generation of UndP-4-aminoarabinose [95]. This intermediate accumulates in polymyxin B-resistant *E. coli* and *Salmonella* strains [95]. Aminoarabinose is added to the 4'-phosphoryl group of lipid A by ArnT (PmrK) [95]. The addition of 4-aminoarabinose to lipid A decreases the net negative charge of this phosphoryl group from -1.5 to 0, resulting in a more than 500-fold increase in polymyxin resistance over a strain defective for lipid A 4-aminoarabinose incorporation [96]. Numerous reports in the literature have associated the *arn* operon to polymyxin B resistance in many different Gram-negative bacterial species [74, 97-99].

1.7.2.2 PmrC, CptA and Polymyxin B Resistance

The addition of pEtN to the lipid A and core moieties of LPS is governed by the pEtN transferases PmrC and CptA in the *Enterobacteriaceae*. Both pEtN transferases are IM proteins, crossing the IM multiple times (Fig. 1.11). The N-terminal of this protein encodes five transmembrane domains and the C-terminal possesses pEtN transferase activity [87]. Addition of pEtN to the lipid A moiety results in a decrease of net negative charge of the phosphoryl groups from -1.5 to -1, resulting only

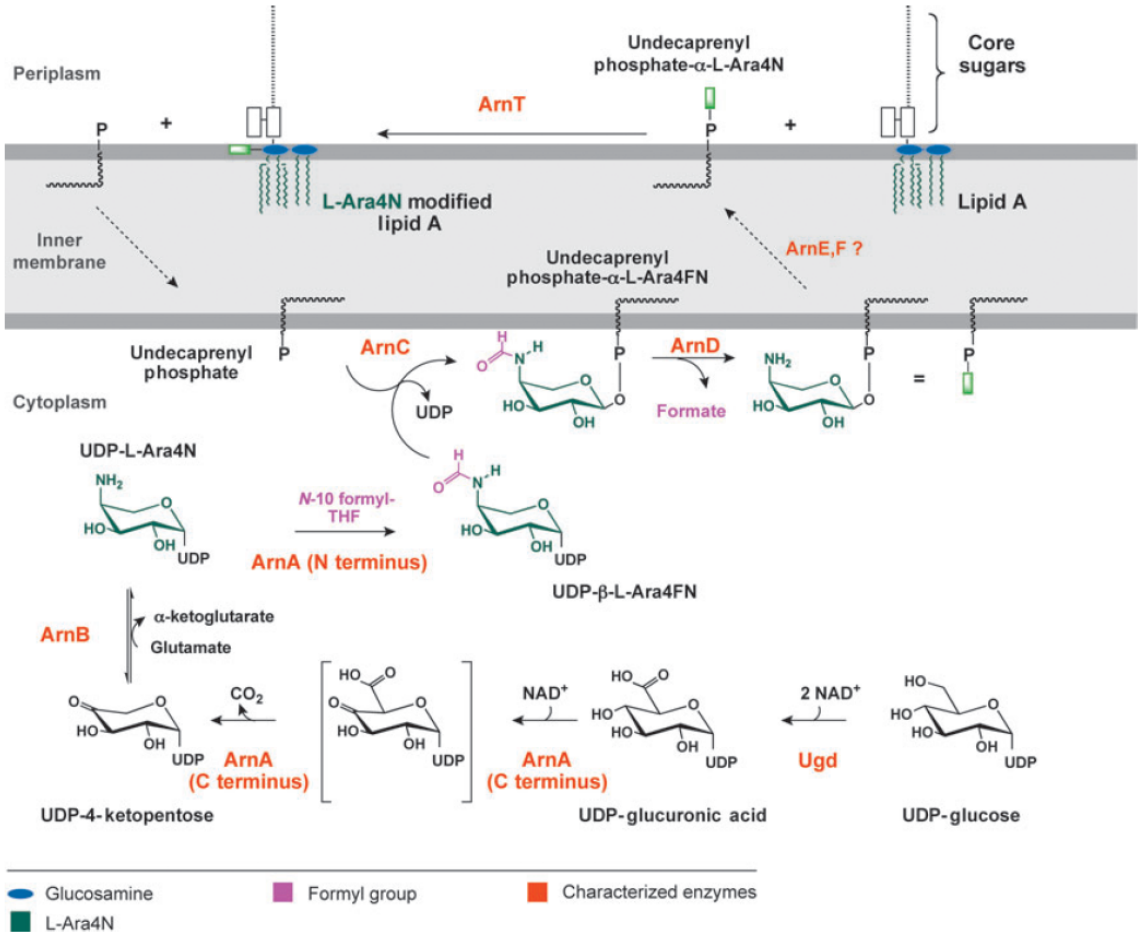

Figure 1.10: The *arn* operon and *ugd* catalyze the addition of 4-aminoarabinose to lipid A. The synthesis and addition of 4-aminoarabinose comprises both cytoplasmic and IM enzymes. [Adapted from Raetz, C.R., *et al*. *Annu Rev Biochem*, 76, 295-329, (2007)].

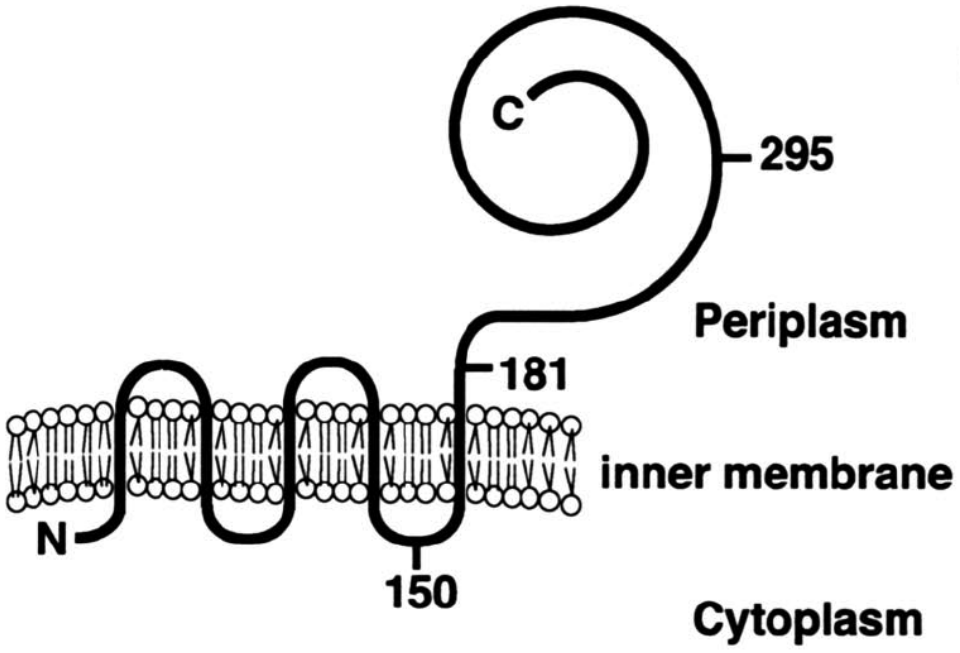

Figure 1.11: The PmrC and CptA pEtN transferases are IM proteins with their active site facing the periplasm. Both PmrC and CptA share this topology, acting on LPS before it is shuttled to the OM. [Adapted from Lee, H., *et al.*, *J Bacteriol*, 186, 4124-4133, (2004)].

in a 3- to 5-fold increase in resistance to polymyxin B over a strain defective for lipid A pEtN incorporation, highlighting the fact that the role of PmrC in polymyxin B resistance may be secondary [96]. As evidence of this claim, PmrC only slightly contributes to survival to a polymyxin B killing assay compared to the *arn* (*pbgP*) operon in *S. enterica*, and therefore it may accomplish different roles in the *Enterobacteriaceae*.

The role of CptA in polymyxin B resistance is even more loosely associated. Compared to the contribution of PmrC-mediated addition of pEtN to lipid A, the effect of the addition of pEtN to the core heptose-I in promoting resistance to polymyxin B is negligible [88]. Therefore, CptA may have other roles in the *Enterobacteriaceae*.

1.7.2.2.1 PmrC has Different Roles in other Gram-Negative Bacteria.

PmrC, in most of the *Enterobacteriaceae*, has been solely studied in its ability to confer resistance to polymyxin B. However, in *Campylobacter jejuni*, PmrC, or EptC as it is called in this species, has various roles. First, EptC was shown to add pEtN to threonine 75 (Thr75) of the FlgG subunit of the flagellar apparatus [100]. An *eptC* mutant was found to be immotile, therefore linking the FlgG pEtN modification to flagellar apparatus function [100]. This finding was extrapolated to be essential in most ε-proteobacteria, as the Thr75 residue of the FlgG subunit is relatively well-conserved. In the same bacterium, EptC was found to add pEtN to another substrate, *N*-linked glycans [101]. *N*-linked glycans are heptasaccharides, encoded by the *pgl* gene cluster, which are either associated to bacterial cell surfaces or released into the environment [101]. Interestingly, it was shown, that although at a lesser rate, *E. coli* PmrC was able to modify *C. jejuni* *N*-linked glycans with pEtN, suggesting that *C. jejuni*, given its reduced genome size, expanded

the number of substrates for EptC-mediated transfer of pEtN. This is evidenced by the fact that it was found that EptC also mediates transfer to the core heptose-I group, whereas members of the *Enterobacteriaceae* have evolved a separate pEtN transferase to accomplish this function (i.e. CptA). With relation to activation of Toll like Receptors (TLRs), *C. jejuni* EptC-modified LPS resulted in increased recognition by the human TLR4/MD2 receptor complex compared to its unmodified counterpart [102]. In addition, chicks, the natural reservoir of *C. jejuni*, were less colonized by the *eptC* mutant compared to the wild-type strain, suggesting a role for EptC in establishing commensalism [102]. Altogether, these data indicate that the role of pEtN modification of LPS may extend beyond AMP resistance.

1.8 Iron and Bacterial Pathogenicity

1.8.1 Iron: Essential for Bacterial Growth

Iron is a key metal in both promoting host immunity and bacterial growth [103]. In a healthy individual, iron is chelated by iron-chelating proteins such transferrin, lactoferrin and ferritin or in association with heme within hemoglobin, limiting the concentration of free iron available to bacteria being in a range of 10^{-11} to 10^{-12}M [103]. Additionally, it is important that iron remains sequestered to proteins due to the ability of free iron to generate free radicals by the Fenton reaction ($Fe^{2+} + H_2O_2 \leftrightarrow Fe^{3+} + OH^- + OH^{\cdot}$), which are capable of damaging host nucleic acids, proteins and lipids [103].

All bacteria require iron for growth, except for the causative agent of Lyme disease, *Borrelia burgdoferi*. The struggle between host and pathogen is the result of the requirement of bacteria for a free iron concentration of 10^{-6} M to 10^{-7} M to accomplish cellular functions such as

replication and DNA synthesis as iron is utilized as a cofactor in many enzymes involved in these processes [104]. Thus, bacteria (including pathogens) have evolved specialized iron-acquisition systems [104]. These systems utilize iron-binding molecules, siderophores, which have a high affinity for Fe^{3+} ($K_d \sim 10^{-40\text{-}50}$M) [105]. In the *Enterobacteriaceae*, the siderophores with the strongest affinity for Fe^{3+} are the ferric enterobactins [106]. Siderophores consist of either phenolic rings or hydroxamate structures with hydroxy, dihydroxybenzoic acid, carboxy or aminohydroxy groups for chelation of Fe^{3+} [106]. Once bound to iron, the siderophore-iron complex binds its cognate receptor on the OM [106]. FepA is the receptor for the ferric enterobactins [106]. Iron is then transferred to the periplasmic protein FepB, a mechanism that is dependent on TonB [106]. Free iron gains access to the bacterial cytosol with the aid of an ATP-dependent permease [106]. In *E. coli*, at least two other iron uptake mechanisms have been described [106, 107]. Once inside the bacterial cytosol, Fe^{3+} is reduced to Fe^{2+} and is either utilized in enzymatic reactions or stored bound to bacterioferritins [106].

Interestingly, mammalian cells have evolved siderophores themselves to counter the action of bacterial siderophores [103]. Siderocalin, also known as lipocalin-2, is a protein that is secreted by neutrophils in response to infection. Siderocalin binds enterobactin and sequesters the siderophore-iron complex, preventing bacterial uptake [103]. Siderocalin, in complex with 2,5-dihydroxybenzoic acid, was actually found to traffic iron to the mitochondria for the synthesis of iron-sulfur proteins [103]. However, pathogens can secrete chemically-altered siderophores to counteract the action of the mammalian siderophores [103].

In most bacteria, gene regulation in response to low iron concentrations in the host is under the transcriptional control of the iron-dependent repressor known as Fur (Ferric uptake repressor) [104]. In the presence of iron, Fur binds the "Fur box", a palindromic sequence,

(GATAATGATAATCATTATC) in the promoters of genes encoding proteins that utilize iron and represses their expression [104, 108]. In the absence of iron, this repression is relieved [104].

In mice, some environments where *Enterobacteriaceae* may encounter micromolar iron concentrations are in the stomach and small intestine (29 to 733 µM) and in the duodenum (10 to 100 µM) [109] . Concentrations of ferric iron in these organs are thought to be in the same range in humans [110]. Interestingly, during septicemia, free iron monitored in the bloodstream of patients was shown to increase from 5 µM to 35 µM [111]. These micromolar concentrations of iron may be able to positively modulate LpxC activity, the *N*-acetylglucosamine deacetylase that is responsible for the catalysis of the committed step in the constitutive lipid A pathway, and hence, in LPS synthesis. LpxC was originally classified as a Zn^{2+} metallo-enzyme, as it exhibits two times more affinity for the Zn^{2+} over the Fe^{2+} ion *in vitro*, but the conditions in which these experiments were done did not take into account the loss in redox potential of iron (Fe^{2+} to Fe^{3+}), which is oxygen-sensitive [28]. Redox potential is more tightly regulated *in vivo*, as the cytoplasm, where LpxC is located, is an overall reducing environment [28]. It was further shown by *in vitro* assays that LpxC bound to Fe^{2+} had a six- to eight-fold increase in catalytic activity over LpxC bound to Zn^{2+}, which is primarily due to an increase in k_{cat} [29].

1.9 OM vesiculation

1.9.1 Structure, Composition and Mechanism of Formation

OM vesiculation is a relatively novel topic of research in the field of bacteriology. However, OM vesicles were first described 50 years ago. In contrast to eukaryotic cells, where membrane vesiculation is known to be involved in storage, trafficking (cell-cell and inter-

organelle communication) and digestion of cellular components, much is still unknown about OM vesiculation in Gram-negative bacteria.

OMVs are constitutively shed during growth by both pathogens and non-pathogens whether in liquid culture, solid culture or biofilm growth [112, 113]. They are produced by blebbing or budding of the OM, in turn, encapsulating periplasmic cargo inside a membrane bilayer composed of OM (Fig. 1.12) [112]. The size of these spheroid vesicles ranges from 10 to 300 nm and they contain LPS, phospholipids, DNA, RNA, and proteins from the cytoplasm, IM and OM [112]. Packaging into vesicles leads to either enrichment or exclusion of specific proteins into these spheroid particles, suggesting that it is not a random process [112]. The key process involved in OM vesiculation appears to be the interaction between the OM and the peptidoglycan layer (Fig. 1.12) [114]. Vesiculation is observed when there is a local decrease in the interactions between OM and peptidoglycan at a specific location [114]. This local decrease in OM-peptidoglycan interaction results in vesicle budding from the OM [114]. The key proteins involved in the interaction between the OM and the peptidoglycan layer are Braun's lipoprotein (Lpp), OmpA and the Tol-Pal system [114]. The major component involved in OM vesiculation is Lpp, the most abundant lipoprotein in *E. coli*, estimated to be present at 750,000 copies per cell, forms a covalent bond between its lysine 58 (lys58) residue and the diaminopimelic acid residue of the peptidoglycan molecule [114]. Lpp is termed free when it is unbound to peptidoglycan, whereas it is in bound form when it is linked to peptidoglycan. The ratio of the free to bound form of Lpp is 2:1. A mutation in the lipid anchor of Lpp, in the lysine 58 residue that forms crosslinks with the peptidoglycan layer (Δlys58) or the deletion of the *lpp* gene leads to OM hypervesiculation, that is, the overproduction of OMVs estimated to be 150-fold higher than the wild-type strain [114].

Additionally, Reg26, also known as MicL, which is a σ^E-dependent small RNA, was found to downregulate the Lpp levels in the cell, leading to OM vesiculation [115].

Pal, another OM lipoprotein, forms, as opposed to Lpp, a non-covalent link with the peptidoglycan layer via an α-helical motif [116]. Pal is part of the Tol-Pal system, which consists of the IM proteins TolA, TolQ, TolR, and the periplasmic protein TolB, which forms a complex with Pal. TolA-TolQ-TolR interact whereas TolB forms a complex with Pal. Both complexes are linked via a TolA-Pal interaction, which is dependent on the proton motive force, suggesting that this interaction is unfavourable but critical to OM integrity [117]. Pal has also been shown to form independent interactions with Lpp, OmpA and TolB [118].

OmpA (Outer membrane protein A), is not classified as an outer membrane porin, such as OmpF and OmpC, but is involved in the structural integrity of the Gram-negative OM. The carboxyl-terminal of OmpA, termed the OmpA-like domain was found to co-crystallize with diaminopimelic acid residue of the peptidoglycan layer [119]. It was further shown that deletion of *ompA* lead to hypervesiculation in *E. coli* [120]. Just as MicL downregulates Lpp levels in the cell, a similar σ^E-dependent small RNA, MicA in *E. coli*, was found to downregulate cellular OmpA levels, resulting in decreased interactions made with the peptidoglycan layer, leading to the production of OMVs [121].

Other plausible mechanisms by which OM vesiculation occurs includes the accumulation of peptidoglycan monomers in the periplasm [122]. In one study, it was shown that a mutant of *Porphorymonas gingivalis* in autolysin, an enzyme responsible for the cleavage of peptidoglycan, produced vesicles with low molecular weight muramyl peptides in their lumen, although vesiculation in this case may be the result of stress response activation due to the accumulation of these peptides [122]. It is suggested by the authors that the accumulation of these peptides would

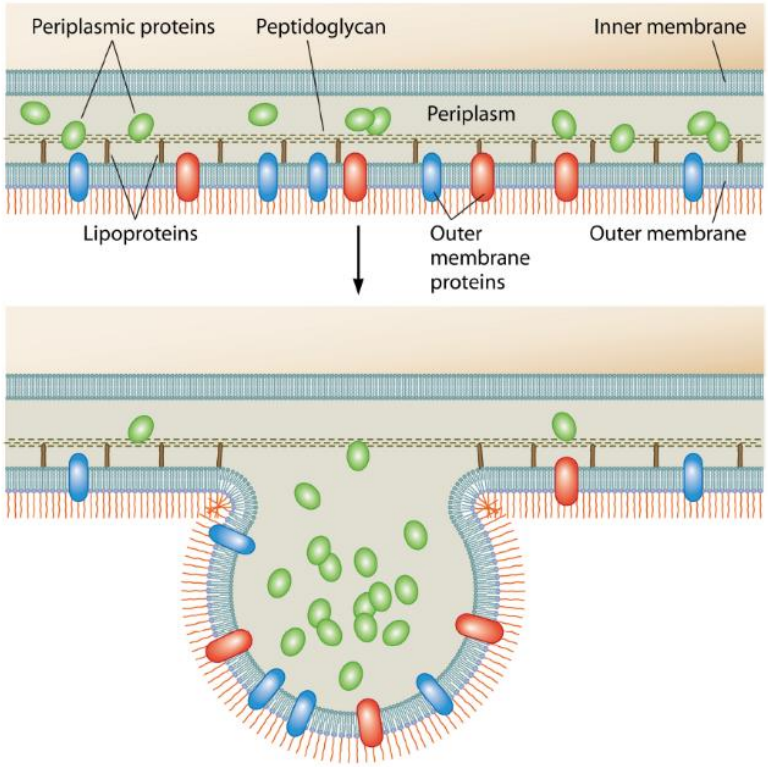

Figure 1.12: **OM vesiculation.** The process of vesiculation consists of a local decrease in the interactions made between the OM and peptidoglycan layer. [Adapted from Ellis T.N., and Kuehn M.J., *Microbiol Mol Biol R*, 74, 81-94 (2010)].

exert a pressure on the OM, generating a curvature, a crucial step in the formation of OMVs [122]. Additionally, OMVs containing these low molecular weight fragments of peptidoglycan collected from *Helicobacter pylori*, *Pseudomonas aeruginosa* and *Neisseria gonorrhoeae* were shown to elicit a NOD-1-dependent innate immune response [123]. Another process by which OM curvature is thought to be generated is by differences in LPS charge of different LPS species [124]. In *P. aeruginosa*, it is thought that the relative concentration of B-band LPS, which possesses a heteropolymeric O-antigen and is more negatively charged than A-band LPS, plays a role in promoting membrane curvatures required for OM budding and vesicle production [124]. This observation leads one to believe that vesicle formation is indeed a regulated process in *P. aeruginosa*.

OM vesiculation has been demonstrated to arise under conditions that activate envelope stress responses, most notably when bacteria experience high growth temperatures resulting in the accumulation of misfolded proteins in the periplasm. These proteins must be exported out of the cell as the increased turgor in the cell envelope leads to envelope stress [125]. Thus, OM vesiculation is an adaptive mechanism that increases bacterial survival to envelope stress. In a wild-type strain, this process involves the periplasmic protein DegP, which acts as a protease when bacteria are shifted from lower to higher temperatures (e.g. 30˚C to 37˚C) and cleaves the misfolded periplasmic proteins [125]. In contrast, an *E. coli degP* mutant strain was shown to hypervesiculate when grown at 37ºC compared to the wild-type strain, as the level of misfolded proteins was exacerbated under this condition [125]. Thus, the OM vesiculation process itself is dependent on the cell envelope stress response, which is also corroborated by the fact that the σ^E envelope stress response regulates the transcription of MicA and MicL under inducing cues of envelope stress.

1.9.2 Function of OMVs

OMVs are secreted by both pathogens and non-pathogens and therefore have various functions. The role of vesiculation in pathogenesis had initially been recorded in experimental animals infected by Gram-negative bacteria. For example, in a rat model of septicemia caused by *E. coli*, LPS and OM protein-containing bacterial fragments were isolated from the serum and were found to be of the same composition than the material shed when the *E. coli* was grown in culture with human serum [126]. They were classified as OMVs as they were composed of LPS, OM proteins and lipoproteins; were larger than 0.1 μm in size; and were, most notably, stable [126]. More importantly, the role of vesicles in diseased human samples caused by bacterial infections has also been reported. In the case of fatal septicemia caused by vesiculating *N. meningitidis*, a level of 1,700 endotoxin units/ml was recorded in the bloodstream of the patient, equivalent to the activity of 170 ng/ml pure *E. coli* LPS, was determined to be caused by the vesicles shed by the infecting bacterium [127].

In terms of general functions, OMVs have been shown to play a role in interspecies competition and collaboration. When nutrients are in limited concentration, OMVs have been documented to contain peptidoglycan hydrolases and to be bactericidal to both Gram-negative and Gram-positive bacteria when co-cultured together [128]. Other enzymes found within the vesicle cargo are β-lactamase, therefore suggesting OMVs act as means that mediate antibiotic resistance [129]. “Community goods” are also released into the environment by the means of OMVs. Xylanase and cellulase released within vesicles benefit the whole of the microbial community, as they degrade complex carbohydrates and make them digestible by most members of the microbial niche [130]. OMVs have also been shown to promote biofilm formation, as DNA found on the outer surface of the vesicle acts as a bridge between the bacterium and biofilm glycopolymers

[130]. Additionally, vesicle-mediated DNA exchange may also be a means by which bacteria exchange genetic material through horizontal gene transfer, which could be very important in understanding how antibiotic resistance is propagated during an infection [131]. In addition, OMVs have been demonstrated to fuse with either the membranes of other bacteria or mammalian cells, resulting in the deliverance of their cargo [112].

In terms of toxins associated with OMVs, the vesicle itself provides protection from proteases and antibodies, provides optimal conditions for toxin folding as well as a vehicle for toxin delivery [132]. For example, heat labile enterotoxin of enterotoxigenic *E. coli* (ETEC) is contained within vesicles and specifically target epithelial and Y1 adrenal cells, triggering their apoptosis [133]. Another toxin that is packaged into vesicles is EHEC hemolysin, which targets host cell mitochondria by first promoting fusion of the vesicle with the host epithelial cell membrane leading to toxin delivery, disrupting the mitochondrial membrane after it is released into the host cytosol, releasing cytochrome c and inducing apoptosis by a mechanism which includes caspase-9 and caspase-3 [133]. In addition, EHEC OMVs have also been shown to contain Shiga toxin, which may exarcebate the pathology caused by this bacterium as the toxin's effect would be long-lasting, sheltered from host proteases [134].

The process by which cargo are packaged into vesicles remains unknown, as there seems to exist a process by which some proteins are selected over others to be packaged into vesicles. Interestingly, in agreement with a regulated packaging process, by proteomic analysis of *Bacteroides fragilis* and *Bacteroides thetaiotaomicron* OMVs, it was revealed that a large subset of OM vesicle cargo proteins were acidic, which may serve as a packaging signal [135].

In terms of triggering potential of the immune system, OMVs, due to their composition (LPS, lipoproteins, toxins, OM porins), have the potential to activate the immune system in

numerous ways, depending on the composition of the vesicle itself [112]. This gives way to the potential of designing OMVs containing specific cellular components to generate a desired immune response. What is interesting about OMVs is that they are more likely to specifically induce the immune system based on a signature response of the bacterial species that produces them rather than elicit the immune responses observed for purified molecules such LPS or toxins, as the concentration of these substituents in the vesicles varies depending on the bacterium [112]. For example, recently, it has been described that one way the microbiota interacts with the host is through OMVs [136]. As evidence for this, *Bacteroides fragilis* was shown to package capsular polysaccharide (PSA) into OMVs to induce $T_{regulatory}$ cells to produce immunomodulatory cytokines (i.e. IL-10) [136]. The capsular PSA containing vesicles prevented experimental colitis in mice, which is synonymous to inflammatory bowel disease in humans [136]. In addition, the OMVs containing capsular polysaccharide were shown to increase $T_{regulatory}$ cell function by enhancing their suppressive capacity [136]. The mechanism was shown to be dependent on TLR2 present on dendritic cells, which induced the expression Gadd45α to induce specific $T_{regulatory}$ cell function in IL-10 secretion [136]. The response to pure PSA, which was not in association with OMVs, did not generate the same immune response, highlighting the importance of OMVs in generating a particular host immune response [136]. This suggests applications for vesicles, such as their potential use in vaccines. In terms of vaccine-based therapies using OMVs in formulations, OMVs, as such, are composed of a natural adjuvant, LPS [112]. In the context of vesicle, it was shown that OM vesicle LPS triggers the immune system differently than purified LPS from whole cells, and is most probably more physiologically relevant to *in vivo* conditions [137]. A difference in triggering potential arises in the bioavailability of LPS from OMVs that reaches deep into tissues and thus have higher biological activity *in vivo* making them suitable candidates for vaccine

adjuvants, whereas purified LPS, which is highly hydrophobic in nature, would quickly bind available receptors and generate an overwhelming immune response, as is the case in septic shock [137]. To date, the only vesicle-based vaccine that has been successful is the vaccine against meningococcal serogroup type B, with a total of 55 million vaccinations (2010) [112]. Hence, future studies in the potential of OMVs for the use in vaccine formulations will be interesting. As proof of the value of utilizing vesicle-based vaccines in the treatment of multi-drug Gram-negative resistant bacterial infections, vaccination of mice with *A. baumannii* OMVs was proven to confer protection from *A. baumannii* infection as well as cure an existing infection in mice [138].

As it is appearing that OMVs may be a more physiologically relevant mean by which pathogens cause disease, preventing vesicle biosynthesis may be an interesting alternative to the inhibition of virulence, and thus serve as a valid alternative to conventional antibiotics.

1.10 Thesis Goals

The overall objective of this project was to determine the role of PmrC- and CptA-mediated pEtN LPS modifications in *C. rodentium*, the murine model pathogen of EHEC and EPEC infections in humans. *C. rodentium* is a convenient model to study the role of PmrAB-regulated pEtN modifications as the *arn* operon is absent in this bacterium. The modification of the lipid A moiety is thus only pEtN-dependent. This is important as 4-aminoarabinose addition to the lipid A moiety's 4'-phosphoryl group has been shown to interfere with pEtN addition in *S. enterica* [139]. Therefore, the contribution of PmrC-mediated resistance to the AMP polymyxin B and to other functions relating to LPS can be fully appreciated in *C. rodentium*. Additionally, the *pmrD* gene is absent from the *C. rodentium* genome, which means that the PmrAB-regulated LPS

modifications can be studied independently of the PhoPQ two-component system. Therefore, seeing as micromolar concentrations of iron is the main activator of the PmrAB two-component system, it was used to induce PmrAB throughout the different experiments in the context of a limiting Mg^{2+} concentration to not interfere with PmrAB signalling.

The first objective was to determine the contribution of PmrAB-regulated LPS modifications in resistance to a variety of antibiotics, as these modifications alter the structure of the LPS layer. We first tested our strains (wild-type *C. rodentium*, Δ*pmrAB*, Δ*pmrC*, Δ*cptA* and Δ*pmrC*Δ*cptA*) for susceptibility against PMB in a minimal inhibitory concentration (MIC) assay. Only two-fold decreases in MIC values were observed for the Δ*pmrAB* and Δ*pmrC*Δ*cptA* strains compared to wild-type *C. rodentium* confirming that pEtN modifications have little impact on PMB resistance in *C. rodentium*. In contrast, we observed that the Δ*pmrAB*, Δ*pmrC*Δ*cptA* and Δ*pmrC* strains had increased sensitivity to hydrophobic antibiotics compared to the wild-type strain. These are antibiotics that must diffuse through the OM LPS barrier to gain access to inside the cell. This phenotype was later attributed to a loss of OM integrity in these strains. Interestingly, both pWSK-*pmrC* and pWSK-*cptA* complementation restored OM integrity in the Δ*pmrC*Δ*cptA* strain, indicating that pEtN modifications have a role in maintenance of OM integrity.

The second objective was to determine the molecular mechanism by which pEtN modifications promote OM integrity. We used a Δ*waaL* background to specifically monitor lipid A-core biosynthesis in the presence of iron, as O-antigen is synthesized via a separate pathway. Thus, the Δ*waaL* and Δ*waaL*Δ*pmrC*Δ*cptA* strains were grown in the presence of increasing concentrations of iron (0, 25, 50 and 100 µM $FeSO_4$) and LPS was extracted from whole-cell lysates of these strains. By anti-KDO immunoblot, it was shown that the Δ*waaL*Δ*pmrC*Δ*cptA* strain demonstrated altered LPS turnover compared to the Δ*waaL* strain under these growth

conditions. It was then determined that the Δ*waaL*Δ*pmrC*Δ*cptA* strain accumulated free lipid A compared to the Δ*waaL* strain as revealed by anti-lipid A immunoblot, suggesting that lipid A turnover, in response to iron, is defective in this strain. Additionally, it was demonstrated that overexpression of LpxC under an arabinose inducible promoter in the Δ*waaL* strain accumulated free lipid A in the presence of high arabinose concentrations, suggesting that the increased lipid A content observed in the Δ*waaL*Δ*pmrC*Δ*cptA* strain may be LpxC-dependent, due the effect of Fe^{2+} on the catalytic activity of this enzyme. It was later confirmed that *pmrC* and *cptA* expression in the Δ*waaL*Δ*pmrC*Δ*cptA* strain decreased free lipid A levels, indicating that pEtN modifications are involved in lipid A turnover. By performing sucrose density gradient centrifugation, the Δ*waaL*Δ*pmrC*Δ*cptA* strain accumulated lipid A-core species throughout its cell envelope under this condition, it was then determined that *pmrC* and *cptA* expression in the Δ*waaL*Δ*pmrC*Δ*cptA* strain promoted transfer of lipid A-core species from the IM to the OM. Finally, it was determined that the response to iron, which is both LpxC-dependent and PmrAB-dependent, resulted in an iron concentration-dependent increase in resistance to novobiocin, a hydrophobic antibiotic, for the Δ*waaL* strain. The Δ*waaL*Δ*pmrC*Δ*cptA* strain failed to grow in a medium containing 50 µM iron or more with novobiocin, highlighting the role PmrC- and CptA-mediated pEtN LPS modifications in reinforcing the OM barrier in response to iron in the growth medium by promoting LPS turnover and transfer to the OM.

The third objective was to determine whether iron influences OM vesiculation in *C. rodentium*. First, vesicles were collected from a *C. rodentium* Δ*waaL* strain grown in minimal media supplemented with increasing iron concentrations (0, 25, 50 and 100 µM $FeSO_4$) and it was determined that OM vesicle release is an iron-dependent mechanism as determined by the increased concentration of the OM protease CroP in the vesicular membranes, most probably due

to the increase LPS content at the OM as a consequence to the response to iron, which leads to vesiculation. Interestingly, it was shown that Δ*waaL*-derived OMVs were more bactericidal against the Δ*waaL*Δ*pmrC*Δ*cptA* strain than against the Δ*waaL* strain. This result suggested that PmrC and CptA are involved in conferring protection against OMVs, as their production is induced by the response to iron.

Altogether, we have unveiled novel roles for PmrAB-regulated pEtN LPS modifications in both LPS transfer from the IM to the OM and OM vesiculation, respectively. We are confident that this information can be helpful in combatting the issue of multi-drug resistant Gram-negative pathogens by understanding how they synthesize their OM and produce OMVs.

PREFACE TO CHAPTER 2

Chapter 2 will look at how at the relationship between pEtN modifications and OM integrity under PmrAB-inducing conditions, which is the presence of micromolar concentrations of iron. Lack of these modifications results in a number of phenotypes. Here, we show that PmrAB-regulated pEtN modification have a direct effect in maintaining OM integrity under PmrAB-inducing conditions.

Chapter 2:

Absence of PmrAB-mediated Phosphoethanolamine Modifications of *Citrobacter rodentium* Lipopolysaccharide Affects Outer Membrane Integrity

Charles Viau[1], Valerie Le Sage[1], Daniel K. Ting[1], Jeremy Gross[1] and Hervé Le Moual[1, 2 *]

[1]*Department of Microbiology and Immunology and* [2]*Faculty of Dentistry,*

McGill University, Montreal, QC, H3A 2B4, Canada

Running title: *Phosphoethanolamine LPS modifications in Citrobacter rodentium*

Keywords: Outer membrane, PmrAB, phosphoethanolamine, lipopolysaccharide, *Citrobacter rodentium*

J Bacteriol. 2011 May;193 (9):2168-76. doi: 10.1128/JB.01449-10.

2.1 ABSTRACT

The PmrAB two-component system of enterobacteria regulates a number of genes whose protein products modify lipopolysaccharide (LPS). The LPS is modified during transport to the bacterial outer membrane (OM). A subset of PmrAB-mediated LPS modifications consists of the addition of phosphoethanolamine (pEtN) to lipid A by PmrC and to the core by CptA. In *Salmonella enterica*, pEtN modifications have been associated with resistance to polymyxin B and to excess iron. To investigate putative functions of pEtN modifications in *Citrobacter rodentium*, Δ*pmrAB*, Δ*pmrC*, Δ*cptA* and Δ*pmrC*Δ*cptA* deletion mutants were constructed. Compared to wild-type, most mutant strains were found to be more susceptible to antibiotics that must diffuse across the LPS layer of the OM. All mutant strains also showed increased influx rates of ethidium dye across their OM, suggesting that PmrAB-regulated pEtN modifications affect OM permeability. This was confirmed by increased partition of the fluorescent dye 1-*N*-phenylnaphthylamine (NPN) into the OM phospholipid layer of the mutant strains. In addition, substantial release of periplasmic β-lactamase was observed for the Δ*pmrAB* and Δ*pmrC*Δ*cptA* strains, indicating loss of OM integrity. This study attributes a new role for PmrAB-mediated pEtN LPS modifications in the maintenance of *C. rodentium* OM integrity.

2.2 INTRODUCTION

The outer membrane (OM) of Gram–negative bacteria is asymmetric with lipopolysaccharide (LPS) forming the outer leaflet [96]. The LPS layer functions as a permeability barrier to antibacterial compounds including lipophilic antibiotics and host antimicrobial peptides (AMPs). Lipophilic antibiotics must cross the OM by diffusion through the LPS layer. AMPs are typically too large to diffuse through porin channels (MW cutoff < 600 Da), they penetrate the OM by perturbing the lateral interactions between neighboring LPS molecules mediated by divalent Mg^{2+} and Ca^{2+} cations. Limiting concentrations of these cations undermine the OM permeability barrier to the action of AMPs and lipophilic antibiotics [24]. Enterobacteria have developed an adaptive response for remodeling the OM by modifying LPS. In response to various environmental signals, the PhoPQ and PmrAB two-component systems (TCS) control these LPS modifications at the transcriptional level [140-142]. LPS modifications decrease OM permeability by adding palmitate to lipid A (*pagP* gene) [95]. They also neutralize negative charges of LPS by adding 4-aminoarabinose (*arn* operon) or phosphoethanolamine (pEtN) (*pmrC* and *cptA* genes) to specific phosphate groups [95, 143]. Early studies have highlighted an association between PmrAB-mediated modifications of LPS and increased resistance of *Salmonella enterica* to the AMP polymyxin B (PMB) [144, 145]. Later studies showed that PmrAB-mediated LPS modifications also have a role in the survival of *S. enterica* to excess iron [71, 146]. In *S. enterica*, the PhoPQ TCS controls the PmrAB TCS and the RcsBCD phosphorelay system [147, 148]. PhoPQ controls PmrAB signaling by promoting expression of the PmrD protein that binds the response regulator PmrA and prevents its dephosphorylation, resulting in sustained activation of PmrA-regulated genes [79, 149].

The extracellular enteric pathogen *Citrobacter rodentium* causes transmissible colonic hyperplasia in mice [150]. *C. rodentium* has similar virulence factors to enteropathogenic *Escherichia coli* (EPEC) and enterohaemorrhagic *E. coli* (EHEC) making it an excellent model organism for the study of these human pathogens. Sequencing of the *C. rodentium* genome revealed striking differences with *S. enterica* [151]. For example, *C. rodentium* does not appear to have the *pmrD* gene, suggesting that PhoPQ does not control PmrA-regulated genes, as observed previously in *Yersinia pestis* [152]. In addition, the PmrA-regulated *arn* operon (also known as *pmrHFIJKLM* operon) is also absent from the *C. rodentium* genome. The *arn* operon is responsible for the addition of 4-aminoarabinose to lipid A, a modification that is central to PMB resistance [85]. These observations are consistent with the fact that *C. rodentium* Δ*phoPQ* does not have increased susceptibility to PMB compared to wild-type [153]. Among the other LPS modifying PmrA-regulated genes, *C. rodentium* possesses the *pmrC* and *cptA* homologues. The *pmrC* and *cptA* genes encode pEtN transferases responsible for mediating the addition of pEtN to the 1' and 4' phosphates of lipid A and to the phosphate of heptose-I found in the LPS core, respectively [95, 143]. Addition of pEtN to lipid A or the LPS core has been shown to have a modest effect on PMB resistance [154-156]. Recently, it was shown that the single pEtN transferase of *Campylobacter jejuni* adds pEtN to both lipid A and the flagellar rod protein FlgG, affecting bacterial motility [157]. This study indicated that pEtN modifications may have other roles.

C. rodentium does not have the ability to modify LPS with 4-aminoarabinose, which interferes with the addition of pEtN to the 4' phosphate of lipid A in *S. enterica* [139]. Therefore, *C. rodentium* is an organism of choice to study the biological function of pEtN modifications. In this study, the objective was to characterize *C. rodentium* deletion mutants of *pmrAB*, *pmrC* and *cptA*. We found that the absence of PmrAB-mediated pEtN modifications of LPS increases OM

permeability to lipophilic compounds and affects OM integrity, highlighting a new role for pEtN modifications.

2.3 MATERIALS AND METHODS

Media and reagents. Bacteria were grown at 37°C with aeration in Luria-Bertani (LB) broth, trypticase soy broth (TSB), or N-minimal medium (pH 7.5) containing 0.2% glucose and supplemented with $MgCl_2$ and $FeSO_4$, as indicated. When appropriate, media were supplemented with chloramphenicol (30 μg/ml) or kanamycin (50 μg/ml). Polymyxin B (PMB), cephalothin, norfloxacin, erythromycin, novobiocin, vancomycin, ethidium bromide (EtBr), 1-*N*-phenylnaphthylamine (NPN) and carbonyl cyanide *meta*-chlorophenylhydrazone (CCCP) were purchased from Sigma. Nitrocefin was from EMD Chemicals. Restriction enzymes and *Pfx* DNA polymerase were from New England Biolabs and Invitrogen, respectively.

Construction of *C. rodentium* deletion mutants. The bacterial strains and plasmids used in this study are listed in Table 1. DNA purification, cloning, and transformation were performed according to standard procedures [158]. The *C. rodentium* Δ*pmrAB*, Δ*pmrC*, Δ*cptA*, Δ*pmrC*Δ*cptA* and Δ*phoPQ*Δ*pmrAB* deletion mutants were generated by *sacB* gene-based allelic exchange [159]. The upstream and downstream sequences of the *cptA*, *pmrC*, and *pmrAB* genes were PCR-amplified from *C. rodentium* genomic DNA using the primers listed in Table 2.1. PCR fragments were gel-purified, digested with the appropriate restriction enzymes (Table 2.1) and ligated into pRE112 cleaved with XbaI and SacI. Resulting plasmids were verified by sequencing, transformed into the *E. coli* χ7213 donor strain and conjugated into the appropriate *C. rodentium* strain. Chromosomal plasmid insertion was selected for by culturing on LB agar supplemented with chloramphenicol. Selected clones were cultured on peptone agar containing 5% sucrose to isolate colonies that were sucrose-resistant. These resulting colonies were also tested for chloramphenicol

sensitivity. Gene deletions were verified by PCR. Plasmids used for complementation were constructed by PCR-amplifying the genes of interest with their promoters from *C. rodentium* genomic DNA using the primers listed in Table 2.1 (*pmrAB*, CR677 and CR680; *pmrC*, CR694 and CR697 and *cptA*, CR756 and CR757). The resulting PCR products were cloned into the XbaI and BamHI or XbaI and SacI restriction sites of plasmid pWSK129, generating plasmids pWSK*pmrAB*, pWSK*pmrC* and pWSK*cptA*. In pWSK*pmrAB, pmrAB* was under control of the constitutive promoter located at the 3' end of the *pmrC* coding region [160].

Construction of chromosomal *lacZ* transcriptional fusions and β-galactosidase assay. The *pmrC* or *cptA* promoters were PCR-amplified using the primers listed in Table 2.1. The PCR-fragments were digested with XbaI and SmaI and ligated upstream of the *lacZ* gene of the suicide vector pFUSE [161]. The resulting constructs were transformed into *E. coli* χ7213, conjugated into the *C. rodentium* wild-type, Δ*phoPQ* and Δ*pmrAB* strains, and selected for by culturing on LB agar supplemented with chloramphenicol. Insertion of the suicide vector was verified by sequencing. β-galactosidase activity assays were performed in triplicate at least three times, as previously described [162].

MIC determination. Minimum inhibitory concentrations (MIC) were determined in 96-well microtiter plates using the broth microdilution method [163]. Briefly, bacterial cultures were grown in TSB, diluted to 5×10^5 CFU/ml in N-minimal medium supplemented with 10 μM $MgCl_2$ and 25 μM $FeSO_4$ and aliquoted into rows of wells. Two-fold serial dilutions of the tested

TABLE 2.0 Bacterial strains and plasmids used in this study

Strain or plasmid	Description	Source or reference
C. rodentium strain		
DBS100	Wild-type *C. rodentium strain* (ATCC51459)	[150]
Δ*phoPQ*	DBS100 Δ*phoPQ*	[153]
Δ*pmrAB*	DBS100 Δ*pmrAB*	This study
Δ*pmrC*	DBS100 Δ*pmrC*	This study
Δ*cptA*	DBS100 Δ*cptA*	This study
Δ*pmrC*Δ*cptA*	DBS100 Δ*pmrC*Δ*cptA*	This study
Δ*phoPQ*Δ*pmrAB*	DBS100 Δ*phoPQ*Δ*pmrAB*	This study
DBS100 *pmrC*::*lacZ*	*pmrC*::*lacZ* in DBS100, Cm^r	This study
Δ*phoPQ pmrC*::*lacZ*	*pmrC*::*lacZ* in Δ*phoPQ* , Cm^r	This study
Δ*pmrAB pmrC*::*lacZ*	*pmrC*::*lacZ* in Δ*pmrAB*, Cm^r	This study
DBS100 *cptA*::*lacZ*	*cptA*::*lacZ* in DBS100, Cm^r	This study
Δ*phoPQ cptA*::*lacZ*	*cptA*::*lacZ* in Δ*phoPQ*, Cm^r	This study
Δ*pmrAB cptA*::*lacZ*	*cptA*::*lacZ* in Δ*pmrAB*, Cm^r	This study
E. coli strain		
χ7213	*thr-1 leuB6 fhuA21 lacY1 glnV44 recA1 asdA4 thi-1* RP4-2-Tc::Mu [*-pir*], Kan^r	[164]
Plasmids		
pRE112	Sucrose sensitive (*sacB*1) suicide vector, Cm^r	[165]

pFUSE	Suicide vector, *lacZYA*, mob^{+} (RP4), ori R6K, Cm^{r}	[161]
pWSK129	Low-copy number cloning vector, Kan^{r}	[166]
pWSK*pmrAB*		This study
pWSK*pmrC*		This study
pWSK*cptA*		This study

TABLE 2.1 Primers used in this study [a]

Primer	Sequence	Usage
CR677	AGCTAGTCTAGATGTTCTCCGGAATGCCACGCAAGC	Δ*pmrAB* 5′F XbaI
CR678	AGCTAGGATATCGGTGTCGCGGGCGGTCAGGATCAG	Δ*pmrAB* 5′R EcoRV
CR679	AGCTAGGATATCGCGGTGATGGGAGTTGAGGATCAG	Δ*pmrAB* 3′F EcoRV
CR680	AGCTAGGAGCTCTTTCGCCGGTCTGCTGATGCTGGC	Δ*pmrAB* 3′R SacI
CR694	GACTAGTCTAGACCAGCAGAATCAGGCCGATAG	Δ*pmrC* 5′F XbaI
CR695	AGCCATGATATCACGGCGTAAATGCGGACTCG	Δ*pmrC* 5′R EcoRV
CR696	AGCTAGGATATCCAGCGGCATCGACAGAAAGAC	Δ*pmrC* 3′F EcoRV
CR697	CAGTGAGAGCTCCCGCTACATTCCAGAAGCCCT	Δ*pmrC* 3′R SacI
CR719	TGACATCTAGAGGAGCTGGGCAAACTACCGCTC	Δ*cptA* 5′F XbaI
CR734	TGCAGGTACCGCTAAATGCGGACGCGGGCTGG	Δ*cptA* 5′R KpnI
CR735	GGTGGGTACCTGCGCTGATTGATTATGACACTCTG	Δ*cptA* 3′F KpnI
CR722	GGCGGAGCTCTCAGGTCGTAGCCCTTCAGCAAC	Δ*cptA* 3′R SacI

CR555	AGCTAGTCTAGAGATCTTAGCCCAGCTTTCGCAGTATCCGGTCTCC	*pmrC::lacZ* 5'F XbaI
CR554	AGCTACCCCGGGAAACCAGCAGCAGCCAGGCGAGCAGTCTGAG	*pmrC::lacZ* 3'R SmaI
CR774	AGCTAGTCTAGAATGCTGGAAATGGTCTTCGCCAAAG	*cptA::lacZ* 5'F XbaI
CR775	AGCTACCCCGGGGCTAAATGCGGACGCGGGCTGG	*cptA::lacZ* 3'R SmaI
CR756	GGTATCTACAGAAATGGTCTTCGCCAAAGCGGAT	pWSK*cptA* 5' XbaI
CR757	GCCAGAGCTCGATGTCCTCAAGTGATTATTGCCGG	pWSK*cptA* 3' SacI

[a] Restriction sites are underlined

antimicrobial compound were added to each row of wells. The plates were incubated at 37°C for 24 h. The lowest concentration of the antimicrobial compound that did not permit any visible growth was determined to be the MIC. Determination of MIC values was repeated, at least three times, until no variation was observed between replicates.

OM permeability assays. N-minimal media supplemented with 1 mM $MgCl_2$ were inoculated (1:80) with LB-grown overnight cultures of the various *C. rodentium* strains. Cultures were grown until an optical density at 600 nm (OD_{600}) of 0.7-0.8. Cells were washed with phosphate-buffered saline (PBS) and resuspended in N-minimal media supplemented with 10 μM $MgCl_2$ and 25 μM $FeSO_4$. At an OD_{600} of ≈1.3, cells were harvested by centrifugation and diluted in PBS to an OD_{600} of 0.4. The assay measuring ethidium influx rates was performed as previously described [167]. Briefly, cells (3 ml) were added to a quartz cuvette with stirring and incubated with 50 μM CCCP for 10 min to inactivate efflux pumps. EtBr was added to these bacterial suspensions at a final concentration of 4 μM. The fluorescence generated from the binding of ethidium to DNA was measured using a Varian Eclipse spectrofluorometer with excitation and emission wavelengths of 545 and 600 nm, respectively. Slit widths were 5 and 10 nm, respectively. The assay monitoring partition of NPN into membrane phospholipids was carried out as described elsewhere [168]. NPN was added at a final concentration of 5 μM to bacteria resuspended in PBS (3 ml). Fluorescence generated by NPN partition into phospholipids was measured as described above with an excitation wavelength of 350 nm, an emission wavelength of 420 nm and slit widths set at 5 nm.

β-lactamase leakage assay. Bacterial cultures were grown as described in the OM permeability assays section. Release of the chromosomally encoded *C. rodentium* β-lactamase (ROD_12321, M.W. 32 kDa) from the periplasm to the supernatant was compared between the various *C. rodentium* strains to assess OM integrity. The chromogenic β-lactam nitrocefin was used as a substrate [169]. In brief, the released β-lactamase fractions were isolated by collecting the supernatant of 1 ml-culture aliquots. The periplasmic β-lactamase fractions were obtained by osmotic lysis of the remaining cells, using the protocol supplied with the Epicentre periplasting kit. Enzymatic assays were performed at 22°C in N-minimal medium and β-lactamase activity was monitored by measuring the absorbance at 482 nm for 30 min using a Powerwave X340 microplate reader (Bio-Tek Instruments). Slopes of OD_{482} as a function of time were calculated to determine β-lactamase activities in both the released and periplasmic fractions [169]. Percentages of β-lactamase released into the culture supernatants were calculated by determining the ratio of β-lactamase activity in the supernatant to total β-lactamase activity (released and periplasmic fractions). Each strain was assayed in triplicates in multiple experiments.

2.4 RESULTS

Transcription of *C. rodentium pmrC* and *cptA* is regulated by PmrAB independently of PhoPQ. The PhoP-regulated *pmrD* gene that connects the *S. enterica* PhoPQ and PmrAB signaling pathways is absent from the *C. rodentium* genome [151]. The *C. rodentium pmrC* and *cptA* promoters contain PmrA-binding sites found in the same context as those described for *S. enterica* [170, 171]. To examine whether expression of *C. rodentium pmrC* and *cptA* is under the control of PmrAB, chromosomal β-galactosidase fusions with the *pmrC* and *cptA* genes were constructed in the wild-type, Δ*phoPQ* and Δ*pmrAB C. rodentium* strains. The *lacZ* reporter strains were grown under PhoPQ- and PmrAB-inducing conditions (10 μM $MgCl_2$ and 25 μM $FeSO_4$). The β-galactosidase activities of the *pmrC*::*lacZ* reporter in the wild-type and Δ*phoPQ* strains were very similar (Fig. 2.0, A). In contrast, expression from the *pmrC*::*lacZ* reporter was not observed in the Δ*pmrAB* strain, indicating that *pmrC* is regulated by PmrAB in *C. rodentium*. Similar results were obtained by using $FeCl_3$ or mild acidic pH (pH 5.5) as PmrAB-inducing conditions (data not shown). Expression from the *cptA*::*lacZ* reporter fusion was marginally affected in the Δ*phoPQ* strain and decreased by 3-fold in the Δ*pmrAB* strain, indicating that *C. rodentium cptA* is at least partly regulated by PmrAB (Fig. 2.0, B). The residual expression from the *cptA* promoter in the Δ*pmrAB* strain suggests that other transcriptional factors regulate *cptA* expression (Fig. 2.0, B). Transcriptional regulation of *C. rodentium pmrC* and *cptA* by PmrAB was further validated by measuring the expression of both reporter fusions in the presence of increasing concentrations of $FeSO_4$ (Fig. 2.0, C). Altogether, these data confirm that PmrAB regulates expression of the *C. rodentium pmrC* and *cptA* genes, as reported previously for *S. enterica* [170, 171]. They also indicate that expression of *pmrC* and *cptA* is independent of PhoPQ.

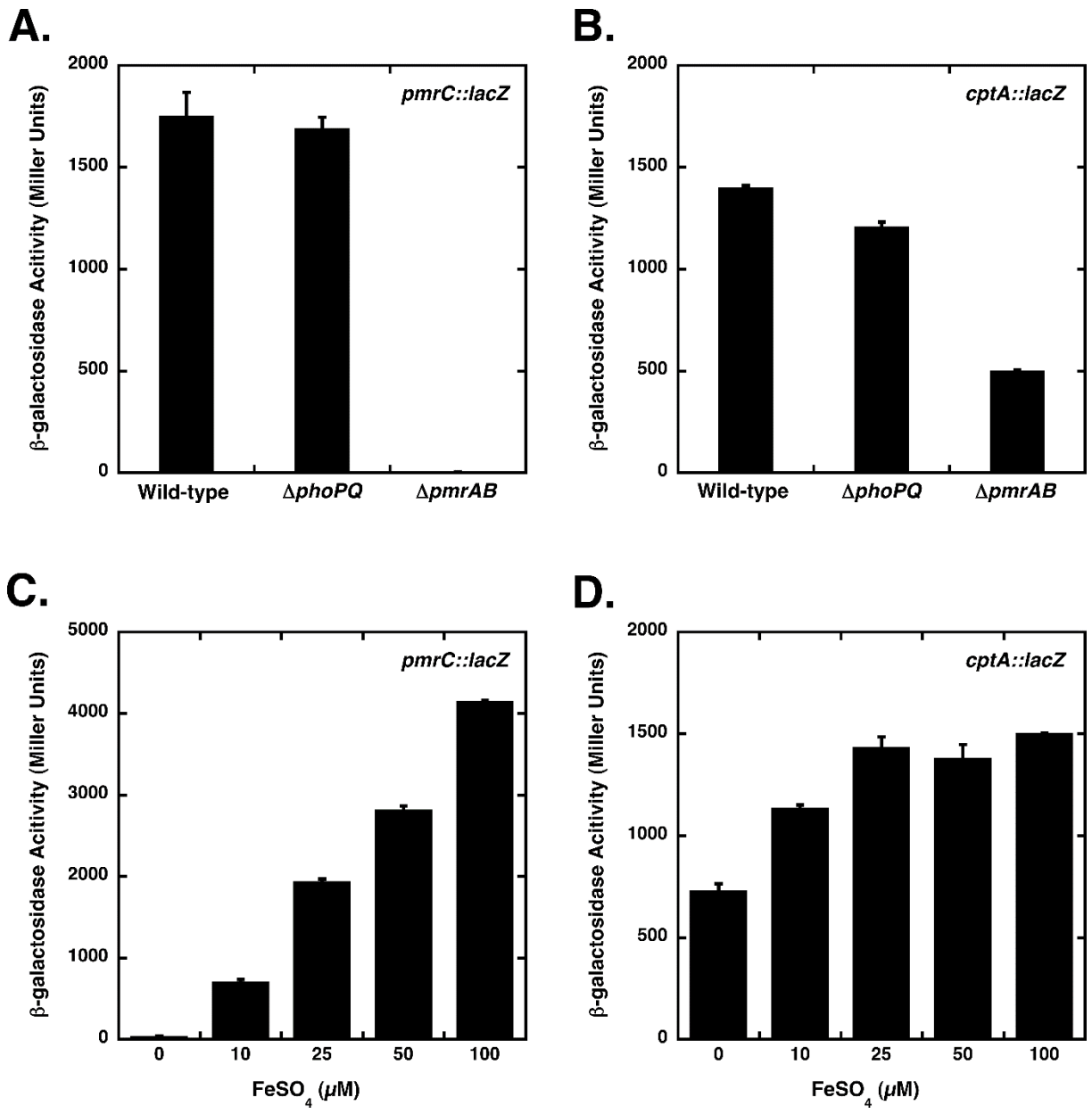

Figure 2.0: Expression of *C. rodentium pmrC* and *cptA* is regulated by PmrAB, independently of PhoPQ. (A) Expression of *pmrC* is strictly regulated by PmrAB. (B) Expression of *cptA* is primarily regulated by PmrAB. β-galactosidase activity from the *pmrC*::*lacZ* (C) and *cptA*::*lacZ* (D) reporter strains in the presence of increasing concentrations of $FeSO_4$. The various *pmrC*::*lacZ* or *cptA*::*lacZ* reporter strains were constructed as described in the Materials and Methods section. Strains were grown up to OD_{600} of 0.4 in N-minimal medium containing 1 mM $MgCl_2$, washed in PBS and resuspended in N-minimal medium supplemented with 10 μM $MgCl_2$ and $FeSO_4$, as indicated. After an additional 90-min incubation at 37°C, β-galactosidase activities were assayed using the $CHCl_3$-sodium dodecyl sulfate permeabilization procedure [162]. Values are means ± standard deviations of three independent experiments.

pEtN modifications protect *C. rodentium* from iron toxicity. PmrAB-regulated LPS modifications have been associated with resistance to excess iron in *S. enterica* [71, 146]. The susceptibility of the *C. rodentium* wild-type, Δ*pmrAB*, Δ*pmrC*, Δ*cptA* and Δ*pmrC*Δ*cptA* strains to $FeSO_4$ was assessed by determining MIC values. As shown in Table 2.2, all mutant strains were more susceptible to excess iron than wild-type. Compared to the wild-type strain, the Δ*cptA* and Δ*pmrC* strains exhibited 2- and 4-fold lower MIC values, respectively. The Δ*pmrC*Δ*cptA* and Δ*pmrAB* strains showed much higher susceptibility to iron with 8- and 16-fold lower MIC values, respectively. Complementation of the mutant strains with the pWSK129-derived pWSK*pmrAB*, pWSK*pmrC* and pWSK*cptA* plasmids restored resistance to iron above wild-type level (Table 2.2). Essentially similar data were obtained with $FeCl_3$ (data not shown). Altogether, the data indicate that pEtN transferases protect *C. rodentium* from excess iron and support previous observations in *S. enterica* [71, 146]. Due to the higher susceptibility of the mutant strains to excess iron, all subsequent experiments were performed in N-minimal medium supplemented with 25 µM of $FeSO_4$, a concentration of iron that induces expression of both *pmrC* and *cptA* (Fig. 2.0, C and D) without affecting growth or viability of the various strains as judged by OD_{600} measurements and survival assays (see Fig. S1 in the supplemental material).

pEtN modifications and PMB resistance. The role of *C. rodentium* PmrC and CptA in PMB resistance was assessed by determining MIC values. In N-minimal medium, MIC values of 2 µg/ml were obtained for all tested strains (Table 2.3). These results indicate that neither PmrC nor CptA is involved in resistance to PMB, at least under these experimental conditions. The data also suggest that no additional PmrAB-regulated *C. rodentium* genes play a role in PMB resistance. In

TABLE 2.2 MIC values of $FeSO_4$ for *C. rodentium* strains

	MIC (μM)
Strains	N-minimal medium [a]
Wild-type	1,600
Δ*pmrAB*	100
Δ*pmrC*	400
Δ*cptA*	800
Δ*pmrC*Δ*cptA*	200
Δ*pmrAB*-pWSK*pmrAB*	> 1,600
Δ*pmrC*-pWSK*pmrC*	> 1,600
Δ*cptA*-pWSK*cptA*	> 1,600

[a] N-minimal medium was supplemented with 10 μM $MgCl_2$.

Table 2.3 MIC values of PMB for *C. rodentium* strains

	MIC (μg/ml)	
Strain	N-minimal medium[a]	LB[b]
Wild-type	2	0.4
Δ*pmrAB*	2	0.2
Δ*pmrC*	2	0.2
Δ*cptA*	2	0.4
Δ*pmrC*Δ*cptA*	2	0.2
Δ*pmrAB*-pWSK*pmrAB*	2	0.4
Δ*pmrC*-pWSK*pmrC*	2	0.4
Δ*cptA*-pWSK*cptA*	2	0.4

[a] N-minimal medium was supplemented with 10 μM $MgCl_2$ and 25 μM $FeSO_4$.

[b] LB was supplemented with 500 μM $FeSO_4$.

LB broth, 2-fold decreases in MIC values were obtained for the Δ*pmrC*, Δ*pmrC*Δ*cptA* and Δ*pmrAB* strains (Table 2.3). These slight differences in MIC values are consistent with previous studies that reported the marginal involvement of *S. enterica* PmrAB-mediated pEtN modifications in PMB resistance [88, 156].

pEtN modifications confer resistance to lipophilic antibiotics. As both PmrC and CptA alter the structure of the LPS layer, susceptibility to different types of antibiotics was examined. Small hydrophilic antibiotics are known to diffuse across porins, whereas lipophilic antibiotics must diffuse across the asymmetrical bilayer of the OM [24]. MIC values were determined for the lipophilic antibiotics novobiocin and erythromycin (Table 2.4). Both the wild-type and Δ*cptA* strains were equally susceptible to novobiocin with MIC values of 16 µg/ml. The MIC for the Δ*pmrC* strain was decreased by 2-fold. In contrast, the MIC for the Δ*pmrC*Δc*ptA* strain showed an 8-fold decrease. Consistently, a 4-fold reduction in MIC value was obtained for the Δ*pmrAB* strain. Complementation of the Δ*pmrAB* and Δ*pmrC* strains with pWSK*pmrAB* and pWSK*pmrC*, respectively, restored the MIC values to wild-type level (16 µg/ml) or to a greater extent (32 µg/ml). Complementation of the Δ*cptA* strain with pWSK*cptA* did not have an observable effect on the MIC value. Interestingly, complementation of the Δ*pmrC*Δ*cptA* strain with pWSK*cptA* or pWSK*pmrC* increased the MIC values to 8 and 16 µg/ml, respectively. A similar trend was observed with erythromycin, with the fold changes being much higher. Erythromycin MIC values were decreased by 16 and 32-fold for the Δ*pmrC* and Δ*pmrC*Δ*cptA*, respectively. All complemented single mutant strains had their MIC values equal to the wild-type value. As for novobiocin, complementation of the Δ*pmrC*Δ*cptA* strain with pWSK*pmrC* more effectively restored resistance to erythromycin than when complemented with pWSK*cptA* (Table 2.4).

Altogether, the data indicate that PmrC-mediated addition of pEtN to LPS may have a preponderant role over the CptA-mediated modification in restricting access of lipophilic drugs across the OM. In addition, the data strongly suggest that modifications introduced by both PmrC and CptA act together to reinforce the LPS permeability barrier.

MIC values were also determined for the hydrophilic antibiotics cephalothin and norfloxacin [172]. For both antibiotics, MIC values for all strains were essentially similar and did not exhibit the susceptibility pattern observed for novobiocin and erythromycin (Table 2.4). Susceptibility to the hydrophilic antibiotic vancomycin, which is too large (M.W. 1450 Da) to diffuse through porins, was also examined. Obtained MIC values reflected the pattern of susceptibility observed for novobiocin and erythromycin (Table 2.4). This pattern of susceptibility was also obtained for SDS, a detergent that is used to assess OM integrity (Table 2.4). These data further support the possibility that pEtN modifications introduced by both PmrC and CptA are involved in the control of OM permeability and/or integrity.

pEtN modifications influence OM permeability to hydrophobic dyes. In *S. enterica*, the PhoPQ-mediated modifications of LPS have been shown to strengthen the OM permeability barrier [167, 173]. To determine the respective contributions of *C. rodentium* PhoPQ and PmrAB in controlling OM permeability, we compared the influx of EtBr into the wild-type, Δ*phoPQ*, Δ*pmrAB* and Δ*phoPQ*Δ*pmrAB* strains. In this assay, diffusion of ethidium across the OM was shown to be the rate-limiting step [167]. Ethidium influx rates were increased by 1.6-fold for the Δ*pmrAB* and Δ*phoPQ*Δ*pmrAB* strains compared to the wild-type strain (Fig. 2.1, A). In contrast, the influx rate for the Δ*phoPQ* strain was similar to the wild-type strain. These observations highlight the importance of the PmrAB TCS in regulating OM permeability in *C. rodentium*. They

TABLE 2.4 MIC values of lipophilic and hydrophilic antibiotics and SDS for *C. rodentium* strains

	MIC (μg/ml)					
Strain	Novobiocin	Erythromycin	Cephalotin	Norfloxacin	Vancomycin	SDS
Wild-type	16	1,024	32	0.008	4	62,500
Δ*pmrAB*	4	32	64	0.016	1	15,625
Δ*pmrC*	8	64	32	0.016	2	31,250
Δ*cptA*	16	1,024	32	0.008	4	62,500
Δ*cptA*Δ*pmrC*	2	32	64	0.008	1	15,625
Δ*pmrAB*-pWSK*pmrAB*	32	1,024	32	0.016	8	62,500
Δ*pmrC*-pWSK*pmrC*	32	1,024	32	0.016	4	62,500
Δ*cptA*-pWSK*cptA*	16	1,024	32	0.016	4	62,500
Δ*cptA*Δ*pmrC*-pWSK*pmrC*	16	1,024	32	0.016	4	62,500
Δ*cptA*Δ*pmrC*-pWSK*cptA*	8	128	32	0.016	2	31,250

are also consistent with the fact that transcriptional regulation of target genes by PmrAB is independent of PhoPQ in *C. rodentium* (Fig. 2.0). To assess whether the PmrC and CptA are involved in reinforcing the OM permeability barrier, influx of ethidium into the Δ*pmrC*, Δ*cptA* and Δ*pmrC*Δ*cptA* strains was monitored (Fig. 2.1, B). The Δ*pmrC*Δ*cptA* and Δ*pmrAB* mutants showed similar ethidium influx rates that were 1.5-fold higher than that of the wild-type strain. Influx rates for the Δ*pmrC* and Δ*cptA* strains were intermediate and consistently higher than that of wild-type. Ethidium influx rates for the complemented strains were either similar (Δ*cptA*-pWSK*cptA*) or slightly lower (Δ*pmrC*-pWSK*pmrC* and Δ*pmrAB*-pWSK*pmrAB*) than that of the wild-type strain (data not shown). These results indicate that both pEtN modifications are required for the strengthening of the OM barrier and support the possibility that PmrC and CptA act in concert in this process.

To further confirm these observations, the partition of the uncharged fluorescent probe NPN into the asymmetric bilayer of these strains was measured. Fluorescence of NPN is weak in aqueous environments but strong in the hydrophobic environment of disrupted membranes [168]. For the Δ*pmrC*Δ*cptA* and Δ*pmrAB* strains, the maximum fluorescence intensities of NPN were approximately 3-fold higher than that of the wild-type strain (Fig. 2.2, A). Fluorescence intensities for the Δ*pmrC* and Δ*cptA* strains were consistently higher than that of wild-type with Δ*pmrC* consistently higher than Δ*cptA* (Fig. 2.2, A). These results are in agreement with the ethidium influx assays (Fig. 2.1). To clarify the individual contributions of PmrC and CptA in reinforcing the OM barrier, the Δ*pmrC*Δ*cptA* strain was complemented with the pWSK*pmrC* or pWSK*cptA* plasmid and assayed for NPN partition (Fig. 2.2, B). In both cases, accumulation of NPN fluorescence was reduced to intermediate levels and complementation with pWSK*pmrC* consistently resulted in a larger reduction of fluorescence intensity (2.2-fold) than

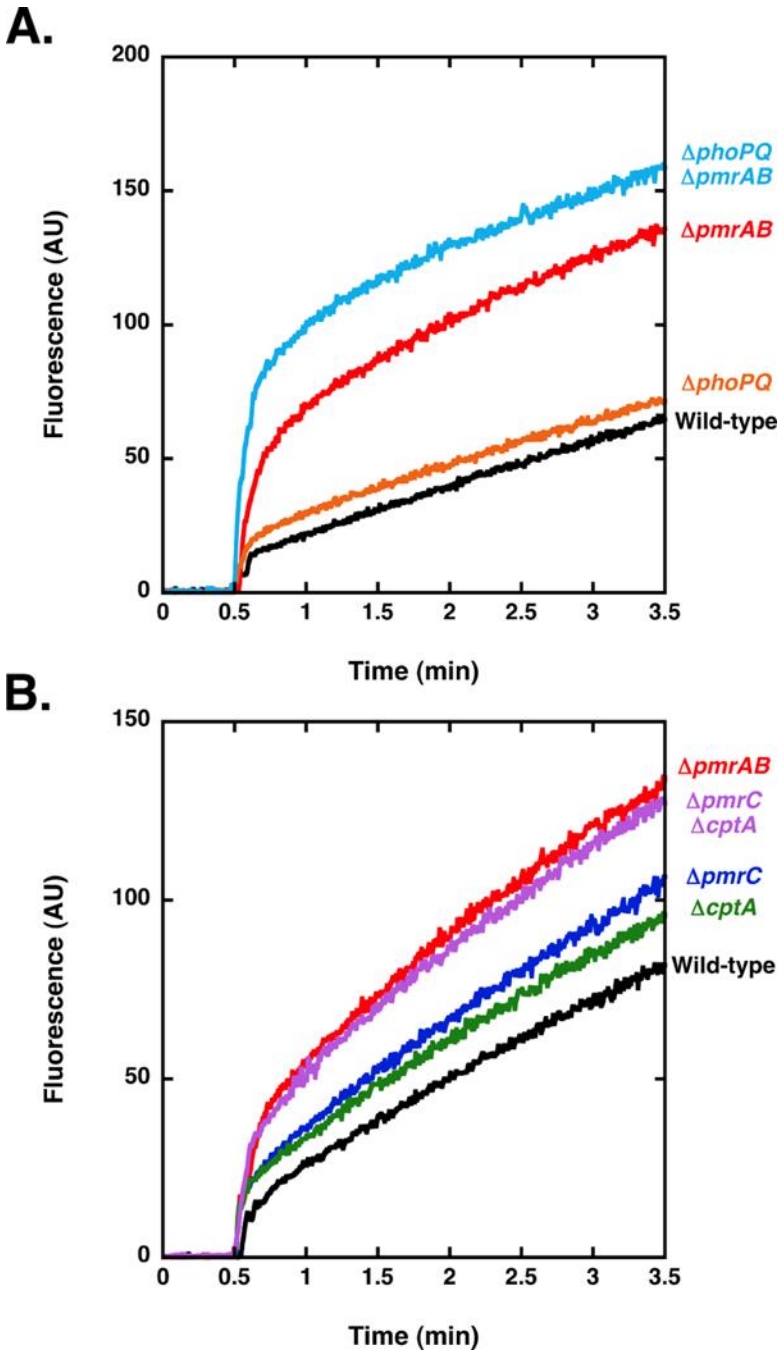

Figure 2.1: Ethidium influx into *C. rodentium* mutant strains. (A) Ethidium influx into the wild-type, Δ*phoPQ*, Δ*pmrAB* and Δ*phoPQ*Δ*pmrAB* strains. (B) Ethidium influx into the wild-type, Δ*pmrC*, Δ*cptA*, Δ*pmrC*Δ*cptA* and Δ*pmrAB* strains. Cells were grown as described under Materials and Methods. Cultures were diluted in PBS to an OD_{600} of 0.4, transferred to a quartz cuvette and stirred for the length of the experiment. EtBr was added at 0.5 min and the influx of ethidium was monitored over 3 minutes by measuring fluorescence emission at 600 nm. Ethidium influx rates were calculated from the linear portions of the curves (1-3.5 min). One representative experiment is shown of three independent experiments. AU, arbitrary units.

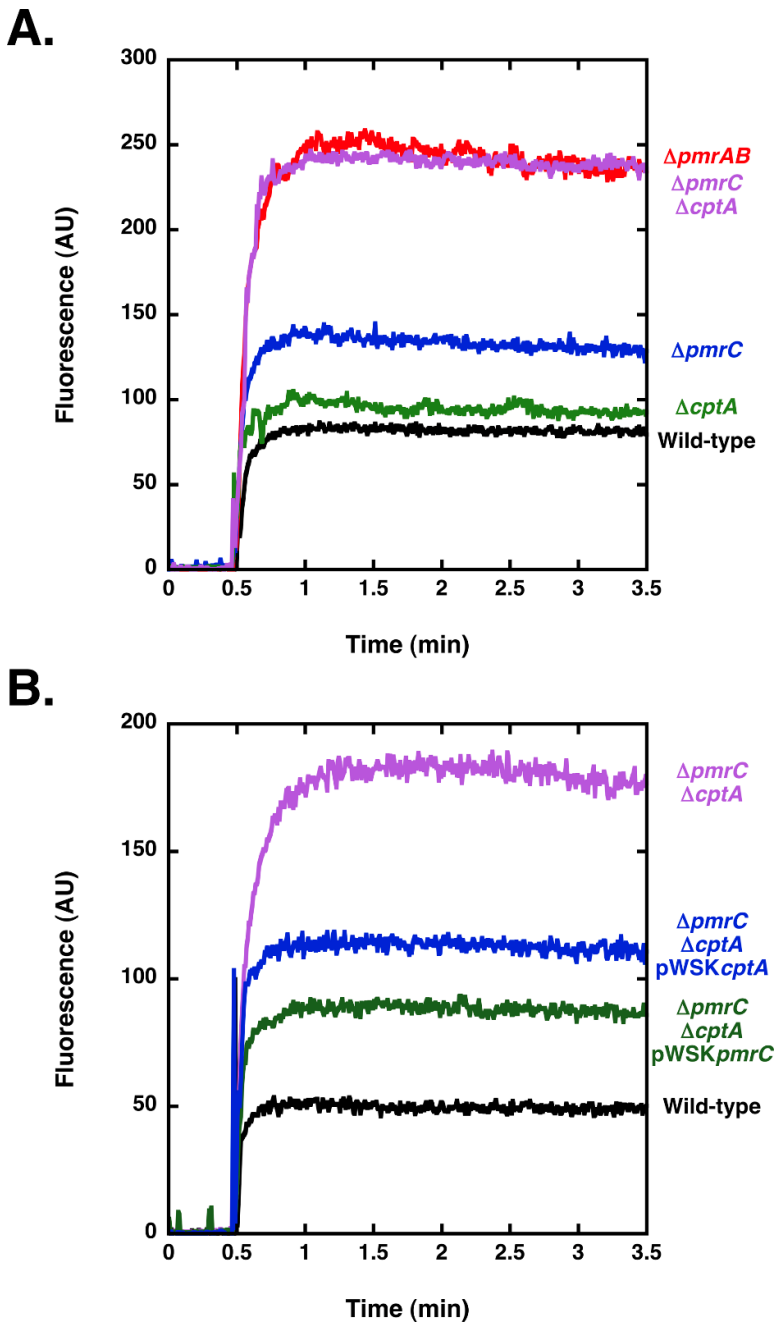

Figure 2.2: Partition of NPN into the OM of *C. rodentium* strains. (A) Change in the fluorescence due to the partitioning of NPN into the OM of the wild-type, Δ*pmrC*, Δ*cptA*, Δ*pmrC*Δ*cptA* and Δ*pmrAB* strains. (B) Change in the fluorescence due to the partitioning of NPN into the OM of the wild-type, Δ*pmrC*Δ*cptA*, Δ*pmrC*Δ*cptA*-pWSK*pmrC* and Δ*pmrC*Δ*cptA*-pWSK*cptA*. Bacterial cultures were grown as described under Materials and Methods, diluted in PBS to an OD_{600} of 0.4 and transferred to a quartz cuvette with stirring. NPN was added at 0.5 min and NPN partition was monitored by measuring fluorescence emission at 420 nm over 3 min. One representative experiment is shown of three independent experiments. AU, arbitrary units.

complementation with pWSK*cptA* (1.8- fold). These results show that both pEtN transferases are required to reach the wild-type level of OM impermeability. They also suggest that PmrC contributes to a larger extent than CptA to the strengthening of the OM barrier.

Lack of pEtN modifications affect OM integrity. To determine whether the weakened OM barrier observed in the absence of *pmrC* and *cptA* is due to strict increased permeability or loss of integrity, release of the endogenous *C. rodentium* β-lactamase into culture supernatants was assessed using the chromogenic substrate nitrocefin [169]. As shown in Fig. 2.3, minimal release of β-lactamase (2-3%) was obtained for the wild-type and Δ*cptA* strains. β-lactamase release was slightly higher (6%) for the Δ*pmrC* strain, although statistically insignificant. More dramatic leakage of β-lactamase (~22%) was measured for the Δ*pmrC*Δ*cptA* and Δ*pmrAB* strains, which represented a 10-fold increase compared to wild-type. These results clearly show that the lack of PmrAB-regulated pEtN transferases affects *C. rodentium* OM integrity. Complementation of the Δ*pmrC*Δ*cptA* strain with pWSK*pmrC* or pWSK*cptA* restored OM integrity to levels close to wild-type. However, analysis of LPS and OM protein profiles revealed that all *C. rodentium* strains exhibited a full-length LPS capped with *O*-polysaccharide and no difference in the amounts of the major OM porins (OmpA, OmpC and OmpF) (Fig. S2). Altogether, these data show that both PmrC and CptA-mediated pEtN modifications are involved in maintaining OM integrity. Furthermore, they support the observation that the PmrC and CptA pEtN transferases are both required and act together in this process.

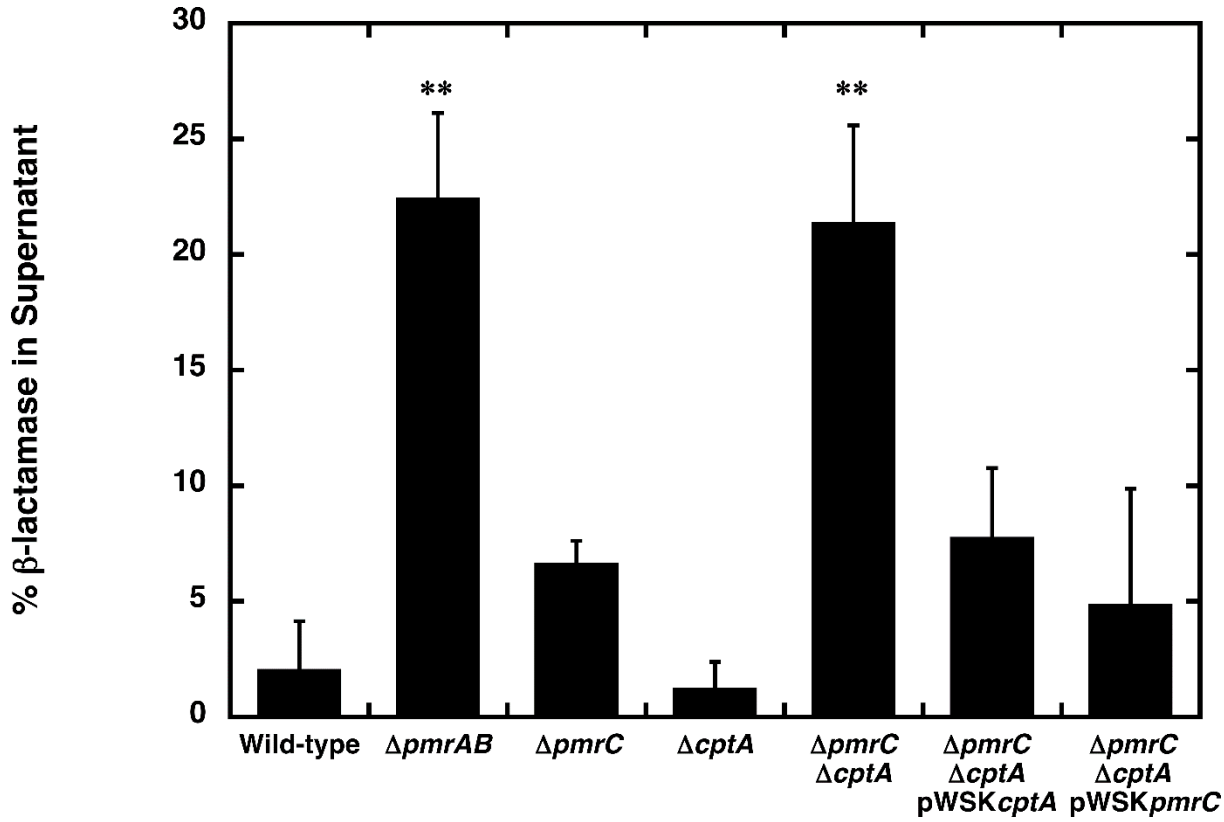

Figure 2.3: Absence of PmrAB-regulated pEtN transferases affects *C. rodentium* OM integrity. Cells were grown as described under Materials and Methods. Culture supernatant and periplasmic fractions from the various *C. rodentium* strains were assayed for β-lactamase activity using nitrocefin as a substrate. The cleavage of nitrocefin was monitored by measuring the absorbance at 482 nm over 30 min. The % of β-lactamase in the culture supernatant was calculated by determining the ratio of β-lactamase activity in the supernatant versus total β-lactamase activity in both fractions. For each strain, total β-lactamase activity was comparable. Values are means of three independent experiments ± standard deviations. **, Dunnett's test $P < 0.01$ compared to wild-type measurements.

2.5 DISCUSSION

The PmrAB-regulated modifications that consist of the addition of 4-aminoarabinose (*arn* operon) and pEtN (*pmrC* and *cptA*) to LPS have been associated with PMB resistance and survival in excess iron in enterobacteria [71, 85, 88, 156]. The *arn* operon, which is absent in *C. rodentium*, has been demonstrated to have a greater role in PMB resistance, compared to the pEtN transferases encoded by *pmrC* and *cptA* [88, 156]. Thus, the biological function of the pEtN transferases PmrC and CptA remains unclear. The fact that PmrC and CptA are required for maintaining OM integrity in *C. rodentium* is a novel finding. Several lines of evidence support this conclusion. First, the Δ*pmrC*, Δ*pmrC*Δ*cptA* and Δ*pmrAB* strains had increased susceptibility to antibiotics that must cross the OM by diffusing through the LPS layer (lipophilic antibiotics and vancomycin). These increases in susceptibility were not observed for hydrophilic antibiotics that pass through porins. Second, permeability of the OM to two different fluorescent dyes (EtBr and NPN) was increased for all mutant strains, most notably for Δ*pmrC*Δ*cptA* and Δ*pmrAB*. Third, β-lactamase release into culture supernatants revealed defects in OM integrity for the Δ*pmrC*Δ*cptA* and Δ*pmrAB* strains.

In MIC experiments, *C. rodentium* mutant strains showed hypersensitivity to ferrous ($FeSO_4$) and ferric ($FeCl_3$) iron, compared to the wild-type strain (Table 3). Our results showed sensitivity to $FeSO_4$ in the following order: Δ*pmrAB* > Δ*pmrC*Δ*cptA* > Δ*pmrC* > Δ*cptA* > wild-type. Restoration of MIC values above wild-type level was observed for the Δ*pmrC*-pWSK*pmrC* and Δ*cptA*-pWSK*cptA* complemented strains, confirming the involvement of both *C. rodentium* PmrC- and CptA-mediated pEtN modifications in resistance to excess iron. In contrast, neither PmrC nor CptA was found to promote *C. rodentium* resistance to PMB in N-minimal medium (Table 2.3). Consistently, complementation with *pmrC*, *cptA* or *pmrAB* from a low-copy number plasmid did not have an effect on PMB resistance under these conditions. However, the Δ*pmrC*,

Δ*pmrC*Δ*cptA* and Δ*pmrAB* strains showed a slight increase in susceptibility to PMB in LB (Table 2.3). These results are in agreement with previous studies that had shown a minor role for pEtN modifications in PMB resistance [88, 156].

Under PmrAB-inducing conditions, PmrC appeared to be more important than CptA in maintaining a robust OM permeability barrier. The Δ*pmrC* strain was consistently more susceptible than wild-type to both lipophilic antibiotics and vancomycin, whereas no change in MIC values was observed for the Δ*cptA* strain (Table 2.4). Although both the Δ*pmrC* and Δ*cptA* strains showed slight increases in OM permeability to EtBr and NPN compared to the wild-type strain, the Δ*pmrC* strain consistently exhibited slightly higher influx of ethidium and accumulation of NPN compared to the Δ*cptA* strain (Fig. 2.1 and 2.2). The greater effect of PmrC over CptA in contributing to the OM permeability barrier may be explained by differences in transcriptional regulation of the *pmrC* and *cptA* genes. β-galactosidase reporter assays showed that *pmrC* and *cptA* expression was upregulated 45- and 2-fold, respectively, in the presence of 25 μM $FeSO_4$ (Fig. 2.0, C and D). Interestingly, the deletion of either *pmrC* or *cptA* did not affect OM integrity, as shown by the insignificant difference in the amounts of β-lactamase released from the periplasm compared to wild-type (Fig. 2.3). In contrast, the Δ*pmrC*Δ*cptA* strain exhibited more dramatic OM defects in all assays, including a large release of β-lactamase indicative of a loss of OM integrity. These findings indicate that PmrC and CptA act together, possibly synergistically, to maintain the OM permeability barrier. This observation is supported by the fact that complementation of the Δ*pmrC*Δ*cptA* strain with either pWSK-*pmrC* or pWSK-*cptA* restored OM integrity although subtle OM permeability defects were still observed (Fig. 2.2, B and 2.3, Table 2.4). Essentially similar results were obtained for the Δ*pmrAB* and Δ*pmrC*Δ*cptA* strains, suggesting that no additional PmrAB-regulated gene is involved in maintaining *C. rodentium* OM integrity. Collectively, these

data show that lack of either *pmrC* or *cptA* leads to increased OM permeability, whereas lack of both pEtN transferases grossly affects the OM, resulting in a loss of integrity.

In a previous study, Chamnongpol *et al.* observed that a *S. enterica pmrA* mutant had increased uptake of vancomycin under PhoPQ- and PmrAB-inducing conditions [146]. This observation is in agreement with the finding that our *C. rodentium* Δ*pmrAB* strain is highly susceptible to lipophilic antibiotics and to vancomycin under similar growth conditions (Table 2.4). This may suggest that the OM strengthening attributed to pEtN transferases, observed in this study, is conserved among enterobacteria that possess the *pmrC* and *cptA* genes. This possibility could be tested by characterizing similar mutations in a *S. enterica* strain deficient in the *arn* operon. Loss of OM integrity that we observed for the Δ*pmrC*Δ*cptA* and Δ*pmrAB* strains has been reported for other gene mutations. For example, a mutation in the *S. enterica waaP* gene, encoding the kinase responsible for the phosphorylation of the core heptose-I, resulted in an unstable OM as well as increased susceptibility to lipophilic antibiotics [40]. Interestingly, both WaaP and CptA act on the same core sugar. Loss of OM integrity was also observed in mutants of the Tol-Pal complex, which serves as a structural link between the peptidoglycan layer and other cell wall components [174].

Finally, previous reports suggested the involvement of the *S. enterica* PmrAB TCS in producing a robust OM permeability barrier under Mg^{2+}-limiting conditions [167, 173]. Here, we have clearly shown the involvement of *C. rodentium* PmrAB in this process. In *S. enterica*, PmrAB is under the control of the PhoPQ TCS, which also regulates its own LPS modifying genes (*pagP*, *pagL* and *lpxO*). *C. rodentium* does not possess the *pagL* and *lpxO* homologues [151], the *pmrD* homologue that bridges the PhoPQ and PmrAB signaling pathways and a homologue to the *arn* operon. The lack of these homologues makes *C. rodentium* the appropriate model to study the

contribution of PmrAB-regulated pEtN transferases in strengthening the OM permeability barrier. The fact that *pagP* appears to be the sole *C. rodentium* LPS-modifying gene directly regulated by PhoPQ could explain the marginal contribution of this TCS to the production of a robust OM permeability barrier (Fig. 2.1, B). The contribution of 4-aminoarabinose modifications in OM strengthening is still unclear. Kawasaki and Manabe showed that a *S. enterica* mutant of *ugd* (*pmrE*), a gene involved in the early steps of 4-aminoarabinose biosynthesis, displayed OM permeability defects similar to a *pmrA* mutant strain [173]. This may suggest that modification of lipid A with 4-aminoarabinose also contributes to OM permeability in *S. enterica*. In conclusion, we have demonstrated that *C. rodentium pmrC* and *cptA* are the PmrAB-regulated genes responsible for maintaining a robust OM permeability barrier.

2.6 SUPPLEMENTARY FIGURES

2.6.1 Figure S1

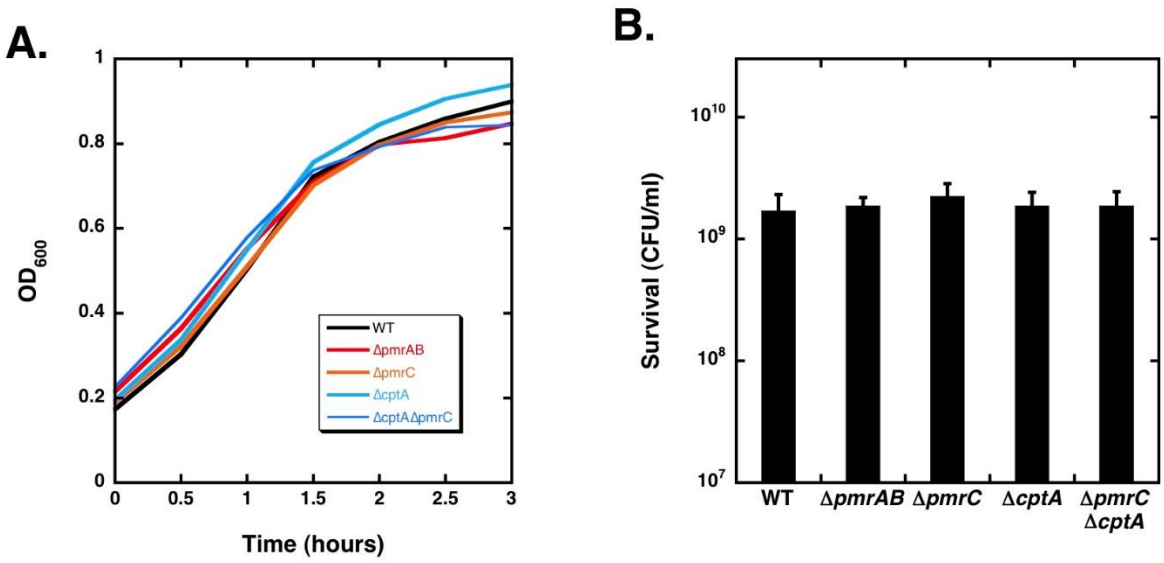

Figure S1: Growth curves and survival assays. (A) Growth curves for *C. rodentium* strains used in this study. Strains were initially grown up to an OD_{600nm} of 0.7-0.8 in N-minimal medium supplemented with 1 mM $MgCl_2$, washed and diluted to an OD_{600nm} of 0.2 in N-minimal medium containing 10 µM $MgCl_2$ and 25 µM $FeSO_4$. Strains were then grown for 3 hours. (B) Strains were initially grown up to an OD_{600nm} of 0.7-0.8 in N-minimal medium supplemented with 1 mM $MgCl_2$, washed and diluted to an OD_{600nm} of 0.7 in N-minimal medium containing 10 µM $MgCl_2$ and 25 µM $FeSO_4$. Strains were grown for 2 h, serially diluted in PBS and plated on LB agar. The CFU/mL values are representative of at least three independent experiments.

2.6.2 Figure S2

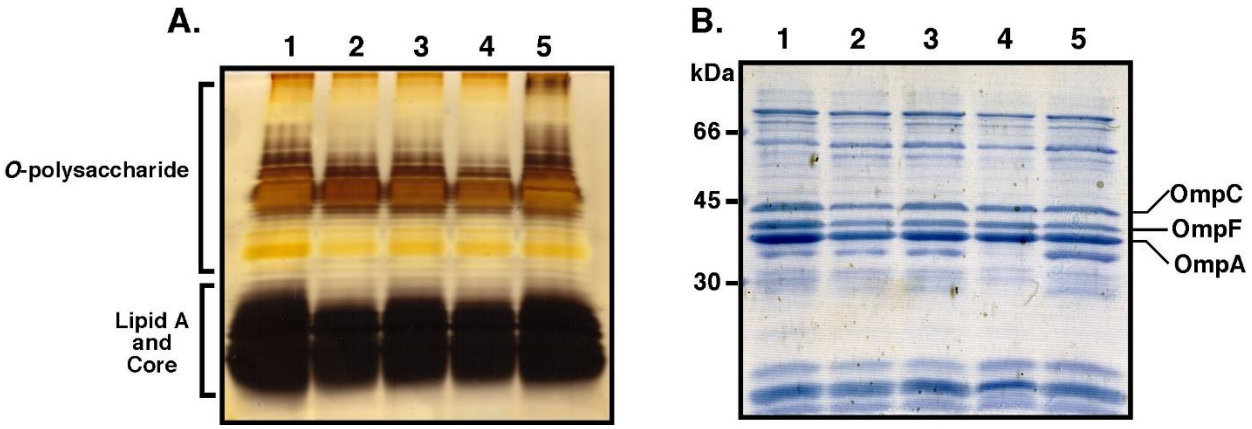

Figure S2: LPS and OMP profiles of strains used in this study. Lane 1, *C. rodentium* wild-type; lane 2, Δ*pmrAB*; lane 3, Δ*pmrC*; lane 4, Δ*cptA*; and lane 5, Δ*pmrC*Δ*cptA.* (A) Whole cell lysate LPS extracts. Strains were initially grown in N-minimal medium supplemented with 1 mM $MgCl_2$ up to an OD_{600nm} of 0.7-0.8, washed with PBS and resupended in N-minimal medium containing 10 µM $MgCl_2$ and 25 µM $FeSO_4$. Strains were grown until an OD_{600nm} of 1.3 before LPS was extracted. (B) OMP profiles. Strains were grown under the same conditions as for LPS analysis, except that a final OD_{600nm} of 2.0 was achieved before OMP extraction was performed.

2.7 ACKNOWLEDGEMENTS

This work was supported by the Canadian Institutes of Health Research (CIHR, MOP-15551) and the Natural Sciences and Engineering Research Council (NSERC, 217482). C.V. was supported by a studentship from the Fonds de la Recherche en Santé du Québec (FRSQ). D.K.T. was the recipient of an NSERC Undergraduate Student Research Award. We thank J.L. Thomassin and J. Brannon for critical reading of the manuscript.

PREFACE TO CHAPTER 3

Chapter 3 looks at the molecular mechanism behind PmrAB-regulated pEtN modification, iron and LPS turnover and how they relate to OM barrier fortification. Iron promotes both PmrAB signalling and increases the activity of LpxC, responsible for the committed step in lipid A biosynthesis, which suggests a link between the two processes. Here, we show that PmrAB-regulated pEtN modifications are involved in the promotion of LPS transfer to the OM, which is induced by iron.

Chapter 3:

PmrAB-regulated Phosphoethanolamine Modifications Promote Lipopolysaccharide Transfer to the Outer Membrane

Charles Viau and Hervé Le Moual*

Department of Microbiology and Immunology, Microbiome and Disease Tolerance Centre, and Faculty of Dentistry, McGill University, Montreal, QC, H3A 2B4, Canada

(IN PREPARATION)

3.1 ABSTRACT

Lipopolysaccharide (LPS) of Gram-negative bacteria is covalently modified in response to environmental changes. The addition of phoshosphoethanolamine (pEtN) to the lipid A and core oligosaccharide of LPS is mediated by PmrC and CptA, respectively. These modifications are controlled by the PmrAB two-component system that responds to micromolar concentrations of Fe^{3+}. In our previous study, these pEtN modifications were shown to be responsible for maintenance of outer membrane (OM) integrity in *Citrobacter rodentium* grown in the presence of iron. To investigate the mechanism by which the addition of pEtN to LPS maintains OM integrity, LPS biosynthesis and transfer of LPS to the OM of the *C. rodentium* Δ*waaL*, Δ*waaL*Δ*pmrC*Δ*cptA*, Δ*waaL*Δ*pmrC*Δ*cptA*/pWSK-*pmrC* and Δ*waaL*Δ*pmrC*Δ*cptA*/pWSK-*cptA* strains were analyzed. Rough strains were used to monitor the production of lipid A-core species, which is essential for LPS biosynthesis, as O-antigen is produced via a separate pathway and is not required for viability. Whole-cell lysate LPS preparations from Δ*waaL* and Δ*waaL*Δ*pmrC*Δ*cptA* strains grown in the presence of increasing iron concentrations showed that iron results in increased LPS biosynthesis. Interestingly, the Δ*waaL*Δ*pmrC*Δ*cptA* strain accumulated free lipid A [lipid A unligated to 3-deoxy-D-manno-octulosonic acid (KDO)]. A similar pattern was observed when LpxC, the enzyme responsible for the committed step in lipid A synthesis, was overexpressed in the Δ*waaL* strain grown in the absence of iron. These results suggest that iron enhances LpxC activity *in vivo*, which results in increased LPS biosynthesis. Plasmid complementation of the Δ*waaL*Δ*pmrC*Δ*cptA* strain with either *pmrC* or *cptA* resulted in decreased free lipid A contents when grown in the presence of iron, suggesting that LPS pEtN modifications are involved in lipid A turnover, and hence LPS turnover. Discontinuous sucrose gradient centrifugation performed with cell envelopes of strains grown in the presence of iron

revealed an accumulation of LPS throughout the cell envelope in the Δ*waaL*Δ*pmrC*Δ*cptA* strain compared to the Δ*waaL* strain. Complementation of this strain with *pmrC* and to a lesser extent *cptA* rescued this phenotype, indicating that pEtN modifications promote LPS transfer to the OM. In addition, the Δ*waaL* strain demonstrated increased resistance to the hydrophobic antibiotic novobiocin in an iron-dependent manner, whereas the Δ*waaL*Δ*pmrC*Δ*cptA* demonstrated increased susceptibility to novobiocin in the same manner, suggesting that the response to iron, which includes PmrAB induction and most probably an increase in LpxC activity, leads to the reinforcement of the OM permeability barrier. Our findings reveal a role for PmrC- and CptA-mediated pEtN modifications in promoting efficient transfer of LPS to the OM as part of the adaptive response to iron.

3.2 INTRODUCTION

The outer membrane (OM) of Gram-negative bacteria is an asymmetric bilayer consisting of an inner leaflet of phospholipids and an outer leaflet of lipopolysaccharide (LPS) [96]. The LPS layer serves as a permeability barrier to antimicrobial compounds such as detergents and antibiotics, which renders Gram-negative bacteria intrinsically more resistant to existing antimicrobial therapies than Gram-positive bacteria. LPS consists of a hydrophobic moiety, lipid A, covalently linked to a hydrophilic moiety, the core oligosaccharide [23]. In some Gram-negative species, the O-antigen is attached to the core oligosaccharide, making the LPS layer smooth as opposed to rough when the O-antigen is lacking in the LPS. LPS biosynthesis is initiated in the bacterial cytoplasm by the *lpx* genes and *waaA* that produce lipid A-KDO_2 [23]. The core oligosaccharide moiety is then ligated to lipid A-KDO_2 by the remaining *waa* gene products one core sugar at a time. Following flipping of lipid A-core by MsbA across the IM, the O-antigen, produced by the *rfb* gene cluster, is added to the lipid A-core precursor by the WaaL O-antigen ligase [23]. Then, LPS subunits are transferred to the OM by the lipopolysaccharide transport (*lpt*) trans-envelope complex, which consists of seven proteins (LptA-G) [41, 175].

Along its transit from the IM to the OM, LPS can be covalently modified in response to changing environmental conditions monitored by the two-component regulatory systems (TCS) PhoPQ, PmrAB and the Rcs phosphorelay system [38, 142, 176, 177]. Among the known modifications of LPS, phosphoethanolamine (pEtN) is added by pEtN transferases to phosphoryl residues resulting in the neutralization of the negative charges [95]. The pEtN transferases PmrC and CptA catalyze the addition of pEtN to the 1-, 4'-phosphate residues of lipid A and to the phosphate residue of the core heptose-I, respectively [95]. Expression of PmrC and CptA is regulated by the PmrAB TCS that is activated by micromolar concentrations of Fe^{3+}, Al^{3+} and

mildly acidic pH in *Salmonella enterica* [38, 142]. Initially, LPS pEtN modifications were associated with bacterial resistance to host cationic antimicrobial peptides. In recent years, a number of novel functions were attributed to pEtN modifications. In addition to LPS, pEtN transferases were also shown to modify specific proteins such as the *Campylobacter jejuni* flagellar protein FlgG and the *Nesseria gonorrhoeae* PilE type IV pilus protein during their transit through the periplasmic space [157, 178]. Remarkably, the sole pEtN transferase (EptC) of *C. jejuni* catalyzes the addition of pEtN to three different substrates: the flagellar protein FlgG, *N*-linked heptasaccharides that are attached to multiple proteins, and the lipid A and core domains of LPS [101, 102, 157]. In addition, pEtN modifications of LPS were shown to affect LPS recognition by the Toll-like receptor 4 (TLR4) and, in turn, modulate the host immune response [179]. These various roles played by pEtN modifications indicate that these modifications result in pleiotropic biological effects.

Citrobacter rodentium is a murine pathogen of the *Enterobacteriaceae* family that causes attaching and effacing lesions similar to those caused by enteropathogenic *Escherichia coli* (EPEC) and enterohemmorhagic *E. coli* (EHEC) in humans. *C. rodentium* possesses four pEtN transferases, including PmrC and CptA. In contrast to other species of the *Enterobacteriaceae* family, the *arn* operon that is responsible for the addition of 4-aminoarabinose to lipid A, a LPS modification that overlaps with PmrC-induced pEtN modifications, is absent from the *C. rodentium* genome [82]. *C. rodentium* PmrAB is also independent of PhoPQ signaling due to the absence of the PhoP-regulated gene encoding the PmrD connector protein [70]. Therefore, *C. rodentium* is an organism of choice to explore the function(s) of LPS pEtN modifications.

Although essential for bacterial growth, high concentrations of iron are toxic to bacteria due to the generation of Fe^{3+} through the Fenton reaction [180]. PmrAB-regulated pEtN

modifications are key components of the adaptive response to iron toxicity, as an *S. enterica pmrA* mutant was shown to accumulate more Fe^{3+} in its OM [76]. In a previous study, we showed that PmrC- and CptA-mediated pEtN modifications modulated OM permeability and were involved in the maintenance of OM integrity in the presence of iron [82]. These novel functions of pEtN modifications were illustrated by the facts that *C. rodentium* Δ*pmrC*Δ*cptA* and Δ*pmrAB* strains displayed higher susceptibility to hydrophobic antibiotics, accumulated higher amounts of fluorescent dyes and showed substantial release of β-lactamase from the periplasm compared to wild-type [82]. This study related the PmrAB-mediated adaptive response to environmental iron to the maintenance of OM integrity.

In this study, we first show that the presence of iron in the growth medium increases LPS biosynthesis in *C. rodentium*, most likely by enhancing LpxC activity, the enzyme responsible for the committed step of lipid A synthesis. We also demonstrate that PmrAB-regulated pEtN modifications promote the efficient transfer of LPS to the OM when iron is present at sublethal concentrations in the environment. Consequently, impaired transfer of LPS to the OM is responsible for the loss of OM integrity and, in turn, increased susceptibility to hydrophobic antibiotics. Hence, this report reveals novel functions of LPS pEtN modifications in the promotion of LPS transfer to the OM as part of the adaptive response to iron.

3.3 MATERIALS AND METHODS

Bacterial strains and growth conditions. Bacterial strains and plasmids used in this study are listed in Table 1. Bacteria were grown at 37°C with aeration in Luria- Bertani (LB) broth, or N-minimal medium (50 mM Bis-Tris, 5 mM KCl, 7.5 mM $(NH_4)_2SO_4$, 0.5 mM K_2SO_4, 1 mM KH_2PO_4, 38 mM glycerol, 0.1% casamino acids, pH 7.5) containing 0.2% glucose and supplemented with $MgCl_2$ and $FeSO_4$, as indicated. When appropriate, media were supplemented with chloramphenicol (30 µg/ml) or kanamycin (50 µg/ml). Briefly, overnight LB cultures were first sub-cultured (1:100 dilution) in 20 ml of N-minimal media supplemented with 0.2 % glucose and 1 mM $MgCl_2$ at 37°C with shaking up to an optical density at 600 nm (OD_{600}) of 0.4. Cultures were washed in 1×phosphate-buffered saline (PBS) and resuspended in 20 ml of either N-minimal media supplemented with 0.2% glucose and 10 µM $MgCl_2$ (PmrAB-non-inducing conditions) or in the same media additionally supplemented with $FeSO_4$, as indicated (PmrAB-inducing conditions). Cultures were grown for an additional 2 h at 37°C with shaking, reaching a final OD_{600} of 1.3.

Construction of the *C. rodentium* deletion mutants. DNA manipulations were performed according to standard procedures [158]. The *waaL* gene was deleted by *sacB* gene-based allelic exchange from the previously described *C. rodentium* wild-type and Δ*pmrC*Δ*cptA* smooth strains to generate the corresponding rough strains [82, 159]. The suicide vector pRE*waaL* was generated by PCR-amplifying the upstream and downstream sequences of the *waaL* gene from *C. rodentium* genomic DNA using the primer pairs listed in Table 2. PCR fragments were gel purified, digested with the appropriate restriction enzymes, and ligated sequentially into pRE112. Resulting plasmids were verified by sequencing, transformed into the *E. coli* χ7213 donor strain and conjugated into

the appropriate *C. rodentium* strains. Chromosomal plasmid insertion was selected for by culturing on LB agar supplemented with chloramphenicol. Selected clones were cultured on peptone agar containing 5% sucrose to isolate colonies that were sucrose resistant. These resulting colonies were also tested for chloramphenicol sensitivity. Gene deletions were verified by PCR using primers CR760 and CR763. Plasmids pWSK-*pmrC* and pWSK-*cptA* expressing *pmrC* and *cptA* under control of their native promoters were previously described [82]. The pBAD-*lpxC* plasmid was constructed by PCR amplifying the *C. rodentium lpxC* gene using the primer pair listed in Table 2. The resulting PCR product was cloned into the SacI and XbaI restriction sites of the pBAD plasmid [82].

LPS preparations and silver staining. Total LPS was isolated from the various *C. rodentium* strains using the hot water-phenol method with modifications [56, 181]. Bacterial cultures were grown as indicated above, centrifuged (10 min, 1,200 × *g*) and normalized to a final OD_{600} of 0.4. Bacterial pellets were resuspended in 300 µl of SDS sample buffer and boiled for 15 minutes. Samples were cooled at room temperature for 15 minutes and 10 µl of a 10 mg/ml solution of proteinase K was added to each sample, and were then incubated at 59ºC for three hours. 200 µl of a phenol solution equilibrated in Tris-HCl pH 7.5 was added to each sample and vortexed vigorously for 15 sec. Samples were heated in a water bath at 65°C for 15 min and vortexed every 5 min for 15 sec. Immediately after this incubation, 1 mL of diethyl ether was added to each sample. Samples were then centrifuged (10 min, 20,600 × *g*) to separate the organic and aqueous phases. The bottom (aqueous) phase (500 µl) was collected and transferred to a new microcentrifuge tube. To increase the purity of the recovered LPS from the whole-cell lysates, another 1 mL of diethyl ether was added to each sample and were centrifuged (10 min, 20,600 ×

TABLE 3.0 Strains and plasmids used in this study

Designation	Description	Reference
Δ*waaL*	DBS100 Δ*waaL*, rough strain	This study
Δ*waaL*Δ*pmrC*Δ*cptA*	DBS100 Δ*waaL*Δ*pmrC*Δ*cptA*	This study
pRE112	Sucrose-sensitive (*sacB1*) suicide vector, Cm^r	[165]
pWSK129	Low-copy number plasmid	[166]
pBAD	Arabinose-inducible expression plasmid	[182]
pRE*waaL*	Δ*waaL* deletion construct in pRE112	This study
pWSK-*pmrC*	*pmrC* cloned into pWSK129	[82]
pWSK-*cptA*	*cptA* cloned into pWSK129	[82]
pBAD-*lpxC*	*lpxC* cloned into pBAD	This study

TABLE 3.1 Primers used in this study

Primers	Sequence	Usage
CR760	AGCTAGTCTAGATATTGCATACGCTTCCGGCGCTCA	Δ*waaL* 5'F XbaI
CR761	TGCAAGGGTACCTCCACAATATGGCGAAGCGAAATGG	Δ*waaL* 5'R KpnI
CR762	AGCTAGGGTACCCCTGCGCGGGAATTTTGAACAGGT	Δ*waaL* 3'F KpnI
CR763	AGCTAGGAGCTCCAGATCCGCCAACGAAGCCCAAAT	Δ*waaL* 3'R SacI
CR941	GGCTGAGCTCGTAATTTGGCGAGATTATACGATGATC	pBAD*lpxC* 5'SacI
CR942	GGCTTCTAGATATGCCAGTACGGTCGATGGTGC	pBAD*lpxC* 3'XbaI

g) once more. The bottom layer (500 µl), consisting of the purified LPS, was collected and transferred to a new microcentrifuge tube. To visualize the LPS banding patterns of the various strains, LPS samples were prepared by adding 50 µl of SDS sample buffer, boiled in water for five minutes and cooled on ice for five minutes. LPS samples were separated by 12.5% SDS-PAGE. Gels were then silver stained with modifications, as described in [183].

Immunoblotting of LPS samples. LPS samples were probed for KDO and free lipid A content using mAb WN1 222.5 and mAb 26.5, respectively (Hycult Biotech) [184, 185]. Following SDS-PAGE, samples were transferred to a polyvinylidene fluoride (PVDF) membrane using a Trans-Blot Semi-Dry Electrophoretic Transfer Cell (Bio-Rad) for 20 minutes at 20 V. Membranes were blocked overnight in 1× Tris-buffered saline (TBS) containing 5% (w/v) non-fat dry milk. Membranes were incubated two hours with the primary antibodies diluted in 1× TBS containing 1% (w/v) nonfat-dry milk (WN1 222.5, 1:10,000; 26.5, 1:1,000) and washed three times in 1× TBS for 10 minutes. Membranes were then incubated one hour with the secondary anti-mouse IgG antibody conjugated to horseradish peroxidase (HRP) at a 1:5,000 dilution in 1× TBS containing 1% (w/v) nonfat-dry milk. Membranes were washed three times in 1× TBS for 10 min and HRP activity was detected using a gel imager (Bio-Rad) following the addition of a chemiluminescent HRP substrate (Millipore).

Discontinuous sucrose density gradient centrifugation. Growth and separation of IM and OM of the various strains by discontinuous sucrose gradient centrifugation was performed as follows. Briefly, bacterial strains subcultured 1:100 from overnight LB cultures into 250 ml of N-minimal

media supplemented with 1 mM $MgCl_2$ and 0.2% glucose and grown and normalized to an OD_{600nm} of 0.4. Bacterial cells were then pelleted (10 min, 1,200 × *g*), washed once with 1× PBS and resuspended in 250 ml of N-minimal media supplemented with 10 µM $MgCl_2$ and with or without 25 µM $FeSO_4$. Bacterial cultures were then grown for an additional two hours, reaching a final OD_{600nm} of ~1.3. Second, spheroplasts were then made by pelleting bacterial cell density corresponding to an OD_{600nm} of 0.7 and resuspending the cells in 1 mL of 10 mM Tris-HCl buffer pH 7.5 containing 0.75 M sucrose. 100 µl of a 100 µg/ml lysozyme solution was then added to each cell suspension and these were incubated on ice for two minutes. 1 ml of an ice-cold 1.5 mM EDTA pH 7.5 solution was added to each of the suspensions. Incubation on ice followed for 60 minutes, with careful shaking every ten minutes, leading to the formation of spheroplasts. Lysis of the spheroplasts was done using a sonic dismembrator (intensity level 6, 3 times, 10 seconds per time and cooled on ice between sonic bursts). Cell lysates were centrifuged (20 min, 1,200×*g*) and cell supernatants were collected. Supernatants were centrifuged (2 h., 140,000 × *g*) using a MLA-80 rotor. Supernatants were decanted and pellets were homogenized using a 26G syringe needle in 800 µl of an ice-cold 3.3 mM Tris-HCl pH 7.5 buffer solution containing 0.25 M sucrose and 1 mM EDTA. Total membranes were collected by centrifugation (2 h., 140,000 × *g*). Total membranes were homogenized using a 26G syringe needle and resuspended in 1 ml of a 25 % sucrose (w/v) containing 5 mM EDTA. Total membrane protein concentration was quantified by absorbance at 280 nm (OD_{280nm}) using a NanoDrop 5000. 100 µl of the total isolated membranes for each strain was then diluted in a 25% sucrose solution buffered with 5 mM EDTA to give a final volume of 500 µl. This total volume of membranes was then applied to the top of a sucrose gradient, consisting of five 2 ml sucrose solutions, ranging from 30 to 50% in concentration, with 5% increments, which were layered onto 0.5 ml of a 55% sucrose. All solutions were buffered by

5 mM EDTA. Gradients were centrifuged at 4ºC (16 h, 150,000 × *g*) using a SW32.1 Ti rotor. 380 µl fractions were collected starting from the top, resulting in 29 total fractions. 10 µl of each odd-numbered fraction was then loaded onto a 20% SDS-PAGE gel. Gel electrophoresis of these fractions was performed at 70 V for 230 min. Inner membrane fractions were identified by measuring the activity of NADH oxidase [186] and the outer membrane fractions were identified by Western blot using a rabbit polyclonal antibody against the outer membrane protease CroP [187].

Minimal inhibitory concentration and survival assays. MIC values for the hydrophobic antibiotic novobiocin (Sigma) were determined in the presence and absence of 25 µM $FeSO_4$, as previously described [82, 163]. For survival assays, bacterial strains were grown in 40 ml N-minimal media in the presence and absence of 25 µM $FeSO_4$, as described above. Once the bacterial density was normalized an OD_{600} of 0.4, the bacterial culture was separated into two flasks. One culture was challenged with 25 µg/ml of novobiocin, while the other served as an untreated control. Cultures were then grown for 2 h at 37°C. Bacterial survival to novobiocin was determined by plating in triplicate on LB plates 10^{-4}, 10^{-6}, 10^{-7},10^{-8} and 10^{-9} dilutions of the culture and incubating overnight at 37°C. Survival was expressed as a percentage by taking the ratio of the CFU/ml determined for the treated culture over the CFU/ml of the untreated control, which was then multiplied by 100%.

3.4 RESULTS

The presence of iron in the medium increases LPS biosynthesis. To determine whether iron-induced pEtN modifications affect LPS turnover, the total LPS content of the *C. rodentium* Δ*waaL* and Δ*waaL*Δ*pmrC*Δ*cptA* strains was compared for cells grown in the presence of increasing iron concentrations (0, 25, 50 and 100 µM $FeSO_4$) (Fig. 3.0, A and B). Δ*waaL* strains were used to monitor the production of lipid A-core species specifically, as O-antigen is synthesized via a separate pathway and is non-essential. LPS was extracted from whole cell lysates, separated by SDS-PAGE and immunoblotted for total LPS content using the WN222.5 mAb against the core KDO moiety (Fig. 3.0, B). The Δ*waaL* strain displayed an increase of LPS production when grown in the presence of $FeSO_4$ concentrations ranging from 0 to 100 µM, reaching maximal production at 50 µM (Fig. 3.0, B). Compared to Δ*waaL*, the Δ*waaL*Δ*pmrC*Δ*cptA* strain displayed a similar increase of LPS production, albeit maximal production was observed at 25 µM $FeSO_4$ (Fig. 3.0, B). Total LPS contents largely decreased at iron concentrations higher than 50 µM for the Δ*waaL* strain and 25 µM for the Δ*waaL*Δ*pmrC*Δ*cptA* strain (Fig. 3.0, B). This is probably due to the fact that the Δ*pmrC*Δ*cptA* strain is more sensitive to high iron concentrations than wild-type, which has been previously documented [82, 180]. These data indicate that the presence of iron enhances LPS biosynthesis in a PmrAB-independent manner and that absence of PmrAB-regulated lipid A-core pEtN modifications results in a dysregulation of LPS turnover. To further characterize the LPS of these strains, immunobloting was performed using the mAb 26.5 that was raised against synthetic lipid A disaccharide [184]. This mAb recognizes free lipid A (i.e. lipid A unligated to KDO), but fails to recognize lipid A ligated to the core domain of LPS [188]. The Δ*waaL* strain did not show any accumulation of free lipid A regardless of the iron concentration (Fig. 3.0, C). In contrast, the Δ*waaL*Δ*pmrC*Δ*cptA* strain accumulated free lipid A when iron is present in the growth

medium (25 - 100 μM $FeSO_4$) (Fig. 3.0, C). Importantly, these data show that free lipid A accumulation is only observed in the strain that is defective for PmrAB-mediated pEtN modifications induced by iron. Taken together, these data suggest that the presence of iron affects LPS turnover through both PmrAB-independent and PmrAB-dependent mechanisms.

Modulation of LpxC activity results in increased LPS biosynthesis. LpxC is the metal-dependent *N*-acetylglucosamine deacetylase responsible for the committed step of lipid A biosynthesis [189]. LpxC was shown to be 6-8 fold more active when Fe^{2+} replaces the Zn^{2+} in its catalytic site, *in vitro* [28, 29]. In an attempt to investigate the PmrAB-independent response to iron, we determined whether increased LPS biosynthesis in *C. rodentium* occurs through a LpxC-dependent mechanism. To demonstrate this, the Δ*waaL*/pBAD-*lpxC* was grown in LB supplemented with increasing concentrations of arabinose (0, 0.002, 0.02 and 0.2%) to induce LpxC expression in a concentration-dependent manner. LPS was extracted and separated by 12.5% SDS-PAGE. An anti-KDO immunoblot was performed to measure the LPS content. The anti-KDO immunoblot showed that LPS biosynthesis increased proportionally to the concentration of arabinose (Fig. 3.1, A). Importantly, free lipid A levels also increased proportionally to the arabinose concentrations (Fig. 3.1, B), confirming that the LpxC expression level correlates with the levels of free lipid A. In addition, this strain showed growth defects at $OD_{600} > 1$ in the presence of 0.2% arabinose (data not shown). Thus, these data indicate that overexpression of LpxC leads to increased LPS production and increased free lipid A content. Together, these results suggest that the increased LPS production induced by the presence of iron may be due to a switch of the metal cofactor in the LpxC active site, which enhances LpxC activity in a PmrAB-independent manner.

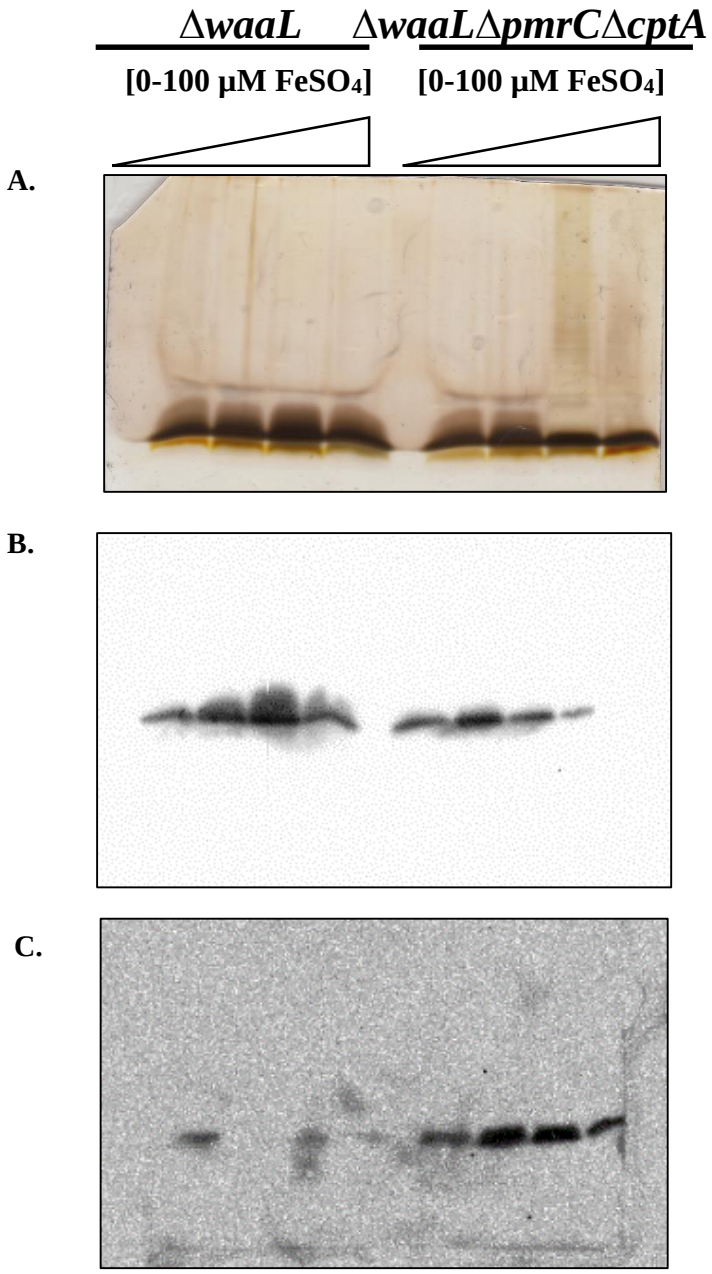

Figure 3.0: Iron increases LPS biosynthesis. Whole-cell lysate LPS preparations of Δ*waaL* and Δ*waaL*Δ*pmrC*Δ*cptA C. rodentium* strains. (A) Silver stain (B) anti-KDO immunoblot and (C) anti-lipid A immunoblot. Briefly, bacterial strains were initially grown in N-minimal media containing 1 mM $MgCl_2$ to an OD_{600} of 0.4, washed once in 1× PBS, and resuspended in equal volumes of N-minimal media containing increasing concentrations of $FeSO_4$ (0 to 100 µM) and LPS was extracted separated by 12.5% SDS-PAGE. Immunoblots were performed to probe for total LPS content using mAb WN222.5, and free lipid A content using mAb 26.5. Results are representative of three separate experiments.

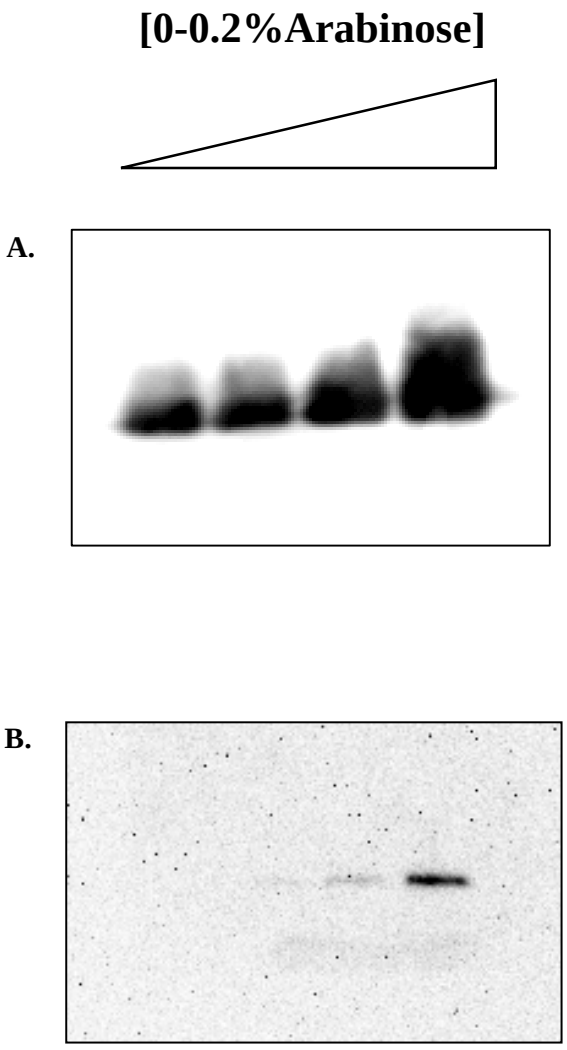

Figure 3.1: LpxC is involved in increased LPS biosynthesis in *C. rodentium*. Whole-cell lysate LPS preparations of Δ*waaL C. rodentium* strain overexpressing *lpxC* from an inducible arabinose promoter. (A) anti-KDO immunoblot and (B) anti-lipid A immunoblot. Strains were grown in LB broth containing increasing concentrations of arabinose inducer (0, 0.002, 0.02 and 0.2%) to induce expression of LpxC from pBAD-*lpxC*. Briefly, strains were initially subcultured 1:100 into 20 mL of LB containing the appropriate concentration of arabinose and grown for 3.5 hours, until the culture containing the highest concentration demonstrated a growth defect. Cultures were then normalized to an OD_{600} of 0.4 and LPS was extracted and separated by 12.5% SDS-PAGE. Immunoblots were performed to probe for total LPS content and free lipid A. Results are representative of three separate experiments.

Role of PmrC- and CptA-mediated pEtN modifications in the response to iron. To investigate the PmrAB-dependent response to iron, we determined the specific roles of PmrC- and CptA-mediated pEtN modifications in LPS turnover. Total LPS was extracted from the *C. rodentium* Δ*waaL*, Δ*waaL*Δ*pmrC*Δ*cptA*, Δ*waaL*Δ*pmrC*Δ*cptA*/pWSK-*pmrC* and Δ*waaL*Δ*cptA*Δ*pmrC*/pWSK-*cptA* strains grown in the presence of 25 μM $FeSO_4$, an iron concentration that produced a maximal iron response without affecting cell growth (Fig. 3.0). Total LPS content did not differ significantly between strains, as determined by anti-KDO immunoblot (Fig. 3.2, B). In contrast, when iron was present in the growth medium, striking differences in free lipid A content was observed (Fig. 3.2, C). In agreement with Fig. 3.0, the only strain that accumulated free lipid A was Δ*waaL*Δ*pmrC*Δ*cptA* (Fig. 3.2, C). Strikingly, complementation of Δ*waaL*Δ*pmrC*Δ*cptA* with either pWSK-*pmrC* or pWSK-*cptA* prevented the accumulation of free lipid A, as revealed by immunoblot against free lipid A (Fig. 3.2, C). Together, these data suggest that PmrC- and CptA-mediated pEtN modifications influence LPS turnover, most notably by preventing the accumulation of free lipid A, which has been related to stress associated with defective LPS transfer to the OM [34, 94].

PmrAB-mediated pEtN modifications promote LPS transfer to the OM. As the Δ*waaL*Δ*pmrC*Δ*cptA* mutant accumulated free lipid A when grown in the presence of iron, we hypothesized that pEtN modifications conferred by PmrC and CptA may be required for efficient LPS transfer from the IM to the OM. To test this possibility, discontinuous sucrose gradient centrifugation was performed with cell envelopes isolated from the the Δ*waaL*, Δ*waaL*Δ*pmrC*Δ*cptA*, Δ*waaL*Δ*pmrC*Δ*cptA*/pWSK-*pmrC* and Δ*waaL*Δ*pmrC*Δ*cptA*/pWSK-*cptA*

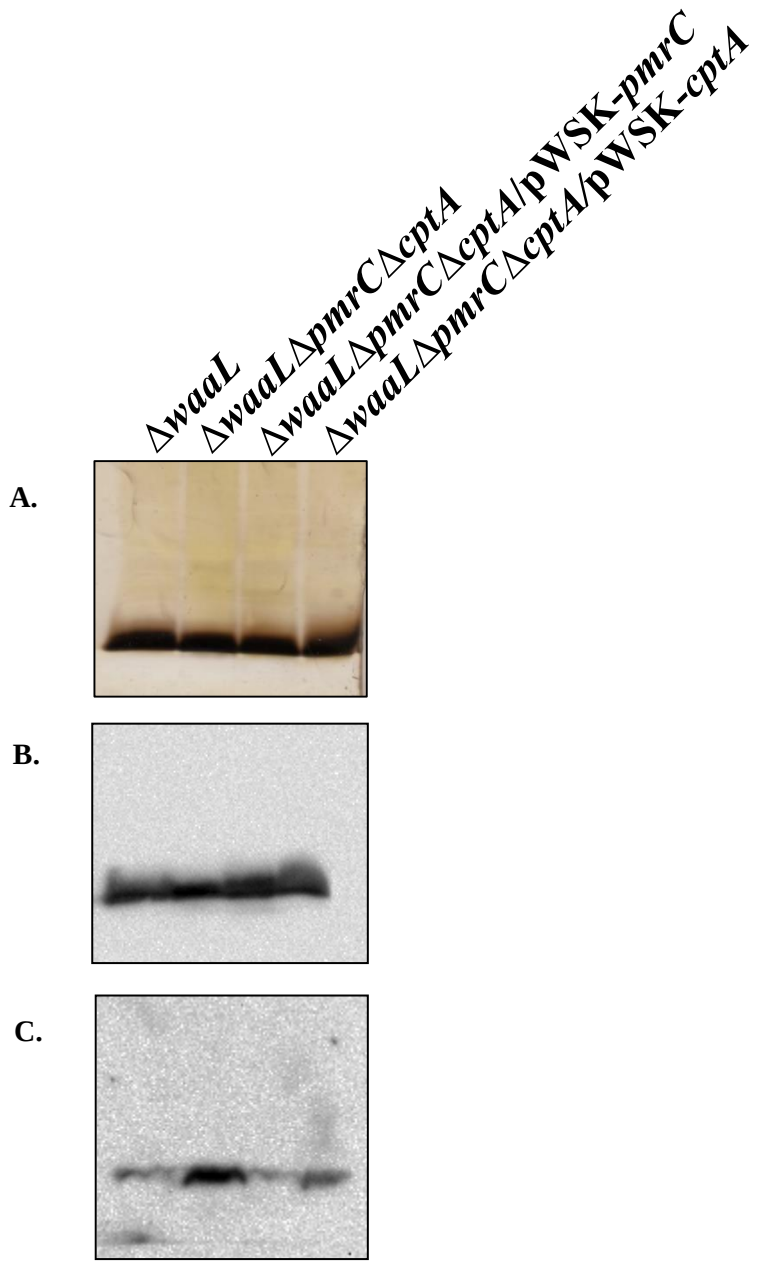

Figure 3.2: The absence of pEtN modifications increases the production of free lipid A in the presence of iron. . (A) Silver stain (B) anti-KDO immunoblot and (C) anti-lipid A immunoblot. Whole-cell lysate LPS extracts of cells normalized to an OD_{600} of 0.4 from Δ*waaL*, Δ*waaL*Δ*pmrC*Δ*cptA*, Δ*waaL*Δ*pmrC*Δ*cptA*/pWSK-*pmrC* and Δ*waaL*Δ*pmrC*Δ*cptA*/pWSK-*cptA C. rodentium* strains. LPS was separated by 12.5% SDS-PAGE and silver-stained using a modified a silver staining protocol (see Materials and Methods section) or probed for total LPS content and free lipid A.

strains grown in the presence of 25 μM $FeSO_4$. Fractions were analyzed by immunoblotting against KDO (Fig. 3.3). The Δ*waaL* strain displayed efficient transfer of LPS to the OM, as LPS was more abundant in the OM fractions. In contrast, the Δ*waaL*Δ*pmrC*Δ*cptA* strain displayed an even accumulation of LPS throughout fractions, indicating that LPS transfer across the cell envelope was defective in this strain. Remarkably, complementation of the Δ*waaL*Δ*pmrC*Δ*cptA* strain complemented with pWSK-*pmrC*, or to a lesser extent pWSK-*cptA*, rescued the Δ*waaL*Δ*pmrC*Δ*cptA* strain by promoting efficient transfer of LPS to the OM (Fig. 3.3). Overall, these results indicate that pEtN modifications conferred by PmrC and CptA in response to iron promote efficient transfer of LPS to the OM. This suggests that inefficient LPS transfer across the cell envelope may be responsible for the loss of OM integrity previously observed in the Δ*pmrC*Δ*cptA* strain [82].

Iron-induced pEtN modifications promote survival to novobiocin. To determine whether efficient LPS transfer across the cell envelope maintains proper integrity of the OM and, thus, increase resistance to hydrophobic antibiotics, MIC values of novobiocin were determined for the various strains grown in the presence of increasing concentrations of $FeSO_4$. Novobiocin is a lipophilic antibiotic that is ineffective against Gram-negative bacteria, as it must diffuse through the OM to access its cytoplasmic target DNA gyrase. For the wild-type strain, the addition of 50 μM $FeSO_4$ resulted in at least a 16-fold increase in the MIC value (Table 3.0). This MIC value decreased at a higher concentration of $FeSO_4$ (100 μM), most probably due to iron toxicity. For the Δ*waaL*Δ*pmrC*Δ*cptA* strain, the addition of 25 μM $FeSO_4$ resulted in a 16-fold decrease in the

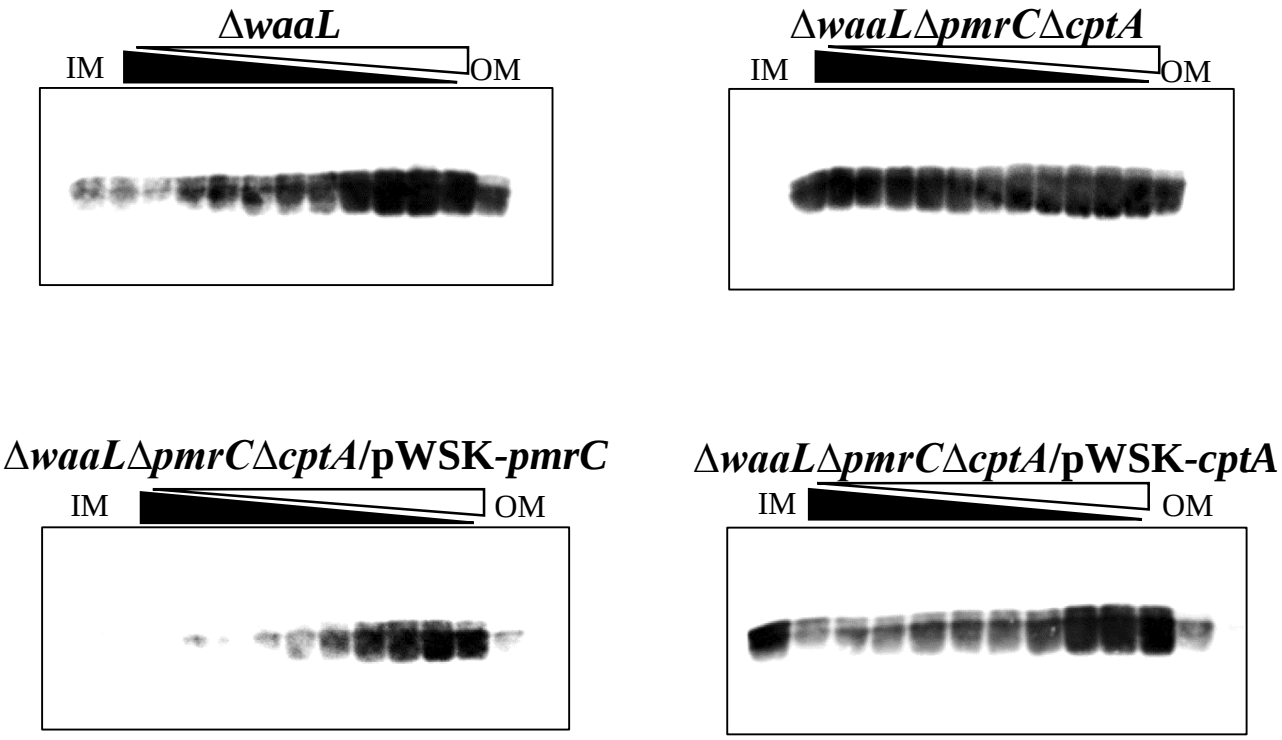

Figure 3.3: pEtN modifications promote LPS transfer to the OM. Discontinuous sucrose gradient fractions representing the IM and OM fractions of Δ*waaL*, Δ*waaL*Δ*pmrC*Δ*cptA*, Δ*waaL*Δ*pmrC*Δ*cptA*/pWSK*pmrC* and Δ*waaL*Δ*pmrC*Δ*cptA*/pWSK*cptA C. rodentium* strains grown in the absence or presence of iron. Strains were grown in the presence of 25 μM $FeSO_4$. Briefly, bacterial strains were grown in N-minimal media containing 1 mM $MgCl_2$, washed in 1× PBS and equal volumes of cells were resuspended in N-minimal media supplemented with iron. Cultures were grown for an additional 2 hours and standardized to an OD_{600nm} of 0.7. Cells were first made into spheroplasts, lyzed and cell membranes were isolated by differential centrifugation and then applied to a discontinuous sucrose density gradient (from 30 to 55%) and centrifuged (16 h, 150,000 × *g*) at 4°C. Fractions were collected starting from the top of the gradient, resulting in 29 total fractions collected. Odd-numbered fraction samples were separated by 20% SDS-PAGE and immunobloting against total LPS was performed. IM and OM fractions were determined using an NADH oxidation assay and by probing for OM porins using a polyclonal CroP antibody, respectively. The level NADH oxidation activities among the different fractions were comparable among the different strains, ensuring that a same amount of total membrane was analyzed. Results are representative of three independent experiments.

MIC value and cells were unable to grow at higher concentrations of $FeSO_4$, indicating a hypersensitivity to iron and/or novobiocin. Strikingly, complementation of Δ*waaL*Δ*pmrC*Δ*cptA* with either pWSK-*pmrC* or pWSK-*cptA* resulted in at least a 4-fold increase of the MIC value regardless of the concentration of $FeSO_4$ in the medium (Table 3.0). To confirm these results, survival assays were performed. Cultures grown in the absence or presence of 25 μM $FeSO_4$ were challenged with novobiocin (25 μg/ml) and the percent survival was determined by serial dilutions. The presence of $FeSO_4$ increased survival of the Δ*waaL* strain from 3% to 47% (Fig. 3.4). In contrast, the Δ*waaL*Δ*pmrC*Δ*cptA* strain did not survive in either condition (Fig. 3.4). The presence of $FeSO_4$ increased survival of the Δ*waaL*Δ*pmrC*Δ*cptA*/pWSK-*pmrC* and Δ*waaL*Δ*pmrC*Δ*cptA*/pWSK-*cptA* strains increased from 42% and 32%, respectively, to 100% for both strains. These data reveal a dual effect of iron. At concentrations between 0 and 50 μM $FeSO_4$, iron leads to increased resistance to hydrophobic antibiotics, such as novobiocin, which is dependent of the level of PmrC- and CptA-mediated LPS pEtN modifications. However, at higher concentrations, iron becomes toxic to the Δ*waaL* strain.

Table 3.2: MIC (µg/ml) of novobiocin in the presence of increasing concentrations of $FeSO_4$

$FeSO_4$ (µM)	0	25	50	100
Δ*waaL*	8	32	>128	8
Δ*waaL*Δ*pmrC*Δ*cptA*	4	0.25	–[a]	–[a]
Δ*waaL*Δ*pmrC*Δ*cptA*/pWSK-*pmrC*	32	>128	>128	>128
Δ*waaL*Δ*pmrC*Δ*cptA*/pWSK-*cptA*	32	>128	>128	>128

–[a,] no observed growth

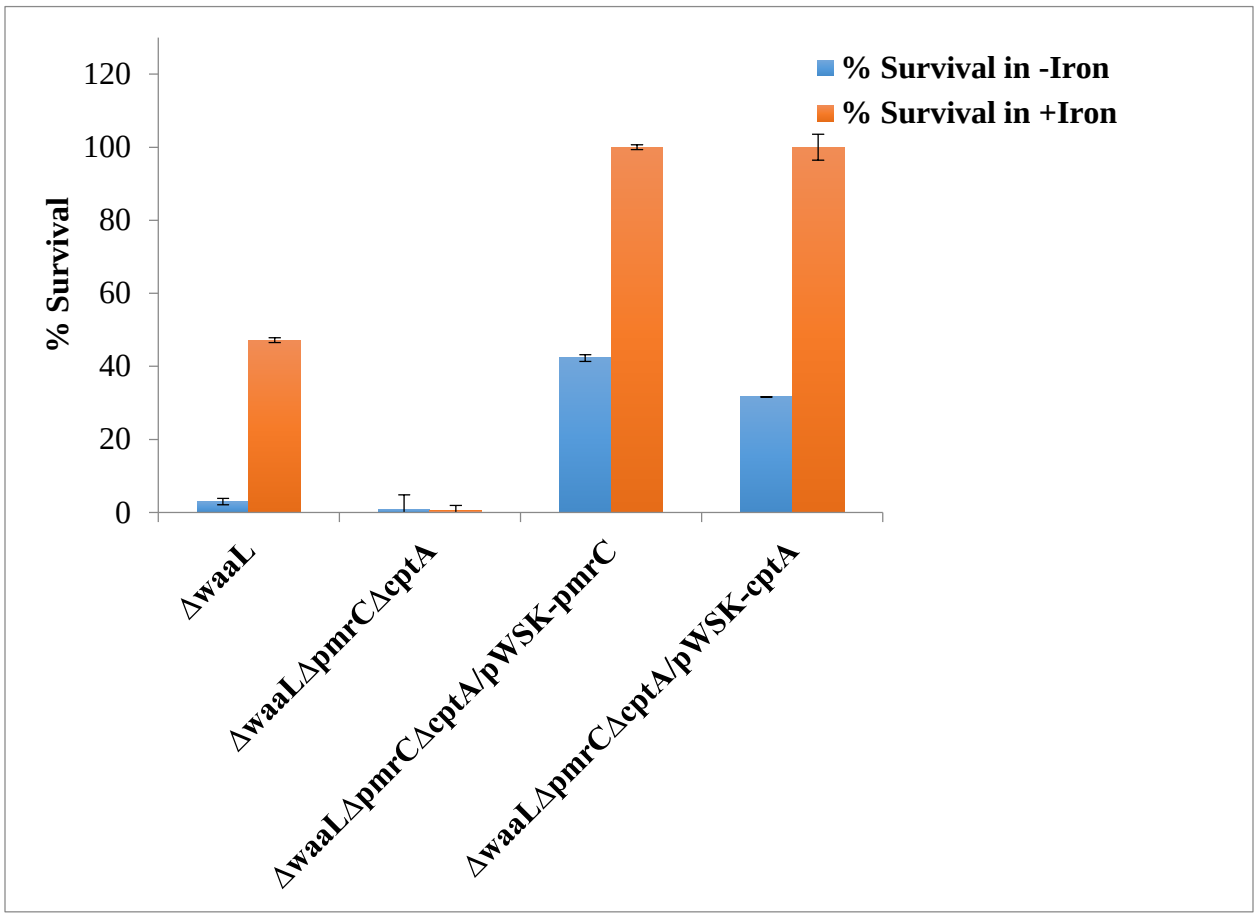

Figure 3.4: Iron increases resistance to novobiocin by a pEtN modification-dependent mechanism. Bacterial strains were initially grown in N-minimal media containing 1 mM $MgCl_2$ up to an OD_{600nm} of 0.4, washed once in 1× PBS, and resuspended into equal volumes of N-minimal media supplemented with or without 25 µM $FeSO_4$. Cultures were then treated with 25 µg/ml novobiocin. Strains were then additionally grown for 2 hours at 37°C. Survival percentage for each strain was determined by calculating the ratio of CFU/ml obtained for the treated culture compared to the CFU/ml obtained for the untreated control culture grown in both the absence (-Iron) or presence (+Iron) of 25 µM $FeSO_4$. Results are representative of the average survival percentage of three independent experiments.

3.5 DISCUSSION

Previous studies have shown that PmrAB-mediated pEtN modifications are important for resistance to iron and hydrophobic antibiotics. This study aimed at deciphering the mechanism by which iron-induced PmrAB-mediated pEtN modifications of LPS affect OM integrity in *C. rodentium*. Here, we showed that iron has a dual effect on LPS transfer to the OM and, in turn, OM integrity. First, the presence of iron in the growth medium resulted in a PmrAB-independent increase of LPS production, most likely through a mechanism that depends on LpxC. Second, the presence of iron also results in the accumulation of free lipid A for strains that are unable to modify LPS with pEtN. This led to the finding that PmrC and CptA-mediated pEtN modifications promote lipid A turnover and transfer of LPS to the OM. Overall, this study details the adaptive response to iron that allows *C. rodentium* to reinforce its OM barrier that consequently results in increased resistance to hydrophobic antibiotics.

First, we showed that the presence of iron results in an overall increase of LPS production in the Δ*waaL* and Δ*waaL*Δ*pmrC*Δ*cptA C. rodentium* strains, indicating that this effect is independent of PmrAB, PmrC and CptA (Fig. 3.0). Since replacement of Zn^{2+} by Fe^{2+} in the LpxC active site has been shown to result in enhanced LpxC activity [28, 29], we hypothesized that the observed increase in LPS production may be the result of this metal switch. To determine whether enhanced LpxC activity results in increased LPS production, *lpxC* was overexpressed from an arabinose inducible promoter in the Δ*waaL* strain. In support of the enhancement of LpxC activity by iron, we found that *lpxC* overexpression leads to increased LPS production and accumulation of free lipid A in this strain (Fig. 3.1). Previous studies have shown that LpxC overexpression is detrimental to bacterial growth [32, 190]. In agreement, induction of *lpxC* expression by more than 0.2% arabinose resulted in bacterial growth arrest at an OD_{600} of 1 (data not shown). Interestingly,

this growth arrest is concomitant with the accumulation of free lipid A under these conditions (Fig. 3.0), however accumulation of lipid A in the Δ*waaL*Δ*pmrC*Δ*cptA* strain when grown in minimal media supplemented with iron did not translate into lethality, suggesting this difference may be due to the growth media used.

In contrast to Δ*waaL*, the Δ*waaL*Δ*pmrC*Δ*cptA* strain accumulated free lipid A when grown in the presence of iron (Figs. 3.0 and 3.2). Complementation of Δ*waaL*Δ*pmrC*Δ*cptA* with either pWSK*pmrC* or pWSK*cptA* prevented accumulation of free lipid A (Fig. 3.2), suggesting that PmrAB-regulated pEtN modifications prevent iron toxicity by positively influencing LPS turnover. Free lipid A accumulation at the IM is potentially lethal, as shown previously for *E. coli* mutants deficient in various enzymes of the lipid A biosynthesis pathway (LpxK, WaaA) or in the ABC transporter MsbA, which is responsible for flipping the lipid A-KDO_2 precursor of LPS across the IM [34, 36, 191]. Since both PmrC and CptA are IM proteins with their active sites facing the periplasm, we hypothesized that the addition of pEtN to lipid A-core may influence LPS transfer to the OM.

Discontinuous sucrose gradients allowed us to examine the transfer of LPS from the IM to the OM. The lack of PmrC- and CptA-mediated pEtN modification resulted in the spreading of LPS throughout the gradient fractions, indicating transport defect (Fig. 3.3). Complementation of the Δ*waaL*Δ*pmrC*Δ*cptA* strain with either pWSK-*pmrC* or pWSK-*cptA* restored efficient transfer of LPS to the OM (Fig. 3.3). The finding that pEtN modifications promote LPS transport to the OM is in good agreement with recent studies examining the role of LPS modifications in other Gram-negative species. In *Burkholderia cepacia*, the addition of 4-aminoarabinose to LPS was found to be essential for LPS transfer to the OM [34, 94]. This modification was essential to the interaction of LPS with LptG, a component of the *lpt* trans-envelope complex. In *Pseudomonas*

aeruginosa, the phosphoryl group present on heptose-I of the core domain, which is modified by CptA, was found to be essential for LPS transport to the OM [39]. These findings suggest that both lipid A and the core domain interact with the LPS transport machinery. LptA is a periplasmic protein that oligomerizes and forms bridges connecting the IM and OM [44]. *In vitro*, LptA was found to interact with the lipid A portion of LPS, regardless of the modification status of lipid A's phosphoryl groups [45]. Therefore, pEtN modifications likely influence the interaction of LPS with another component of the Lpt trans-envelope complex.

In our previous study, we reported that PmrC appears to be more important than CptA in maintaining OM integrity under PmrAB-inducing conditions [82]. This conclusion is supported by the fact that complementation of the Δ*waaL*Δ*pmrC*Δ*cptA* strain with pWSK-*pmrC* resulted in more efficient LPS transfer to the OM than complementation with pWSK-*cptA* (Fig. 3.3), suggesting that pEtN addition to lipid A is more important than pEtN addition to the core for efficient transport to the OM. In contrast, complementation of the Δ*waaL*Δ*pmrC*Δ*cptA* strain with either pWSK-*pmrC* or pWSK-*cptA* prevented the formation of free lipid A (Fig. 3.2), suggesting that both PmrC and CptA indeed play a role in lipid A turnover, and qualitative differences in their ability to do so may be due to the relative expression of the genes encoding both pEtN transferases under PmrAB-inducing conditions compared to non-inducing conditions, which was found to be 45-fold for *pmrC* and only two-fold for *cptA* [82].

Both survival experiments and MIC values determination revealed that the presence of physiological concentrations of iron (25 μM) increases resistance to novobiocin for the Δ*waaL* strain (Fig. 3.4, Table 3.0). These results show that the adaptive response to iron described in this study (Fig. 3.5) leads to increased resistance to hydrophobic antibiotics. The adaptive response to iron has been documented to increase resistance to Fe^{3+} cell-mediated toxicity, but never has it

been linked to antibiotic resistance [192]. The finding that complementation of the Δ*waaL*Δ*pmrC*Δ*cptA* strain with either pWSK-*pmrC* or pWSK-*cptA* leads to exacerbated resistance to novobiocin (Fig. 3.4, Table 3.0) shows that the pEtN transferases play a key role in promoting resistance to hydrophobic antibiotics by reinforcing the OM barrier. Hence, this study highlights the importance of physiological conditions in studying antibiotic resistance, as iron is a critical metal for both host and bacterium [103, 106]. This conclusion is further supported by the fact that complementation of the Δ*waaL*Δ*pmrC*Δ*cptA* strain with either *pmrC* or *cptA* precludes the toxic effect of iron observed for the Δ*waaL*Δ*pmrC*Δ*cptA* strain and to a lesser extent the Δ*waaL* strain at higher iron concentrations (Table 3.0). These results indicates that inhibition of the pEtN transferases PmrC and CptA is likely to make *C. rodentium* and possibly other Gram-negative bacteria susceptible to antibiotics that are otherwise ineffective against these pathogens. In addition, it is unlikely that targeting these non-essential enzymes would generate resistance [20].

The concentrations of iron used throughout this study (i.e. micromolar range) are consistent with the concentrations encountered by *C. rodentium* and other bacterial pathogens during host infection. In the gastrointestinal tract of mice, iron is found at concentrations ranging from 10-100 µM [109]. This suggests that the iron adaptive response described in this study is likely to occur *in vivo*. This conclusion is supported by previous studies showing that the *S. enterica* PmrAB is expressed and activated by the environmental conditions of the murine gastrointestinal tract [72]. Looking at free iron in the bloodstream, the concentration in serum was found to increase from 5 to 35 µM in patients with sepsis syndrome [111]. Therefore, our findings are likely to be relevant in vivo during sepsis and the adaptive response to iron is likely to increase antibiotic resistance.

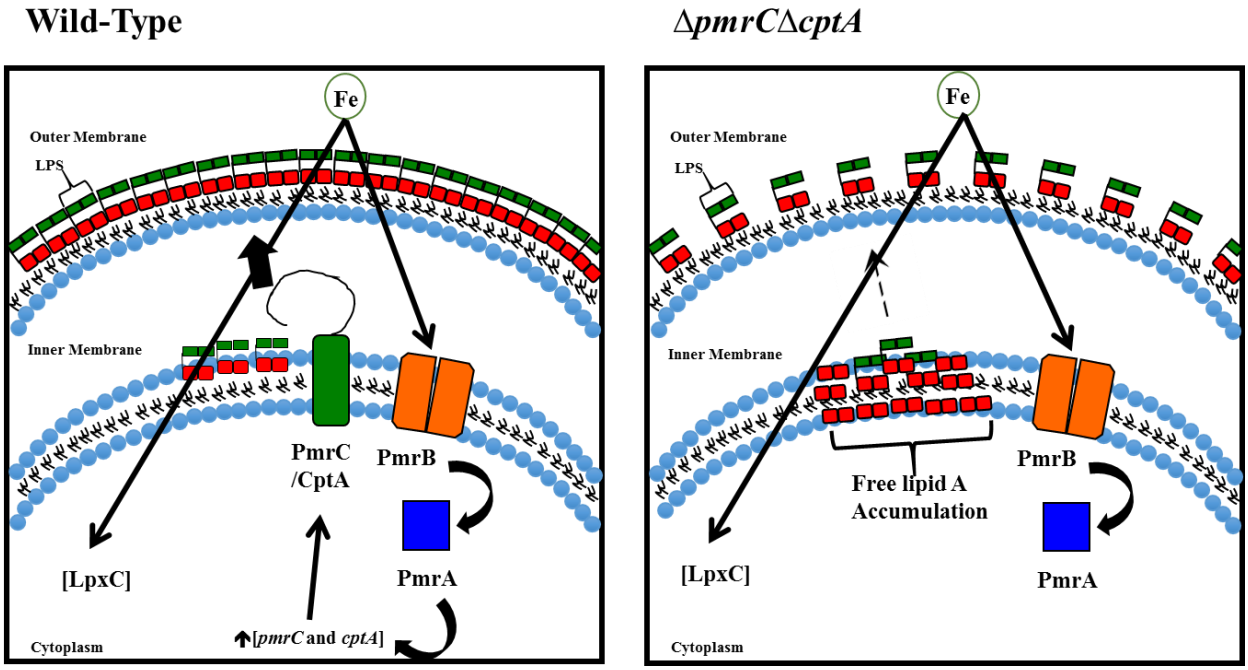

Figure 3.5: **Iron increases both LPS production and expression of *pmrC* and *cptA* to increase the OM permeability barrier**. The interplay between the iron-mediated increase of LPS production, most likely dependent on an increase of LpxC catalytic efficiency, and the iron-mediated upregulation of expression of the pEtN transferases PmrC and CptA in the IM by PmrAB increase the OM permeability barrier in a concentration-dependent manner. The addition of pEtN to LPS would then be a means by which Gram-negative bacteria efficiently transfer LPS subunits to the OM when LPS production is increased.

In summary, the dual effect of iron on both LPS production and expression of PmrAB-regulated pEtN transferases is a novel aspect of the iron adaptive response (Fig. 3.5) that could be targeted to combat the emerging threat of multidrug resistant Gram-negative pathogens. Inhibition of these pEtN transferases could be a novel adjunct therapeutic approach to render Gram-negative bacteria susceptible to existing antibiotics that are not currently used in the clinical setting against Gram-negative infections.

3.6 SUPPLEMENTARY FIGURES

3.6.1 Figure S1

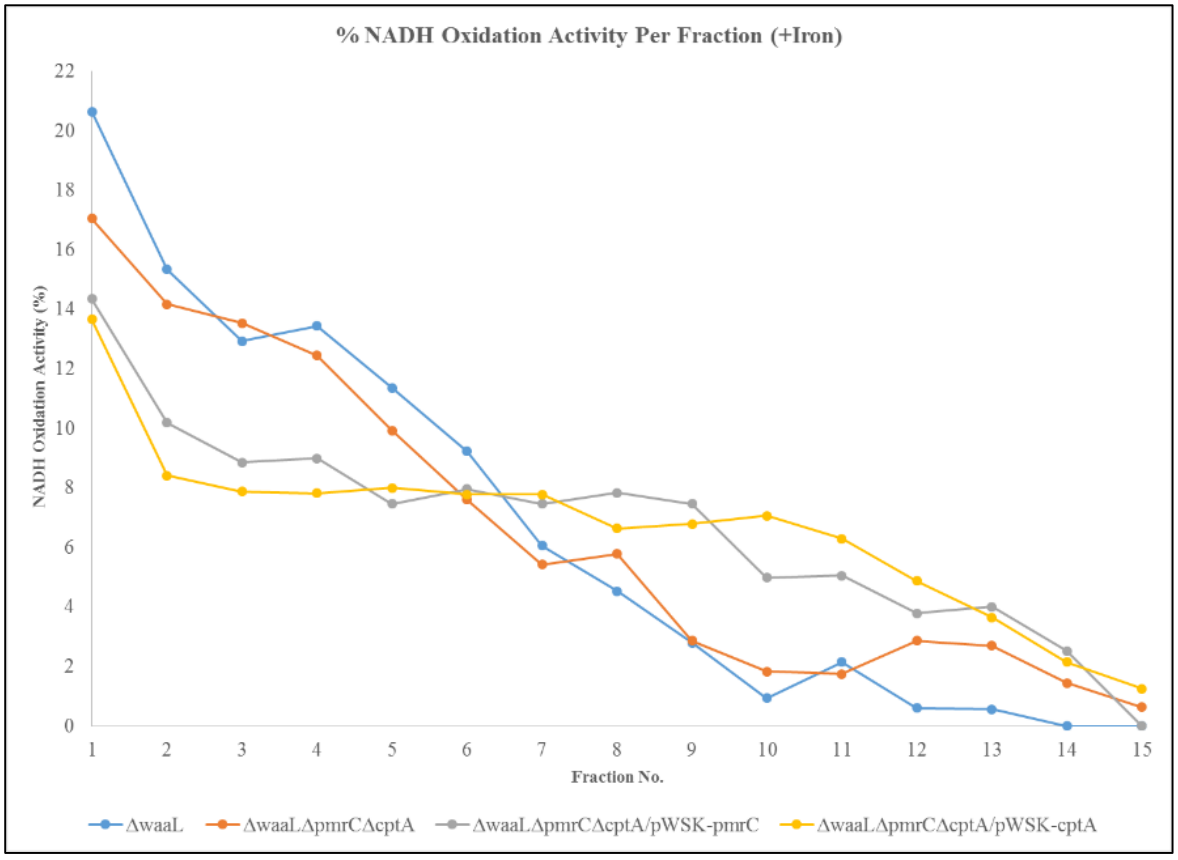

Figure S1: NADH oxidation of collected fractions from strains grown in the absence (-Iron) or presence (+Iron) of 25 µM $FeSO_4$. Strains grown in the presence of 25 µM $FeSO_4$. Membranes fractions were incubated with 0.12 mM β-NADH and the rate of decrease of the absorbance value at 340 nm was monitored over ten minutes. Rates were measured and used to calculate the %NADH activity value for each fraction, where % NADH activity = absolute value (rate of fraction)/absolute value (the total of rates of all fractions) ×100 %. Fractions with higher %NADH activity are representative of IM fractions. Data is cumulative of three separate experiments.

3.6.2 Figure S2.

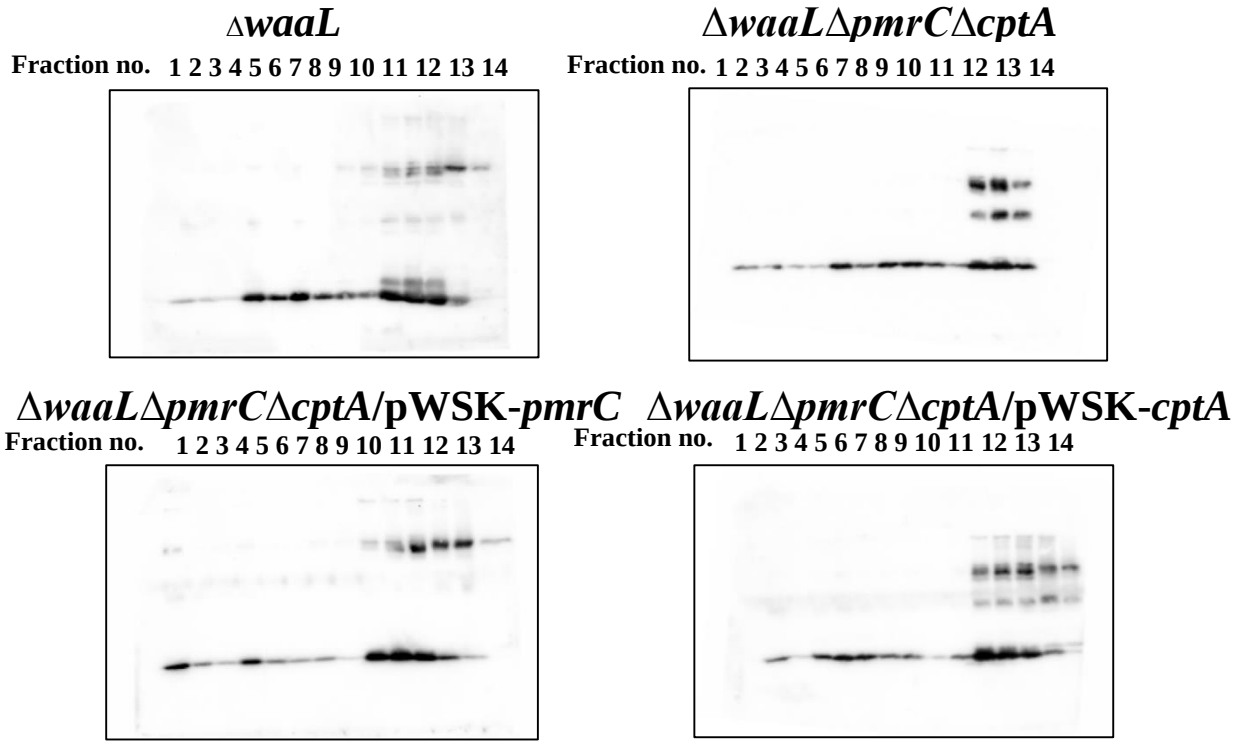

Figure S2: Anti-CroP Western Blot revealing presence of OM proteins in collected fractions. Strains grown in the presence of 25 μM $FeSO_4$. The Anti-CroP primary antibody crossreacts with OM proteins, delineating the OM fractions in the collected samples. Data is representative of three separate experiments.

3.8 ACKNOWLEDGEMENTS

This work was supported by Natural Sciences and Engineering Research Council (NSERC, RGPIN-217482) and the Canadian Institutes of Health Research (CIHR, MOP-15551). C.V. was supported by a NSERC graduate scholarship.

PREFACE TO CHAPTER 4

Chapter 4 looks at the relationship between iron, OM vesiculation and PmrAB-regulated LPS modifications. The mechanism by which OMVs are produced in bacteria is still unknown, although there are some known proteins that are involved in OM vesiculation, such as OmpA and Lpp. Here, we show that iron is involved in the process of vesiculation.

Chapter 4:

The Presence of Iron Influences Outer Membrane Vesiculation.

Charles Viau and Hervé Le Moual*

Department of Microbiology and Immunology, Microbiome and Disease Tolerance Centre,

and Faculty of Dentistry, McGill University, Montreal, QC, H3A 2B4, Canada

***Corresponding author:** Hervé Le Moual, Department of Microbiology and Immunology, McGill University, 3775 University Street, Montreal, QC, H3A 2B4, Canada, Tel: 5143986235; Fax: 5143987052; E-mail: **herve.le-moual@mcgill.ca**

(IN PREPARATION)

4.1 ABSTRACT

Outer membrane vesicles (OMVs) are used by Gram-negative bacteria to cause pathogenesis, as the presence of vesicles has been associated with severe bacterial infections. However, the mechanism of vesicle formation in bacteria is still unclear, although strong evidence indicates a dissociation of the OM from the peptidoglycan layer at specific areas in the bacterial cell envelope, leading to local budding from the OM. Here, we show that OM vesicle (OMV) production by *Citrobacter rodentium* is enhanced by increasing iron concentrations (0, 25, 50 and 100 µM $FeSO_4$), as determined by the presence of the OM protease CroP in OMVs. From a previous report, we concluded that these growth conditions were PmrAB-inducing, resulting in the induction of *pmrC* and *cptA*, two genes encoding phosphoethanolamine (pEtN) transferases that catalyze the addition of pEtN to the lipid A 1- and 4'- phosphoryl groups and to the heptose-I phosphoryl group of lipopolysaccharide (LPS), respectively. As OMVs have been documented to have bactericidal effects, we conducted a minimal inhibitory concentration (MIC) assay to determine the relative toxicity of the isolated vesicles against the *C. rodentium* Δ*waaL* and Δ*waaL*Δ*pmrC*Δ*cptA* strains. Interestingly, the vesicles isolated from the *C. rodentium* Δ*waaL* strain were found to be more bactericidal against the Δ*waaL*Δ*pmrC*Δ*cptA* strain than the Δ*waaL* strain in the presence of iron, suggesting that PmrC and CptA confer protection from these toxic effectors. Thus, the adaptative response to iron requires PmrAB induction as to protect bacteria from the vesicles that are formed.

4.2 INTRODUCTION

Outer membrane (OM) vesicles are closed spheroid particles of various sizes (ranging from 10 to 300 nm in diameter) composed of proteins, lipoproteins and lipopolysaccharide (LPS) released from Gram-negative bacteria during all phases of growth [114, 132]. Bacterial vesiculation and OM vesicle trafficking are not well understood mechanisms, as opposed to the eukaryotic counterparts. A general consensus is that outer membrane (OM) vesiculation is dependent on the dissociation between the OM and the peptidoglycan layer. These interactions include OM proteins and lipoproteins such OmpA, Lpp, and Pal of the Tol/Pal system which interact, both covalently and non-covalently, with the peptidoglycan meshwork [114]. For example, Lpp, the most abundant lipoprotein in *E.coli* estimated at 750,000 copies/cell, was found to specifically interact with lysine 58 of diaminopimelic acid, and truncation of the C-terminus of the protein, where the interaction was mapped, lead to hypervesiculation in the *E. coli* mutant strain [193]. Therefore, a decrease in the number of the local interactions between the OM and peptidoglycan is thought to promote budding and ultimately results in the production of OMVs. Interestingly, vesiculation is thought to increase in periods of environmental stresses, such as the ones inducing the σ^E response in Gram-negative bacteria [194].

OMVs may carry different enzymes for multiple functions. These functions include interbacterial competition, collaboration and pathogenesis [112, 132]. OMVs have been shown to contain autolysins and hydrolases to kill competing bacteria as well as xylanase and cellulase to degrade complex carbohydrates for the benefit of the whole bacterial community [112, 130]. OMVs from pathogenic Gram-negative bacteria have been shown to carry toxins and proteases as cargo which serve to propagate infection [112, 195]. Vesicles may act as virulence factors as well, as they are composed of LPS, the Toll Like Receptor 4 agonist [112]. The vesicle itself provides

protection to their cargo proteins, as they are protected from environmental proteases. Consequently, OMVs have been found in the blood of patients having died of fatal septicemia and in the cerebrospinal fluid of infants having died of meningitis [127, 196].

In the *Enterobacteriaceae*, covalent LPS modifications are regulated by a mechanism which includes two-component systems in Gram-negative bacteria, a system that consists of a sensor histidine kinase and a cognate response regulator, which respond to environmental signals [38]. The main two-component system regulator of covalent LPS modifications in the *Enterobacteriaceae* is the PmrA-PmrB (PmrAB) two component system. PmrAB also responds to low pH (5.5), as well as to micromolar concentrations of Fe^{3+} and Al^{3+}, although activation by Al^{3+} is only 50% compared to the activation level of Fe^{3+} in *S. enterica* [66, 71]. PmrAB regulates the transcription of the *arn* operon (also known as the *pmrHFJIKLM* operon) which catalyzes the addition of aminoarabinose to the 4'-phosphoryl group of lipid A and *pmrC* and *cptA*, which encode phosphoethanolamine (pEtN) transferases that catalyze the addition of pEtN to the 1- and 4'-phosphoryl groups of lipid A and to the core heptose-I phosphoryl group, respectively [38]. Most notably, in *S. enterica*, addition of aminoarabinose and pEtN to the lipid A moiety of LPS has been associated with increased resistance to the AMP polymyxin B, with aminoarabinose addition having a greater effect than pEtN addition in decreasing the negative charge associated to the lipid A phosphoryl groups [85, 87, 96]. In contrast to *S. enterica*, *Citrobacter rodentium* does not possess the *arn* operon and thus serves as a convenient model to study functions specifically associated to PmrAB-regulated pEtN modifications. More recently, PmrC (or EptC in *Campylobacter jejuni*) was found to catalyze the addition pEtN to the FlgG subunit and to the *N*-heptasaccharides found on the surface of the bacterium, indicating that this pEtN transferase has

multiple functions in *C. jejuni* [100, 101]. Therefore, by extending these findings to other Gram-negative bacteria, LPS covalent modifications may have undescribed roles yet to be uncovered.

We recently demonstrated that the *C. rodentium* Δ*waaL*Δ*pmrC*Δ*cptA* strain had a defect in LPS turnover compared to the wild-type strain (in a Δ*waaL* background) when grown in the presence of micromolar concentrations of iron, a PmrAB-inducing condition (manuscript in preparation). This strain was found to accumulate free lipid A, that is lipid A unligated to core sugars, when grown in the presence of iron. This observation indicates a defect in LPS turnover in this strain most probably at the level of lipid A itself as iron has been shown to positively modulate the activity of LpxC, the *N*-acetylglucosamine deacetylase, responsible for the committed step in the constitutive lipid A pathway. PmrC- and CptA-mediated pEtN modifications were shown to first, decrease the accumulation of free lipid A in the Δ*waaL*Δ*pmrC*Δ*cptA* strain and to second, promote transfer of LPS subunits from the IM to the OM by sucrose density gradients, albeit to different extents. Therefore, we attributed a novel role to pEtN modifications in promoting LPS transfer to the OM under PmrAB-inducing conditions.

Here, we describe a novel role of iron itself promoting vesiculation, in minimal media containing iron concentrations up to 100 µM $FeSO_4$ for the *C. rodentium* Δ*waaL* strain, most probably through a mechanism dependent on LpxC and PmrAB-mediated pEtN LPS modifications. Second, we show that isolated vesicles from the Δ*waaL* strain are more bactericidal against the Δ*waaL*Δ*pmrC*Δ*cptA* strain than the Δ*waaL* strain, both in the presence and absence of iron, highlighting the role of PmrC and CptA in conferring protection against OMVs.

4.3 MATERIALS AND METHODS

Bacterial strains and growth conditions. Bacterial strains and plasmids used in this study are listed in Table 4.0. Bacteria were grown at 37°C with aeration in Luria- Bertani (LB) broth, or N-minimal medium (50 mM Bis Tris, 5 mM KCl, 7.5 mM $(NH_4)_2SO_4$, 0.5 mM K_2SO_4, 1 mM KH_2PO_4, 38 mM glycerol, 0.1% casamino acids, pH 7.5) containing 0.2% glucose and supplemented with $MgCl_2$ and $FeSO_4$, as indicated. Briefly, for the experiments done with iron, the *C. rodentium* Δ*waaL* was initially subcultured (1:100) from an overnight culture of LB into 200 ml of N-minimal media containing 1 mM Mg^{2+} and supplemented with 0.2% glucose. The culture was grown until an OD_{600} of 0.4 was achieved. The volume of culture was separated into four (50 ml) and these volumes were centrifuged (1,200 × *g*, 10 min). Bacterial pellets were washed once in 1× phosphate buffered saline (PBS) and centrifuged once again (1,200 × *g*, 10 min). Bacterial pellets were then resuspended in 50 ml of N-minimal media supplemented with 0.2% glucose, 10 µM Mg^{2+} and either 0, 25, 50 or 100 µM $FeSO_4$. Bacterial cultures were then grown for an additional two hours, until the OD_{600nm} reached a value of 1.

OM vesicle collection. 15 ml of bacterial supernatant was centrifuged, and the resulting supernatants was passed through a 0.45 micron filter for sterilization purposes. Supernatants were then applied to Amicon Ultra 15 mL Filters and the supernatants were concentrated according to the manufacturer's specifications. The resulting concentrated supernatants (less than 200 µl) were centrifuged (1 h., 140,000 × *g*) and the resulting pellets, consisting of vesicles, were resuspended in 200 µl of sterile 1× PBS pH 7.5. Vesicle protein concentration for each growth condition was determined by measuring the optical density at 280 nm and the concentrations obtained were usually in the range of 4 mg/ml.

Table 4.0: Strains and plasmids used in this study

Designation	Description	Reference
Δ*waaL*	DBS100 Δ*waaL*, rough strain	This study
Δ*waaL*Δ*pmrC*Δ*cptA*	DBS100 Δ*waaL*Δ*pmrC*Δ*cptA*	This study
pWSK-*pmrC*	*pmrC* cloned into pWSK129	[82]
pWSK-*cptA*	*cptA* cloned into pWSK129	[82]

Gel electrophoresis and Western blotting. Vesicle samples were diluted 1:1000 in sterile 1× PBS to reach a final concentration of 4 µg/ml for each growth condition. 10 µl of the diluted vesicle sample was first diluted 1:1 in 2× SDS sample buffer and 10 µl of each sample was resolved by 12.5% SDS-PAGE at 100 V for 100 minutes. Transfer onto a polyvinylidene membrane of the separated samples was then achieved using a semi-dry transfer apparatus at 20 V for 20 minutes. Membranes were then blocked overnight at 4ºC in 5% milk in 1× tris buffered saline (TBS). The following day, membranes were initially probed using a primary rabbit polyclonal anti-CroP anti-sera diluted 1:2,000 for 2 h on a rocking platform at room temperature. Membranes were then washed with 0.1% milk in 1× TBS three times for 10 min each time. Following the washes, membranes were probed with a secondary mouse anti-rabbit antibody conjugated to horseradish peroxidase for 1 h on a rocking platform at room temperature. Membranes were washed following the previous procedure. Blots were developed with 800 µl of HRP reagent using a gel box imager and software.

Minimal Inhibitory Concentration (MIC) determination. To determine whether the isolated vesicles were bactericidal, a concentration range of vesicles, as determined by the OD_{280nm}, was tested on the Δ*waaL* strain in the presence or absence of iron using a minimal inhibitory concentration assay. Bacteria were first subcultured from an overnight culture into 10 ml of trypticase soy broth (TSB) and grown to an OD_{600} of 0.46, representing a bacterial concentration of 5×10^5 CFU/ml. 20 µl of this culture was then subcultured into 10 ml of N-minimal media supplemented with 0.2% glucose containing either only 10 µM $MgCl_2$ (- iron) or 10 µM $MgCl_2$ and 25 µM $FeSO_4$ (+ iron). 90 µl of the diluted culture was then added to a row of 96-well microtiter plate. A serial dilution of vesicles using a starting concentration of 256 µg/ml diluted

two-fold to a final concentration of of 1 µg/ml was added to the same row. Plates were incubated for 16 hours at 37ºC and the minimal concentration of vesicles that allowed growth was determined for both conditions.

4.4 RESULTS

***C. rodentium* produces OMVs in media supplemented with iron.** The *C. rodentium* Δ*waaL* rough LPS strain was used to determine whether iron induces the production of OMVs. Briefly, this strain was grown in N-minimal media supplemented with increasing concentrations of iron (0, 25, 50 and 100 μM $FeSO_4$), and OMVs were collected by differential centrifugation from the culture supernatants for each condition. Sample aliquots were then loaded on SDS-PAGE and the samples were then probed for the OM protease CroP using a polyclonal antibody. The iron concentrations used reflect the concentrations used in our previous report that demonstrates an iron-dependent increase in LPS production when grown in iron concentrations ranging from 0 to 50 μM. From Fig. 4.0, we observe an iron-dependent increase in the amount of CroP detected in OMVs, as determined by the intensity of the band present at 32 kDa. In addition, the polyclonal antibody used also cross-reacts with LPS. Similarly, the intensity of LPS increases in an iron-dependent manner from 0 to 100 μM $FeSO_4$. This observation, coupled with the increase of CroP under the same conditions, suggests that the Δ*waaL* strain is producing vesicles in an iron-dependent manner under our experimental conditions. These samples were plated on LB plates to determine whether they were sterile. No colony growth was observed (data not shown), indicating that the samples contained OMVs as they were devoid of bacterial cells. The association of LPS with OM proteins is well-documented [197, 198]. In addition, the observation that CroP and LPS concentrations increase concomitently is consistent with the fact that the samples indeed contain OMVs, seeing as OM proteins require LPS to be properly folded in the OM. Altogether, these data suggest that the surplus in LPS production, promoted by iron, is converted into the production of OMVs.

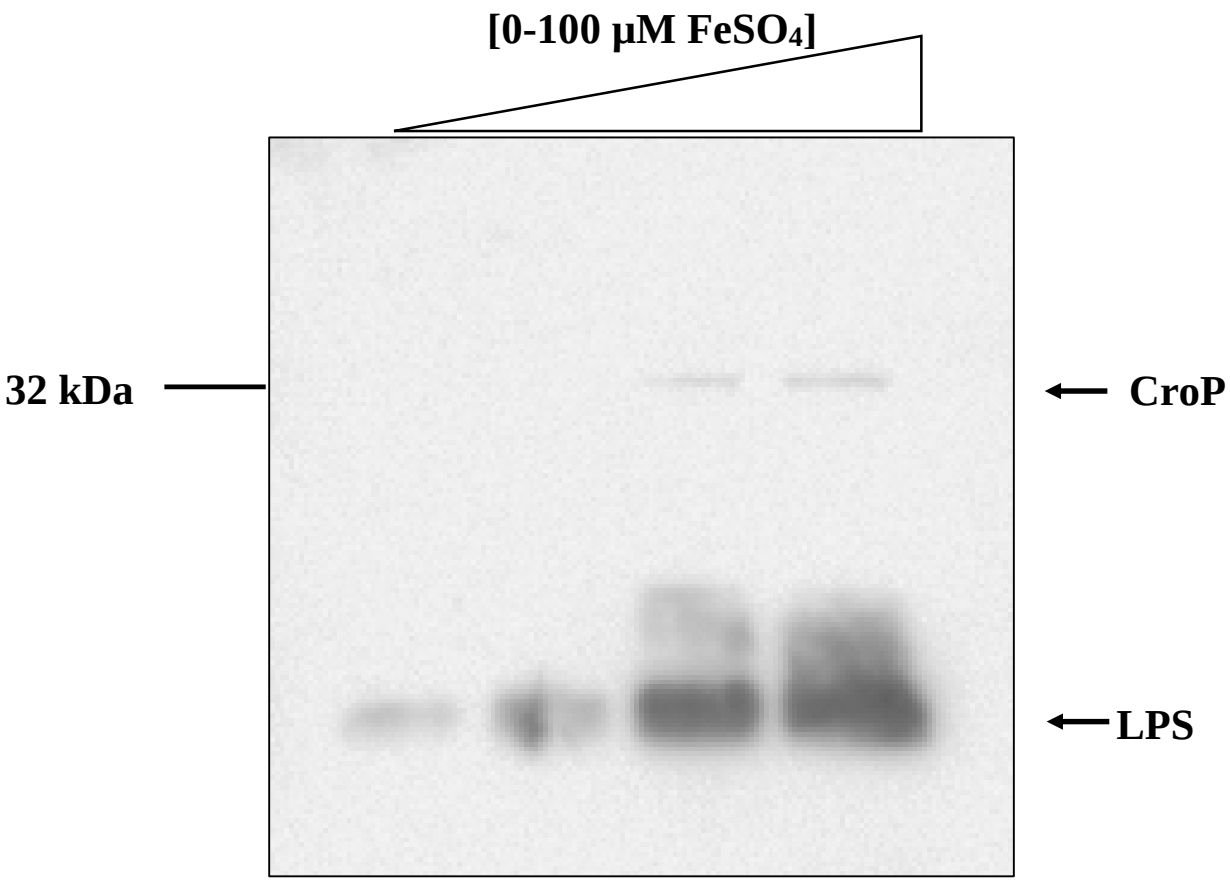

Figure 4.0: Iron induces OM vesiculation. The Δ*waaL* strain was grown in increasing concentrations (0, 25, 50 and 100 µM $FeSO_4$) and vesicles were isolated from the corresponding supernatants. An anti-CroP Western blot using a polyclonal antibody to detect OMVs by the level of CroP. The antibody also detects LPS. Results are representative of three independent experiments.

***C. rodentium*-derived OMVs are bactericidal to the Δ*waaL* strain grown in the absence of iron.** As many reports in the literature have stated that OMVs are bactericidal especially when they originate from pathogens, we tested whether the OMVs collected from the Δ*waaL* strain grown in 100 µM $FeSO_4$ were bactericidal. A MIC assay was then performed using a concentration range of vesicles, from 0 to 128 µg/ml, as determined by the OMV protein concentration that inhibits the growth of a constant concentration of Δ*waaL* and Δ*waaL*Δ*pmrC*Δ*cptA* bacterial cells. From Table 4.1, growth inhibition was monitored in the absence (-Iron) or presence (+Iron) of 25 µM $FeSO_4$. In the absence of iron, the minimal concentration of vesicles that inhibited Δ*waaL* growth was 8 µg/ml and for the Δ*waaL*Δ*pmrC*Δ*cptA* strain, it was 0.25 µg/ml of OMVs. These results suggest that *pmrC* and *cptA* are involved in the OM barrier protection against vesicle-mediated bactericidal effects. In agreement with this observation, in the presence of 25 µM $FeSO_4$, the minimal concentration of OMVs that inhibited growth was greater than 128 µg/ml, whereas the MIC value did not change for the Δ*waaL*Δ*pmrC*Δ*cptA* strain. Taken together, these data suggest that the OMVs collected from the Δ*waaL* strain grown in high iron are bactericidal. In addition, the bacterial response to micromolar iron concentrations shields bacteria from the bacteriostatic effects of OMVs. The iron response includes the induction of PmrAB, which consequently leads to OM barrier fortification through the expression of *pmrC* and *cptA*, which counteracts specifically the bactericidal effect of OMVs.

Table 4.1: MIC of vesicles for Δ*waaL* and Δ*waaL*Δ*pmrC*Δ*cptA* strains

Strain and Condition	MIC of Vesicles (µg/ml)
Δ*waaL* (-Iron)	8
Δ*waaL*Δ*pmrC*Δ*cptA* (-Iron)	0.25
Δ*waaL* (+Iron)	>128
Δ*waaL*Δ*pmrC*Δ*cptA* (+Iron)	0.25

4.5 DISCUSSION

The mechanism of OM vesiculation in Gram-negative bacteria remains unclear. Release of OMVs depends on a local decrease of the number of contacts made between the OM and peptidoglycan, through regulation of such OM proteins and lipoproteins such as OmpA and Lpp, which are known to interact with the peptidoglycan meshwork [114]. Here, we showed that the production of OMVs is dependent on the iron concentration in the medium. This observation implies that LPS biosynthesis, through modulation of LpxC activity by iron, itself is involved in OM vesiculation, thus adding a novel twist to understanding the mechanism by which Gram-negative bacteria produce OMVs.

We had previously showed that the *C. rodentium* Δ*waaL* exhibits an iron-dependent increase in LPS production in minimal media containing 0 to 50 μM $FeSO_4$, whereas total LPS content decreased when this strain was grown in the presence of 100 μM $FeSO_4$. Where does all the extra LPS go? Seeing that the Δ*waaL* did not demonstrate any growth defects in any of the iron concentrations used, we speculated that the extra LPS may have been secreted into the supernatant and hence, we decided to see whether we could isolate vesicles from these culture supernatants, as LPS is rarely secreted in its pure form due to its aggregative property [112]. To our surprise, by probing for CroP, an OM protease found in *C. rodentium*, we found that it was detectable in the culture supernatants grown with 50 and 100 μM $FeSO_4$ along with a crossreacting LPS band, which highly suggests the presence of vesicles in these samples (Fig. 4.0). Thus, the response to iron, which includes PmrAB induction, may include an envelope stress response, such as σ^E, Cpx or Rcs. OM vesiculation has been attributed to the σ^E response, as it has been shown to promote transcription of two sRNAs, MicA and MicL, which bind the *ompA* and *lpp* mRNAs, respectively, thereby decreasing the cellular levels of these proteins [115, 121, 194]. As the role of OmpA and

Lpp in maintaining OM integrity have been previously described, a decrease in these components of the cell envelope results in OM vesiculation [114]. Interestingly, RseB, an IM regulator of the σ^E response that exerts its effect by binding and stabilizing the periplasmic domain of RseA, which sequesters σ^E in the cytoplasm, was found to bind LPS [199]. Therefore, we suggest that the response to micromolar concentrations of iron induces the σ^E response, due to an increase in LPS biosynthesis. Unsequestered periplasmic LPS, meaning LPS unbound by any chaperone, is likely present under our experimental conditions, as the cell envelopes were found to demonstrate a dramatic increase in LPS content with the addition of 25 µM $FeSO_4$ to the growth medium compared to the absence of iron (data not shown). The addition of 50 or 100 µM $FeSO_4$ should even have a more dramatic effect in activating the σ^E response, and thus induce OM vesiculation.

Interestingly, the *C. rodentium*-derived OMVs were shown to be bactericidal against the Δ*waaL* strain in the absence of iron, whereas the addition of iron to the growth medium resulted in protection from these effectors (Table 4.1). Therefore, the bacterial response to iron, which includes the production of OMVs, would also include protection against these vesicles. *C. rodentium* OMVs are probably intrinsically toxic towards the other members of the microbiota, allowing *C. rodentium* to outcompete the other bacteria comprising the community. The effector of the vesicle that gives it its toxic effect remains to be identified. OMVs from *Citrobacter freundii* were shown to be bactericidal against Gram-positive and Gram-negative bacteria due to the presence of peptidoglycan hydrolases [128]. Do *C. rodentium* OMVs contain similar enzymes which are responsible in killing competing bacterial species? CroP, the main OM protease of *C. rodentium*, has been shown to cleave antimicrobial peptides. But may it cleave bacterial products? The study of the bactericidal activity of OMVs produced by a *C. rodentium* Δ*croP* strain will shed some light on this question.

Altogether, our data suggest that OMVs, as produced by the response to iron, is a novel topic that should be investigated given the importance of iron in host-pathogen interaction. Therefore, OMVs represent a novel interface of this interaction that may be physiologically relevant than bacterial cell-host interaction.

ACKNOWLEDGEMENTS

This work was supported by Natural Sciences and Engineering Research Council (NSERC, RGPIN-217482) and the Canadian Institutes of Health Research (CIHR, MOP-15551). C.V. was supported by a NSERC graduate scholarship.

PREFACE TO CHAPTER 5

Chapter 5 recapitulates the main findings of this thesis and discusses what experiments could be performed in the future.

Chapter 5: Conclusions and Future Perspectives

5.1 Conclusions

The main conclusion of the work presented in this thesis is that PmrC- and CptA-mediated pEtN modifications possess roles extending beyond simply conferring resistance to AMPs. They are a means by which *C. rodentium*, and most probably other members of the *Enterobacteriaceae*, promote LPS transfer to the OM when iron is present in the environment. These pEtN modifications are required because iron positively enhances the activity of LpxC, responsible for the committed step of lipid A synthesis, and hence increases LPS production. Therefore, lack of PmrAB-regulated pEtN modifications results in a loss of OM integrity, due to the inability of the mutant (Δ*pmrC*Δ*cptA*) to properly deliver LPS to its final destination, the OM. This phenotype results in increased susceptibility to hydrophobic antibiotics as there are breaches in the OM of this mutant, as well as in the accumulation of free lipid A when this strain is grown in the presence of micromolar concentrations of iron. This conclusion is supported by experimental facts. First, complementation of the Δ*pmrC*Δ*cptA* strain with either pWSK-*pmrC* or pWSK-*cptA* reinforced the OM permeability barrier, which is depicted by the increased resistance of the Δ*pmrC*Δ*cptA*/pWSK-*pmrC* and Δ*pmrC*Δ*cptA*/pWSK-*cptA* strains to hydrophobic antibiotics and SDS, as well as decreased permeability to EtBr and NPN. Second, complementation of the Δ*waaL*Δ*pmrC*Δ*cptA* strain with either pWSK-*pmrC* or pWSK-*cptA* decreased the level of free lipid A in this strain, indicating that pEtN modifications promote LPS turnover. Third, to make the link between the effect of pEtN modifications on both membrane integrity and LPS turnover, it was shown that PmrC and CptA promoted transfer of LPS subunits to the OM. Thus, the role of PmrAB-regulated pEtN modifications is central to OM biogenesis in *C. rodentium* and in probably most other members of the *Enterobacteriaceae*.

The function of pEtN-modified LPS at the OM was then studied. The initial question posed was where does the surplus of LPS, as induced by iron, go? Supernatants from the various strains were then analyzed for vesicles. The Δ*waaL* strain displayed an iron-dependent increase in the concentration of vesicles isolated from the supernatant, suggesting that the mechanism of vesicle formation is dependent on the concentration of iron in the medium. This suggests that the Gram-negative bacterial response to micromolar concentrations of iron, as mediated in part by LpxC and PmrAB, includes the production of vesicles (Fig. 5.0). To verify whether these vesicles were bioactive, they were incubated with the Δ*waaL* and Δ*waaL*Δ*pmrC*Δ*cptA* strains to determine if they were bactericidal, as vesicles isolated from pathogens have been noted to contain hydrolases. Δ*waaL*-derived OMVs were found to be bactericidal against the Δ*waaL*Δ*pmrC*Δ*cptA* strain and less toxic towards the Δ*waaL* strain itself, indicating that the response to iron, which includes PmrAB transcription of *pmrC* and *cptA*, confers protection against the OMVs it produces. Therefore, the response to iron includes protection against potentially destructive effectors.

Most importantly, the work in this thesis has demonstrated a relationship between iron, PmrAB-regulated LPS modifications, more specifically PmrC- and CptA-mediated pEtN modifications, LPS transfer to the OM and OMV production. The surplus of LPS produced, as triggered by iron, is ultimately secreted as part of OMVs. As the Δ*pmrC*Δ*cptA* strain accumulates free lipid A in the presence of iron that is not converted into LPS and demonstrates an accumulation of LPS through its cell envelope, it is safe to assume that PmrC and CptA aid in the process of OM vesiculation. Thus, pEtN modifications do possess multiple roles in *C. rodentium* that are most probably conserved throughout *Enterobacteriaceae*.

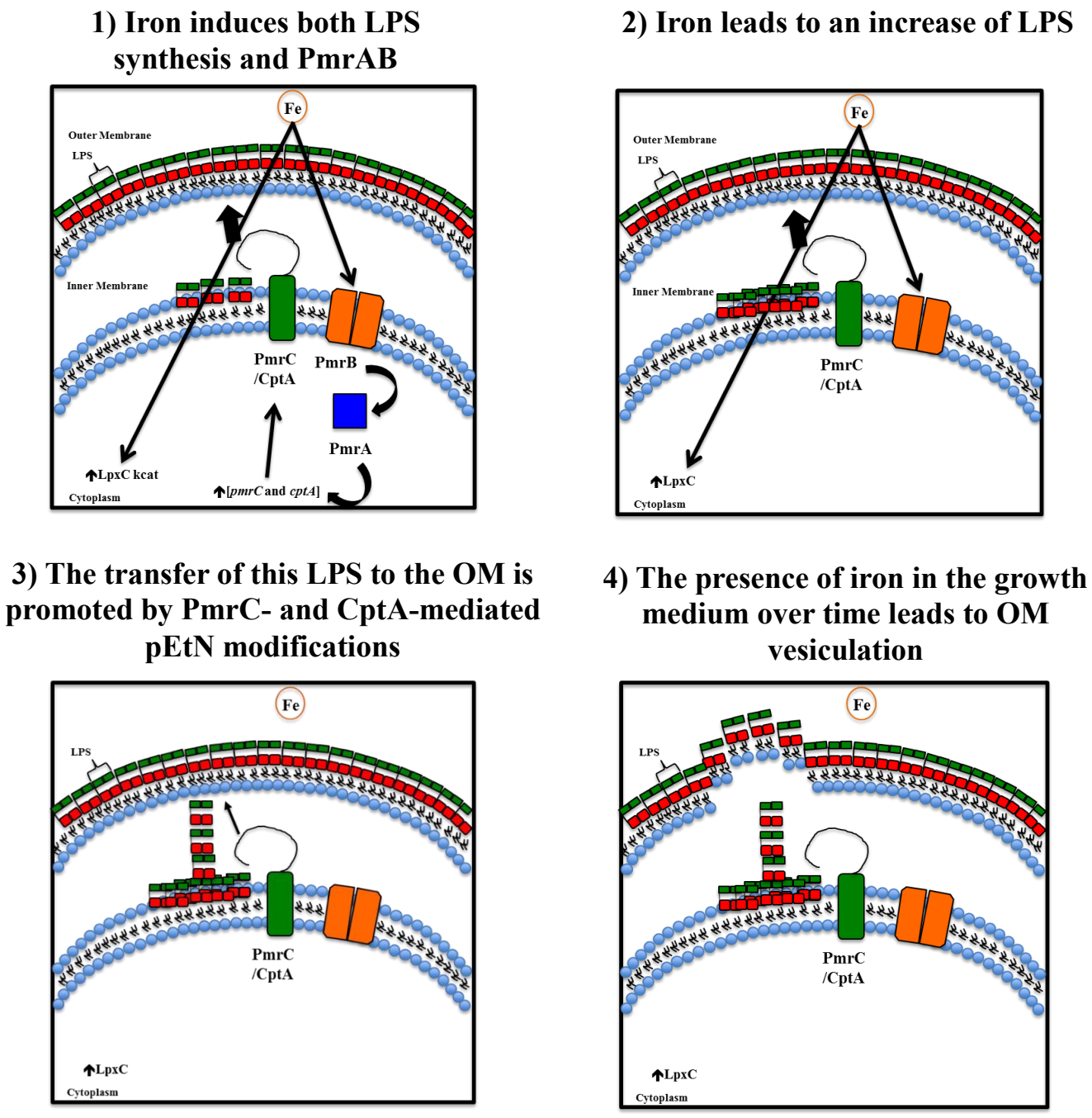

Figure 5.0: The response to micromolar concentrations of iron leads to OM vesiculation in *C. rodentium*.

PmrC and CptA may play as such underscribed but yet important roles in Gram-negative infections in response to an environment where micromolar concentrations of iron are found. Known examples of such environments include the gastrointestinal tract and the bloodstream during the late stages of sepsis [110, 111]. In understanding antibiotic resistance, the environment in which bacteria are found is usually overlooked but is crucial such as the case presented in this thesis. The addition of iron to the growth medium fortifies the OM barrier, an observation that would have been overlooked if the wild-type strain were grown in standard laboratory media, which have undefined concentrations of iron. Thus, inhibiting the pEtN transferases, which act as virulence factors as they are not required for cell viability, may render Gram-negative pathogens more susceptible to the immune system and to antibiotic treatment. Thus, inhibitors of PmrC and CptA could render antibiotics that do not cross the OM useful against Gram-negative bacteria and alleviate the pressure of finding novel antibiotics.

In addition, the finding that adding iron in micromolar concentrations to the growth medium induces OM vesiculation in a wild-type strain may be useful knowledge for the development of vaccines using OMVs as adjuvants. Understanding the mechanism of OM vesiculation provides many advantages. One of these advantages is that, as opposed to non-native OM vesicles, which are generated by mechanical disruption of bacteria, OMVs, as produced by the response to iron may be more physiologically active, given that they are generated naturally by bacteria.

5.2 Future Perspectives

5.2.1 Visualization of the Δ*waaL*Δ*pmrC*Δ*cptA* strain grown in the presence of iron

All of the data presented up to now suggest that the *C. rodentium* Δ*waaL*Δ*pmrC*Δ*cptA* strain exhibits a LPS turnover defect, more specifically at the level of lipid A, and transfer of LPS subunits to the OM when grown in the presence of micromolar concentrations of iron. This phenotype is reminiscent of the Lpt-depleted strains described by Sperandeo *et al*. [55]. These strains exhibited periplasmic invaginations under depletion of Lpt proteins, as described by transmission electron microscopy, which represented accumulation of LPS in the periplasm. An experiment to do for this project would be to describe the Δ*waaL*Δ*pmrC*Δ*cptA* strain grown in the absence or presence of iron to the determine effect of iron on LPS transfer to the OM. The procedure to follow is described in Ogura *et al*. [200].

5.2.1.1 Transmission electron microscopy

Bacterial cells (*C. rodentium* Δ*waaL* and Δ*waaL*Δ*pmrC*Δ*cptA*) will be subcultured from an overnight culture (1:100) into 40 ml of N-minimal media supplemented with 0.2% glucose containing 1 mM $MgCl_2$ and grown at 37ºC until an optical density at 600 nm (OD_{600nm}) of 0.4 is reached. An equal volume of cells (20 ml) for each strain will be centrifuged (10 min, 1,200 × *g*) and washed once in 20 ml of 1× PBS. Cells will be centrifuged once more (10 min, 1,200 × *g*) and resuspended into 20 ml N-media supplemented with 0.2% glucose containing either 10 µM $MgCl_2$ or 10 µM $MgCl_2$ and 25 µM $FeSO_4$. Cells will be grown for an additional two hours at 37ºC until an OD_{600nm} of ~1 is reached. Cells will then be diluted to a final OD_{600nm} of 0.5 and 1 ml of the diluted culture will be fixed with glutaraldehyde at a final concentration of 3%, followed by post-fixation with 1% (w/v) OsO_4. The fixed cells will be dehydrated through a graded ethanol series and embedded in Spurr's low viscosity embedding medium. Ultrathin section of the fixed cells will be prepared using an ultramicrotome (LKB2088 Ultratome V) equipped with glass knives and

stained with 2% (w/v) uranyl citrate and Reynolds lead citrate stain. The ultra-thin bacterial sections will then be viewed under a transmission electron microscope operating at 100 kV. The Δ*waaL* strain will be used as a negative control for this experiment, as no membrane invaginations are expected to be visualized under these conditions.

5.3 Identification of LPS Species Transferred to the OM by PmrC versus CptA.

As it is suggested that PmrC- and CptA- mediated pEtN modifications have different roles, the current hypothesis is that they promote transfer of distinct LPS species to the OM.

5.3.1 Whole-cell lysate LPS extraction of wild-type *C. rodentium*, Δ*pmrC*Δ*cptA*, Δ*pmrC*Δ*cptA*/pWSK-*pmrC* and Δ*pmrC*Δ*cptA*/pWSK-*cptA*.

Previously, sucrose gradient centrifugation was performed using rough LPS strains (Δ*waaL*, Δ*waaL*Δ*pmrC*Δ*cptA*, Δ*waaL*Δ*pmrC*Δ*cptA*/pWSK-*pmrC* and Δ*waaL*Δ*pmrC*Δ*cptA*/pWSK-*cptA*) to monitor LPS transfer efficiency from the IM to the OM, it is important not to neglect the contribution of O-antigen in the transfer of LPS subunits to the OM. The current hypothesis is that lipid A-core pEtN modifications, mediated by PmrC and CptA, promote transfer of lipid A-core subunits to the OM, over full-length LPS capped with O-antigen.

A first experiment to perform is a whole-cell lysate LPS extraction of cells grown in minimal media containing increasing concentrations of iron (0, 25, 50 and 100 µM $FeSO_4$) to determine whether there is an increase in the population of lipid A-core species over full-length LPS over the concentration range of iron tested. Cultures will then be normalized to an OD_{600nm} of

0.4 and centrifuged (10 min, 1,200 × *g*). Bacterial pellets will then resuspended in 300 µl of SDS sample buffer and boiled for 15 minutes. Samples will be cooled at room temperature for 15 minutes and 10 µl of a 10 mg/ml solution of proteinase K will be added to each sample, and will then be incubated at 59ºC for 3 hours. 200 µl of a phenol solution equilibrated in Tris-HCl pH 7.5 will be added to each sample and vortexed vigorously for 15 seconds. Samples will be heated in a water bath at 65°C for 15 min and vortexed every 5 min for 15 seconds. Immediately after this incubation, 1 ml of diethyl ether will be added to each sample. Samples will then be centrifuged (10 min, 20,600 × *g*) to separate the organic and aqueous phases. The bottom (aqueous) phase (500 µl) will then be collected and transferred to a new microcentrifuge tube. To increase the purity of the recovered LPS from the whole-cell lysates, another 1 mL of diethyl ether will be added, and each sample will be centrifuged once more (10 min, 20,600 × *g*). The bottom layer (500 µl), consisting of the purified LPS, will then be collected and transferred to a new microcentrifuge tube.

5.3.1.1 Preliminary results

Preliminary results demonstrate that, in response to iron, wild-type C. *rodentium*, which is a smooth LPS-producing bacterial species, promotes transfer of short LPS species in response to iron (Fig. 5.1). The Δ*pmrAB* strain demonstrates a defect in LPS turnover in the presence of iron, as was determined for the Δ*waaL*Δ*pmrC*Δ*cptA* strain. The defect is present at the level of lipid A-core species when comparing wild-type *C. rodentium* and Δ*pmrAB* grown under the same conditions (Fig. 5.1). Hence, these results suggest PmrAB, as well as the covalent LPS modifications it regulates, most notably the pEtN modifications conferred by PmrC and CptA, promote the transfer of lipid A-core species to the OM in the presence of iron. When relating this

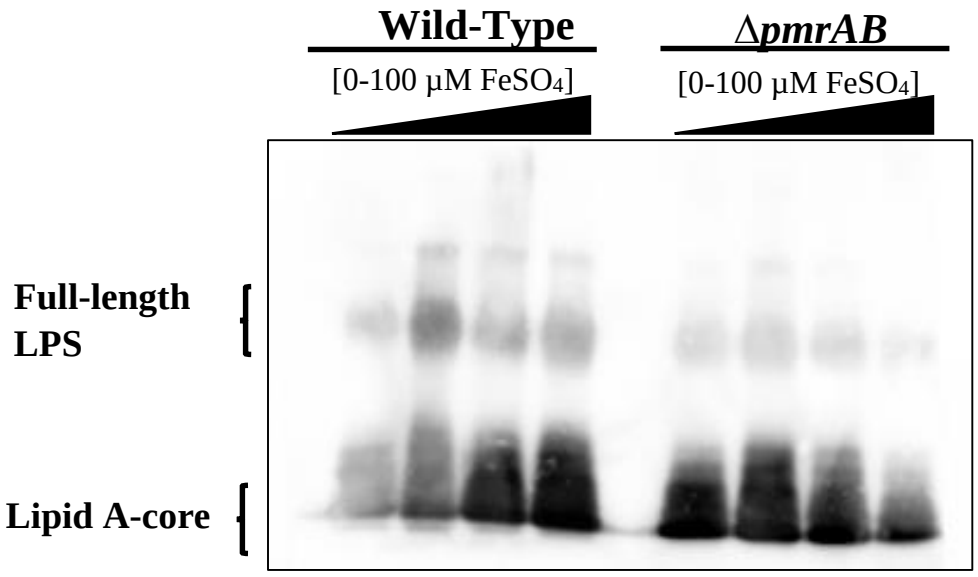

Figure 5.1: Iron promotes biosynthesis of short LPS species in wild-type *C. rodentium*. Bacterial strains were grown in N-minimal media containing 0, 25, 50 or 100 µM $FeSO_4$. LPS was extracted from whole-cell lysates using the hot water-phenol method, separated by 12.5% SDS-PAGE and probed for KDO content by anti-KDO immunoblot.

observation to physiological conditions, members of the *Enterobacteriaceae* have been shown to shorten their LPS layer in response to hostile conditions, such as in the gastrointestinal tract or within macrophages, where free iron and magnesium concentrations may induce the PmrAB and PhoPQ two-component systems, respectively [38].

5.3.2 Identification of LPS core species transferred to the OM by PmrC and CptA.

As the hypothesis is that PmrC and CptA mediate the transfer of lipid A-core species to the OM in response to PmrAB-inducing conditions, most notably micromolar concentrations of iron, the rough LPS (Δ*waaL*) strains will be utilized to describe the LPS structure promoted by both pEtN transferases. The hypothesis is that the PmrC-mediated pEtN modification promotes biosynthesis and transfer of lipid A-KDO_2, as the KDO residues are added in the inner leaflet of the IM, before PmrC can act on the LPS subunit at the outer leaflet of the IM. CptA, however, only adds pEtN on the heptose-I residue phosphoryl group, therefore a larger lipid A-core species is predicted to be synthesized and transferred to the OM by the CptA-conferred pEtN modification. The differences in LPS composition may explain the differential roles and expression levels of *pmrC* and *cptA in vivo*. Therefore, the analysis of the core is most important to decipher which LPS species are promoted by each pEtN modification. The procedure to identify the core residues present by mass spectrometry in each strain is described in St. Michael *et al*.[201].

5.3.2.1 Gas liquid chromatography mass spectrometry

Briefly, the Δ*waaL*, Δ*waaL*Δ*pmrC*Δ*cptA*, Δ*waaL*Δ*pmrC*Δ*cptA*/pWSK-*pmrC* and Δ*waaL*Δ*pmrC*Δ*cptA*/pWSK-*cptA* strains will be grown in the presence or absence of iron to

determine the relative abundance of each core type in both conditions, as described previously. Pellets will be freeze-dried and then washed with organic solvents (1× ethanol, 2× acetone, 2× light petroleum ether) to remove contaminating lipids. LPS will be extracted by the hot water phenol method as described previously and the collected aqueous phase will be dialyzed against dH_2O for 48 hours. The retentate will be freeze-dried and resuspended in dH_2O and treated with DNase and RNase for four hours at 37ºC, followed by a treatment with proteinase K for four hours at 37 ºC. Small peptides will be removed by dialysis, and the retentate will be once again freeze-dried. The retentate will be diluted in water and centrifuged (15 min, 8,000 × *g*). The supernatant will then be centrifuged (5 h, 100,000 × *g*). The pellet will represent purified LPS. The purified LPS will be resuspended in sterile dH_2O and freeze-dried. The core oligosaccharide will be isolated from the purified LPS samples by treatment with acetic acid at 100ºC for 1.5 hours. Insoluble lipid material will be removed by centrifugation (5,000 × *g*). Core oligosaccharide samples will be hydrolyzed using trifluoroacetic acid at 100ºC for four hours. The resulting hydrolysate will be reduced using $NaBD_4$ for 16 hours in H_2O and acetylated with Ac_2O at 100ºC for two hours, using sodium acetate as a catalyst. Samples will then be analyzed by mass spectrometry.

As for expected results, the core samples of the Δ*waaL* and Δ*waaL*Δ*pmrC*Δ*cptA* strains are expected to show numerous peaks by mass spectrometry, given the expression levels of *pmrC* and *cptA* in both the presence and absence of micromolar concentrations of iron. As for the complemented strains, we expect one peak for the Δ*waaL*Δ*pmrC*Δ*cptA*/pWSK-*pmrC* sample corresponding to KDO, whereas more than one peak is expected for the Δ*waaL*Δ*pmrC*Δ*cptA*/pWSK-*cptA* core sample, given the hypothesis that core oligosaccharide is composed of more than only KDO residues in this strain.

5.4 Analysis of the Δ*ybiP* strain

Performing a BlastN search using the nucleotide sequence of *pmrC* as a query returns *cptA* (*yjiP*), *eptB* and an ORF encoding a putative pEtN transferase called *ybiP*. The function of EptB has been described, as it catalyzes the addition of pEtN to the outer most KDO residue of the core in response to micromolar concentration of Ca^{2+} [202]. However, the LPS moiety to which YbiP adds pEtN is unknown.

5.4.1 Preliminary results

By determining the MIC of novobiocin for the Δ*ybiP* strain in the absence or presence of iron, we determined whether the effect on the MIC of novobiocin is iron-dependent, and whether the Δ*ybiP* strain acts like wild-type *C. rodentium* or the Δ*waaL* strain under these conditions. From Table 5.0, we observe that the Δ*ybiP* acts like a rough LPS strain as it demonstrates increased resistance to novobiocin compared to the wild-type strain in the absence of iron in the media. However, the Δ*ybiP* does not display the iron-dependent increase in novobiocin resistance that the Δ*waaL* strain does in response to the addition of 25 μM $FeSO_4$ to the growth medium. This effect may be due to defective transfer of full-length LPS rather than deficient biosynthesis of full-length LPS, which is the case for the *waaL* deletion mutants.

5.4.2 Analysis of the Δ*ybiP* strain cell envelope by discontinuous sucrose gradient centrifugation.

Strain	**MIC (-iron) (µg/ml)**	**MIC (+iron) (µg/ml)**
Wild-type *C. rodentium*	4	8
Δ***waaL***	8	32
Δ***ybiP***	32	32

Table 5.0. MIC values of novobiocin for wild-type *C. rodentium*, Δ*waaL* and Δ*ybiP* in the absence (-iron) or presence (+iron) of 25 µM $FeSO_4$.

As the Δ*ybiP* strain is non-responsive to iron in not having an increased MIC to novobiocin in minimal media supplemented with $FeSO_4$, the following experiments will be done in N-minimal media supplemented with 1 mM $MgCl_2$. The variable will be time as opposed to the response to iron. We assume that the accumulation of full-length LPS in the IM of Δ*ybiP* strain to increase with time compared to the wild-type *C. rodentium*. Bacterial strains (wild-type and Δ*ybiP*) will be subcultured 1:100 from overnight LB cultures into 250 ml of N-minimal media supplemented with 0.2% glucose and 1 mM $MgCl_2$ and grown with shaking at 37ºC for three hours (3 h. time point). A volume corresponding to an OD_{600nm} of 0.7 will be centrifuged (10 min, 1,200 × *g*) and the pellets will be kept on ice. Bacterial cultures will then grown for an additional three hours, after which a second volume corresponding to an OD_{600nm} of 0.7 will be collected and centrifuged (10 min, 1,200 × *g*) to collect the bacterial pellets corresponding to this time point (6 h) . Spheroplasts will then be made resuspending the bacterial pellets corresponding to both time points (3 h and 6 h) in 1 mL of 10 mM Tris-HCl buffer pH 7.5 containing 0.75 M sucrose. 100 µl of a 100 µg/ml lysozyme solution will then be added to each cell suspension and these will be incubated on ice for two minutes. 1 ml of an ice-cold 1.5 mM EDTA pH 7.5 solution will then be added to each of the suspensions. Incubation on ice for one hour will follow, with careful shaking every 10 minutes, resulting in the formation of spheroplasts. Lysis of the spheroplasts will be performed using a sonic dismembrator (intensity level 6, 3 times, 10 seconds per time and cooled on ice between sonic bursts). Cell lysates will then be centrifuged (20 min, 1,200 × *g*) and cell supernatants will be collected. Supernatants will be centrifuged (2 h., 140,000 × *g*) using a MLA-80 rotor. Supernatants will be decanted and pellets will be homogenized using a 26G syringe needle in an ice-cold 3.3 mM Tris-HCl pH 7.5 buffer solution containing 0.25 M sucrose and 1 mM EDTA. Total membranes will be collected by centrifugation for two hours. Total membranes will be

homogenized using a 26G syringe needle and resuspended in 1 ml of a 25 % sucrose (w/v) containing 5 mM EDTA. Membranes will then be diluted with a 25% sucrose solution buffered with 5 mM EDTA to give a final volume of 500 µl. This total volume of membranes will be then applied to the top of a sucrose gradient, consisting of five 2 ml layers of sucrose solutions, ranging from 30 to 50% with 5% increments, unto 0.5 ml of a 55% layer, all buffered by 5 mM EDTA. Gradients will then be centrifuged at 4ºC (16 h, 150,000 × *g*) using a SW32.1 Ti rotor. 380 µl fractions will be collected starting from the top, resulting in a total of 29 fractions. 10 µl of each odd-numbered fraction will then then loaded onto a 20% SDS-PAGE gel.

As for expected results, the Δ*ybiP* strain will probably accumulate full-length LPS in its IM over the time period of the experiment compared to the wild-type strain. If pEtN addition to LPS promotes the transfer of LPS to the OM, YbiP-mediated addition of pEtN would regulate the transfer of full-length LPS.

5.5 Characterization of OMVs produced by Δ*waaL*

The observation that the *C. rodentium* Δ*waaL* strain produces OMVs in response to micromolar iron concentrations requires further confirmation. The evidence of LPS and OM protease concentrations increasing with iron concentration in the medium suggest that this strain is in fact producing OMVs. The procedure to follow to visualize OMVs produced by the strains is by cryo-transmission electron microscopy as described in Perez-Cruz *et al*. [203].

5.5.1 Cryo-transmission electron microscopy of Δ*waaL* OMVs

The *C. rodentium* Δ*waaL* strain will be grown in media containing increasing concentration of iron (0, 25, 50 and 100 µM $FeSO_4$). Briefly, bacterial colonies will be cryo-immobilized using a high-pressure freezer. Frozen samples will then be freeze-substituted in a automatic freeze substitution system, where the substitution was performed in pure acetone containing 2% (w/v) OsO_4 and 0.1% (w/v) uranyl acetate at 90ºC for 72 hours. The temperature will be gradually decreased (5°C/hour) to 4°C, held constant for two hours, and then finally increased to room temperature and maintained for one hour. Samples will be washed for one hour in acetone at room temperature and infiltrated in a graded series of Epon-acetone mixtures: 1:3 for two hours, 2:2 for two hours, 3:1 for 16 hours, and pure Epon 812 for 30 hours. Samples will be embedded in fresh Epon and polymerized at 60°C for 48 hours. Ultra-thin sections will be cut with UCT ultramicrotome and mounted on carbon-coated copper grids. Sections will be post-stained with 2% (w/v) aqueous uranyl acetate and lead citrate and examined in an electron microscope at an acceleration voltage of 120 kV.

The number of vesicles observed for the Δ*waaL* strain grown in the presence of increasing concentrations of iron is hypothesized to increase, as accumulation of unsequestered LPS in the periplasmic space should induce vesiculation by the σ^E response through a mechanism dependent on RseB. These experiments will in fact confirm the interrelation between iron, PmrAB-regulated covalent LPS modifications and OM vesiculation.

5.6 Determination of the envelope stress responses that are activated in the response to iron

To gain a better understanding of the bacterial response to micromolar iron, the stress responses that may be activated by such a signal will be monitored. Thus, expression of the σ^E,

Cpx, Bae and Rcs response will have to be determined. As the response to iron includes an increase in LPS production by the bacteria, it is safe to assume that periplasmic LPS accumulation may serve as inducing signal. RseB, a regulator of the σ^E response, senses unsequestered periplasmic LPS (Fig. 5.2) [199]. In this sense, expression of *lptA* and *lptB*, components of the *lpt* transenvelope complex, has been shown to be regulated by the σ^E response and may suggest a role of this stress response in increasing LPS transport to the OM in response to iron, which both induce LpxC-mediated lipid A synthesis and PmrAB-dependent pEtN transferase expression, necessary for LPS transfer under this condition.

5.6.1 Stress response reporters

The four stress responses will be monitored using a combination of qPCR coupled to β-galactosidase experiments. Keeping in mind that the envelope of the Δ*waaL*Δ*pmrC*Δ*cptA* may be altered in response to iron, it will be interesting to monitor the stress response induction in this strain compared to the Δ*waaL* strain as well as Δ*waaL*Δ*pmrC*Δ*cptA*/pWSK-*pmrC* and Δ*waaL*Δ*pmrC*Δ*cptA*/pWSK-*cptA* strains, thereby evaluating the role of pEtN modifications in regulating individual stress responses.

As for the reporters themselves, the σ^E response will be monitored by the expression level of *rpoE*, which encodes the σ^E factor itself, the Cpx response will be monitored by the expression level of *cpxP*, an IM sensor of misfolded proteins, the Bae response by the expression level of *mdtA*, component of a multi-drug efflux pump, and the Rcs response by the expression level of *wcaD*, a RcsB-regulated gene involved in the production of colanic acid. For example, due to the defect in LPS turnover and transfer to the OM, resulting in a loss of OM integrity, the Δ*waaL*Δ*pmrC*Δ*cptA* may respond by promoting the Rcs response, leading to the production of

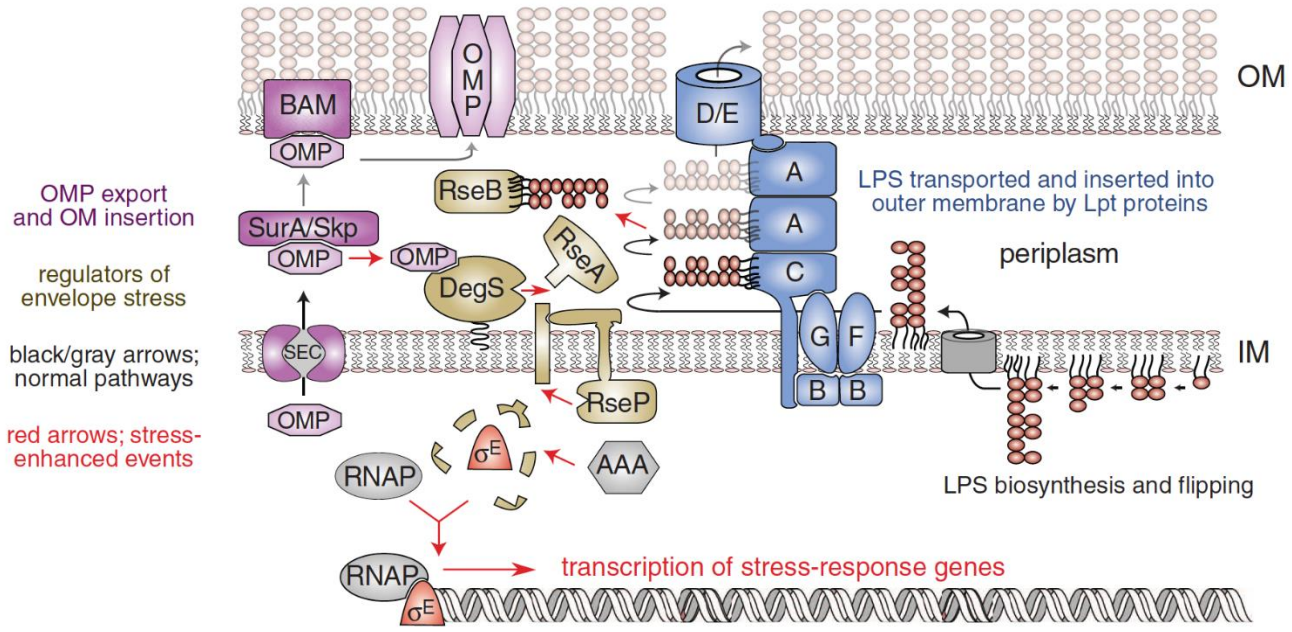

Figure 5.2: RseB senses unsequestered LPS in the periplasm, which in turn activates the σ^E stress response. The presence of micromolar iron concentrations in the growth medium, which induces LPS production in Gram-negative bacteria, may induce the σ^E response by an RseB-dependent mechanism. [Adapted from Lima, S. *et al.*, *Science*, 340, 837-841, (2013)].

colanic acid-modified LPS, reflected by the increased level of expression of *wcaD*. Since a WaaL+ strain is required for production of this modified species of LPS. The smooth LPS *C. rodentium* strain should be used in these experiments.

A set of experiments monitoring expression of the aforementioned reporters will be done initially, including the Δ*waaL* and Δ*waaL*Δ*pmrC*Δ*cptA* strains grown in minimal media containing increasing concentrations of iron (0, 25, 50 and 100 μM $FeSO_4$) to determine whether some stress response are iron-dependent and whether they are pEtN-modification dependent. Another set will include the Δ*waaL* and Δ*waaL*Δ*pmrC*Δ*cptA*/pWSK-*pmrC* and Δ*waaL*Δ*pmrC*Δ*cptA*/pWSK-*cptA* strains grown in the absence or presence of 25 μM $FeSO_4$ to determine the relative contribution of each pEtN modification in promoting or preventing stress responses. Once specific stress responses have been elucidated, transcriptional *lacZ* constructs of genes regulated by the stress response regulon will be made to gain an overview of the stress response involved in the bacterial response to iron.

5.7 Assaying of OMV function in terms of CroP proteolytic activity

Recently, it has been shown that the *Y. pestis* OM Pla protease was able to degrade Fas ligand (FasL), resulting in the prevention of host cell apoptosis and inflammation (Fig. 5.3), extending the role of Pla to cleavage of host immune effectors, as opposed to only cleavage of the fibrinolytic factor plasminogen [204].

The *C. rodentium* OM protease CroP has been shown to degrade AMPs such as C18G and LL37 [153]. However, given that CroP has been found present in OMVs and the fact that packaging of proteins into OMVs is not a random process, its role may be extended beyond

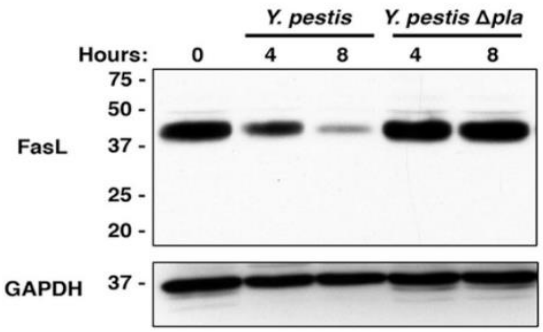

Figure 5.3: *Y. pestis* Pla cleaves FasL from KFL-9 cells, whereas the Δ*pla* strain is unable cleave the immune effector. [Figure adapted from Caulfield *et al*. *Cell Host & Microbe* 15, 424–434, (2014)].

cleavage of host AMPs. Using the same approach as Caulfield *et al*. [203], the objective is to screen the potential of isolated vesicles from *C. rodentium* strain to cleave immune effectors. Similarly to the association of CroP with OMVs produced by *C. rodentium*, Pla was also found present on OMVs produced by *Yersinia pestis* [204], highlighting the fact that OM proteases may have access to substrates which were previously unknown. Although *Y. pestis* and *C. rodentium* have different niches, as they are intracellular and extracellular pathogens, respectively, both have to interact with the host to cause disease. Recently, it has been shown that enterohemmorhagic *E. coli* (EHEC), for which *C. rodentium* is used as the infection model in mice, employs OMVs containing hemolysin that permeabilize host endothelial cell microvasculature and intestinal cell mitochondria [195]. The fact that EHEC produces OMVs in the gut suggests that *C. rodentium* may do the same. As the concentration of free iron in the mouse gut is sufficiently high to induce the formation of vesicles, the role of CroP in OMVs may be as important as the one attributed to Pla in causing *Y. pestis* pathogenesis. In conclusion, there may be unidentified targets of CroP yet to be uncovered just as the observation that Pla cleaves FasL.

5.8 Characterization of the *arn* operon in *C. rodentium*

As *C. rodentium* does not possess the *arn* operon, perhaps by being solely a murine pathogen, this bacterial species did not experience the same evolutionary pressure to polymyxin B that other Gram-negative species did (i.e *Salmonella*, *Pseudomonas* and *Acinetobacter*), given the potential of the *arn* operon to increase resistance to this AMP 500-fold compared to a strain which does not possess it [96]. The *arn* operon with its native promoter from *S. typhimurium* 14028S was cloned into the pACYC184 vector and electroporated into wild-type *C. rodentium* to evaluate its function.

The hypothesis is that 4-aminoarabinose shares the conserved function of promoting LPS transfer to the OM in bacteria that possess this LPS modification, as in *B. cenopacia* [94]. The battery of experiments (MIC assays with hydrophobic antibiotics, permeability to ethidium bromide assay, β-lactamase release assay, and sucrose density gradient centrifugation using pACYC-*arn* complemented strains) will have to probably be done in N-minimal media supplemented with 50 μM $FeSO_4$ rather than 25 μM $FeSO_4$ to see any potential effect. This concentration coincides with the concentration that produced the maximum output of LPS in the Δ*waaL* strain, and therefore, any effect of 4-aminoarabinose incorporation should be observed at this concentration. The *arn* operon can also be studied in a PmrA constitutive background (*pmrA*505), to ensure that expression of the operon at a maximal level.

Altogether, by addressing these research questions, we will elucidate the functions of covalent LPS modifications and their importance in LPS turnover and OM biogenesis. By doing so, we hope to unveil novel targets to combat Gram-negative multi-drug resistance.

REFERENCES

1. Fischbach, M.A. and C.T. Walsh, *Antibiotics for emerging pathogens.* Science, 2009. **325**(5944): p. 1089-93.
2. Khabbaz, R.F., et al., *Challenges of infectious diseases in the USA.* Lancet, 2014. **384**(9937): p. 53-63.
3. Nordmann, P., et al., *The emerging NDM carbapenemases.* Trends Microbiol, 2011. **19**(12): p. 588-595.
4. Mundy, R., et al., *Citrobacter rodentium of mice and man.* Cell Microbiol, 2005. **7**(12): p. 1697-706.
5. Collins, J.W., et al., *Citrobacter rodentium: infection, inflammation and the microbiota.* Nat Rev Microbiol, 2014. **12**(9): p. 612-23.
6. Wright, G.D., *Something old, something new: revisiting natural products in antibiotic drug discovery1.* Can J Microbiol, 2014. **60**(3): p. 147-154.
7. Bumann, D., *Has nature already identified all useful antibacterial targets?* Curr Opin Microbiol 2008. **11**(5): p. 387-392.
8. Falagas, M.E. and P.I. Rafailidis, *Nephrotoxicity of Colistin: New Insight into an Old Antibiotic.* Clin Infect Dis, 2009. **48**(12): p. 1729-1731.
9. Cassir, N., J.-M. Rolain, and P. Brouqui, *A new strategy to fight antimicrobial resistance: the revival of old antibiotics.* Front Microbiol, 2014. **5**.
10. Park, Y.K., et al., *A single clone of Acinetobacter baumannii, ST22, is responsible for high antimicrobial resistance rates of Acinetobacter spp. isolates that cause bacteremia and urinary tract infections in Korea.* Microb Drug Resist, 2010. **16**(2): p. 143-9.
11. Martinez, J.L. and F. Baquero, *Mutation Frequencies and Antibiotic Resistance.* Antimicrob Agents Chemother, 2000. **44**(7): p. 1771-1777.
12. McManus, M., *Mechanisms of bacterial resistance to antimicrobial agents.* Am J Health-Syst Ph, 1997. **54**(12): p. 1420-1433.
13. Rawat, D. and D. Nair, *Extended-spectrum beta-lactamases in Gram Negative Bacteria.* J Glob Infect Dis, 2010. **2**(3): p. 263-74.
14. Pages, J.M., C.E. James, and M. Winterhalter, *The porin and the permeating antibiotic: a selective diffusion barrier in Gram-negative bacteria.* Nat Rev Microbiol, 2008. **6**(12): p. 893-903.
15. Blair, J.M. and L.J. Piddock, *Structure, function and inhibition of RND efflux pumps in Gram-negative bacteria: an update.* Curr Opin Microbiol, 2009. **12**(5): p. 512-9.
16. Poole, K., *Stress responses as determinants of antimicrobial resistance in Gram-negative bacteria.* Trends Microbiol, 2012. **20**(5): p. 227-234.
17. Kohanski, M.A., et al., *A Common Mechanism of Cellular Death Induced by Bactericidal Antibiotics.* Cell, 2007. **130**(5): p. 797-810.
18. Pankey, G.A. and L.D. Sabath, *Clinical Relevance of Bacteriostatic versus Bactericidal Mechanisms of Action in the Treatment of Gram-Positive Bacterial Infections.* Clin Infect Dis, 2004. **38**(6): p. 864-870.
19. King, A.M., et al., *Aspergillomarasmine A overcomes metallo-beta-lactamase antibiotic resistance.* Nature, 2014. **510**(7506): p. 503-6.
20. Clatworthy, A.E., E. Pierson, and D.T. Hung, *Targeting virulence: a new paradigm for antimicrobial therapy.* Nat Chem Biol, 2007. **3**(9): p. 541-8.

21. Lengeler, J.W., Drews, Gerhart, Shlegel, Hans G. , *Biology of Prokaryotes*. 1999, Stuttgart, Germany.: Blackwell Science.
. 955.
22. Swoboda, J.G., et al., *Wall teichoic acid function, biosynthesis, and inhibition.* Chembiochem, 2010. **11**(1): p. 35-45.
23. Raetz, C.R.H. and C. Whitfield, *Lipopolysaccharide Endotoxins.* Annu Rev Biochem, 2002. **71**(1): p. 635-700.
24. Delcour, A.H., *Outer membrane permeability and antibiotic resistance.* BBA - Proteins and Proteomics, 2009. **1794**(5): p. 808-816.
25. Abdelraouf, K., et al., *Characterization of Polymyxin B-Induced Nephrotoxicity: Implications for Dosing Regimen Design.* Antimicrob Agents Chemother, 2012. **56**(9): p. 4625-4629.
26. Whitfield, C. and M.S. Trent, *Biosynthesis and export of bacterial lipopolysaccharides.* Annu Rev Biochem, 2014. **83**: p. 99-128.
27. Raetz, C.R.H., et al., *Discovery of new biosynthetic pathways: the lipid A story.* J Lipid Res, 2009. **50**(Supplement): p. S103-S108.
28. Gattis, S.G., M. Hernick, and C.A. Fierke, *Active Site Metal Ion in UDP-3-O-((R)-3-Hydroxymyristoyl)-N-acetylglucosamine Deacetylase (LpxC) Switches between Fe(II) and Zn(II) Depending on Cellular Conditions.* J Biol Chem, 2010. **285**(44): p. 33788-33796.
29. Hernick, M., et al., *Activation of Escherichia coli UDP-3-O-[(R)-3-hydroxymyristoyl]-N-acetylglucosamine Deacetylase by Fe2+ Yields a More Efficient Enzyme with Altered Ligand Affinity.* Biochemistry, 2010. **49**(10): p. 2246-2255.
30. Barb, A.W., et al., *Inhibition of lipid A biosynthesis as the primary mechanism of CHIR-090 antibiotic activity in Escherichia coli.* Biochemistry, 2007. **46**(12): p. 3793-802.
31. Lin, L., et al., *Inhibition of LpxC protects mice from resistant Acinetobacter baumannii by modulating inflammation and enhancing phagocytosis.* mBio, 2012. **3**(5).
32. Langklotz, S., M. Schakermann, and F. Narberhaus, *Control of lipopolysaccharide biosynthesis by FtsH-mediated proteolysis of LpxC is conserved in enterobacteria but not in all gram-negative bacteria.* J Bacteriol, 2011. **193**(5): p. 1090-7.
33. Tomaras, A.P., et al., *LpxC inhibitors as new antibacterial agents and tools for studying regulation of lipid a biosynthesis in Gram-negative pathogens.* mBio, 2014. **5**(5): p. e01551-14.
34. Zhou, Z., et al., *Function of Escherichia coli MsbA, an Essential ABC Family Transporter, in Lipid A and Phospholipid Biosynthesis.* J Biol Chem, 1998. **273**(20): p. 12466-12475.
35. Reynolds, C.M. and C.R. Raetz, *Replacement of lipopolysaccharide with free lipid A molecules in Escherichia coli mutants lacking all core sugars.* Biochemistry, 2009. **48**(40): p. 9627-40.
36. Garrett, T.A., N.L.S. Que, and C.R.H. Raetz, *Accumulation of a Lipid A Precursor Lacking the 4'-Phosphate following Inactivation of the Escherichia coli lpxKGene.* J Biol Chem, 1998. **273**(20): p. 12457-12465.
37. Westphal, K., et al., *A trapping approach reveals novel substrates and physiological functions of the essential protease FtsH in Escherichia coli.* J Biol Chem, 2012. **287**(51): p. 42962-71.
38. Chen, H.D. and E.A. Groisman, *The biology of the PmrA/PmrB two-component system: the major regulator of lipopolysaccharide modifications.* Annu Rev Microbiol, 2013. **67**: p. 83-112.

39. DeLucia, A.M., et al., *Lipopolysaccharide (LPS) Inner-Core Phosphates Are Required for Complete LPS Synthesis and Transport to the Outer Membrane in Pseudomonas aeruginosa PAO1.* mBio, 2011. **2**(4).
40. Yethon, J.A., et al., *Salmonella enterica Serovar TyphimuriumwaaP Mutants Show Increased Susceptibility to Polymyxin and Loss of Virulence In Vivo.* Infect Immun, 2000. **68**(8): p. 4485-4491.
41. Sperandeo, P., G. Deho, and A. Polissi, *The lipopolysaccharide transport system of Gram-negative bacteria.* Biochim Biophys Acta, 2009. **1791**(7): p. 594-602.
42. Freinkman, E., et al., *Regulated assembly of the transenvelope protein complex required for lipopolysaccharide export.* Biochemistry, 2012. **51**(24): p. 4800-6.
43. Okuda, S., E. Freinkman, and D. Kahne, *Cytoplasmic ATP hydrolysis powers transport of lipopolysaccharide across the periplasm in E. coli.* Science, 2012. **338**(6111): p. 1214-7.
44. Merten, J.A., K.M. Schultz, and C.S. Klug, *Concentration-dependent oligomerization and oligomeric arrangement of LptA.* Protein Sci, 2012. **21**(2): p. 211-8.
45. Tran, A.X., M.S. Trent, and C. Whitfield, *The LptA protein of Escherichia coli is a periplasmic lipid A-binding protein involved in the lipopolysaccharide export pathway.* J Biol Chem, 2008. **283**(29): p. 20342-9.
46. Villa, R., et al., *The Escherichia coli Lpt transenvelope protein complex for lipopolysaccharide export is assembled via conserved structurally homologous domains.* J Bacteriol, 2013. **195**(5): p. 1100-8.
47. Tran, A.X., C. Dong, and C. Whitfield, *Structure and functional analysis of LptC, a conserved membrane protein involved in the lipopolysaccharide export pathway in Escherichia coli.* J Biol Chem, 2010. **285**(43): p. 33529-39.
48. Freinkman, E., S.S. Chng, and D. Kahne, *The complex that inserts lipopolysaccharide into the bacterial outer membrane forms a two-protein plug-and-barrel.* Proc Natl Acad Sci U S A, 2011. **108**(6): p. 2486-91.
49. Grabowicz, M., J. Yeh, and T.J. Silhavy, *Dominant negative lptE mutation that supports a role for LptE as a plug in the LptD barrel.* J Bacteriol, 2013. **195**(6): p. 1327-34.
50. Ruiz, N., et al., *Nonconsecutive disulfide bond formation in an essential integral outer membrane protein.* Proc Natl Acad Sci U S A, 2010. **107**(27): p. 12245-50.
51. Malojcic, G., et al., *LptE binds to and alters the physical state of LPS to catalyze its assembly at the cell surface.* Proc Natl Acad Sci U S A, 2014. **111**(26): p. 9467-72.
52. Qiao, S., et al., *Structural basis for lipopolysaccharide insertion in the bacterial outer membrane.* Nature, 2014. **511**(7507): p. 108-11.
53. Srinivas, N., et al., *Peptidomimetic antibiotics target outer-membrane biogenesis in Pseudomonas aeruginosa.* Science, 2010. **327**(5968): p. 1010-3.
54. Werneburg, M., et al., *Inhibition of lipopolysaccharide transport to the outer membrane in Pseudomonas aeruginosa by peptidomimetic antibiotics.* Chembiochem, 2012. **13**(12): p. 1767-75.
55. Sperandeo, P., et al., *Functional analysis of the protein machinery required for transport of lipopolysaccharide to the outer membrane of Escherichia coli.* J Bacteriol, 2008. **190**(13): p. 4460-9.
56. Sperandeo, P., et al., *Characterization of lptA and lptB, two essential genes implicated in lipopolysaccharide transport to the outer membrane of Escherichia coli.* J Bacteriol, 2007. **189**(1): p. 244-53.

57. Meredith, T.C., et al., *Modification of lipopolysaccharide with colanic acid (M-antigen) repeats in Escherichia coli.* J Biol Chem, 2007. **282**(11): p. 7790-8.
58. Martorana, A.M., et al., *Complex transcriptional organization regulates an Escherichia coli locus implicated in lipopolysaccharide biogenesis.* Res Microbiol, 2011. **162**(5): p. 470-82.
59. Gunn, J.S. and S.I. Miller, *PhoP-PhoQ activates transcription of pmrAB, encoding a two-component regulatory system involved in Salmonella typhimurium antimicrobial peptide resistance.* J Bacteriol, 1996. **178**(23): p. 6857-64.
60. Monsieurs, P., et al., *Comparison of the PhoPQ regulon in Escherichia coli and Salmonella typhimurium.* J Mol Evol, 2005. **60**(4): p. 462-74.
61. Groisman, E.A., *The Pleiotropic Two-Component Regulatory System PhoP-PhoQ.* J Bacteriol, 2001. **183**(6): p. 1835-1842.
62. Shin, D. and E.A. Groisman, *Signal-dependent binding of the response regulators PhoP and PmrA to their target promoters in vivo.* J Biol Chem, 2005. **280**(6): p. 4089-94.
63. Prost, L.R., et al., *Activation of the bacterial sensor kinase PhoQ by acidic pH.* Mol Cell, 2007. **26**(2): p. 165-74.
64. Bader, M.W., et al., *Recognition of antimicrobial peptides by a bacterial sensor kinase.* Cell, 2005. **122**(3): p. 461-72.
65. Nishino, K., et al., *Identification of the lipopolysaccharide modifications controlled by the Salmonella PmrA/PmrB system mediating resistance to Fe(III) and Al(III).* Mol Microbiol, 2006. **61**(3): p. 645-54.
66. Perez, J.C. and E.A. Groisman, *Acid pH activation of the PmrA/PmrB two-component regulatory system of Salmonella enterica.* Mol Microbiol, 2007. **63**(1): p. 283-93.
67. Prost, L.R. and S.I. Miller, *The Salmonellae PhoQ sensor: mechanisms of detection of phagosome signals.* Cell Microbiol, 2008. **10**(3): p. 576-82.
68. Wosten, M.M. and E.A. Groisman, *Molecular characterization of the PmrA regulon.* J Biol Chem, 1999. **274**(38): p. 27185-90.
69. Lejona, S., et al., *Molecular characterization of the Mg2+-responsive PhoP-PhoQ regulon in Salmonella enterica.* J Bacteriol, 2003. **185**(21): p. 6287-94.
70. Chen, H.D. and E.A. Groisman, *The Biology of the PmrA/PmrB Two-Component System: The Major Regulator of Lipopolysaccharide Modifications.* Annual Review of Microbiology, 2013. **67**(1): p. 83-112.
71. Wosten, M.M., et al., *A signal transduction system that responds to extracellular iron.* Cell, 2000. **103**(1): p. 113-25.
72. Merighi, M., et al., *Resolvase-in vivo expression technology analysis of the Salmonella enterica serovar Typhimurium PhoP and PmrA regulons in BALB/c mice.* J Bacteriol, 2005. **187**(21): p. 7407-16.
73. Zhao, Y., et al., *Identification of genes affecting Salmonella enterica serovar enteritidis infection of chicken macrophages.* Infect Immun, 2002. **70**(9): p. 5319-21.
74. Gunn, J.S., et al., *Genetic and functional analysis of a PmrA-PmrB-regulated locus necessary for lipopolysaccharide modification, antimicrobial peptide resistance, and oral virulence of Salmonella enterica serovar typhimurium.* Infect Immun, 2000. **68**(11): p. 6139-46.
75. Fields, P.I., et al., *Mutants of Salmonella typhimurium that cannot survive within the macrophage are avirulent.* Proc Natl Acad Sci U S A, 1986. **83**(14): p. 5189-93.

76. Kato, A., et al., *Reciprocal control between a bacterium's regulatory system and the modification status of its lipopolysaccharide.* Mol Cell, 2012. **47**(6): p. 897-908.
77. Soncini, F.C., E.G. Véscovi, and E.A. Groisman, *Transcriptional autoregulation of the Salmonella typhimurium phoPQ operon.* J Bacteriol, 1995. **177**(15): p. 4364-71.
78. Shin, D., et al., *A positive feedback loop promotes transcription surge that jump-starts Salmonella virulence circuit.* Science, 2006. **314**(5805): p. 1607-9.
79. Kox, L.F., M.M. Wosten, and E.A. Groisman, *A small protein that mediates the activation of a two-component system by another two-component system.* EMBO J, 2000. **19**(8): p. 1861-72.
80. Cheng, H.Y., Y.F. Chen, and H.L. Peng, *Molecular characterization of the PhoPQ-PmrD-PmrAB mediated pathway regulating polymyxin B resistance in Klebsiella pneumoniae CG43.* J Biomed Sci, 2010. **17**: p. 60.
81. Winfield, M.D. and E.A. Groisman, *Phenotypic differences between Salmonella and Escherichia coli resulting from the disparate regulation of homologous genes.* Proc Natl Acad Sci U S A, 2004. **101**(49): p. 17162-7.
82. Viau, C., et al., *Absence of PmrAB-mediated phosphoethanolamine modifications of Citrobacter rodentium lipopolysaccharide affects outer membrane integrity.* J Bacteriol, 2011. **193**(9): p. 2168-76.
83. Bishop, R.E., et al., *Transfer of palmitate from phospholipids to lipid A in outer membranes of gram-negative bacteria.* EMBO J, 2000. **19**(19): p. 5071-80.
84. Guo, L., et al., *Lipid A acylation and bacterial resistance against vertebrate antimicrobial peptides.* Cell, 1998. **95**(2): p. 189-98.
85. Gunn, J.S., et al., *PmrA-PmrB-regulated genes necessary for 4-aminoarabinose lipid A modification and polymyxin resistance.* Mol Microbiol, 1998. **27**(6): p. 1171-82.
86. Evans, M.E., D.J. Feola, and R.P. Rapp, *Polymyxin B sulfate and colistin: old antibiotics for emerging multiresistant gram-negative bacteria.* Ann Pharmacother, 1999. **33**(9): p. 960-7.
87. Lee, H., et al., *The PmrA-regulated pmrC gene mediates phosphoethanolamine modification of lipid A and polymyxin resistance in Salmonella enterica.* J Bacteriol, 2004. **186**(13): p. 4124-33.
88. Tamayo, R., et al., *Identification of cptA, a PmrA-regulated locus required for phosphoethanolamine modification of the Salmonella enterica serovar typhimurium lipopolysaccharide core.* J Bacteriol, 2005. **187**(10): p. 3391-9.
89. Delgado, M.A., C. Mouslim, and E.A. Groisman, *The PmrA/PmrB and RcsC/YojN/RcsB systems control expression of the Salmonella O-antigen chain length determinant.* Mol Microbiol, 2006. **60**(1): p. 39-50.
90. Pescaretti, M.d.l.M., et al., *The PmrA/PmrB regulatory system controls the expression of the wzzfepE gene involved in the O-antigen synthesis of Salmonella enterica serovar Typhimurium.* Microbiology, 2011. **157**(9): p. 2515-2521.
91. Herrera, C.M., J.V. Hankins, and M.S. Trent, *Activation of PmrA inhibits LpxT-dependent phosphorylation of lipid A promoting resistance to antimicrobial peptides.* Mol Microbiol, 2010. **76**(6): p. 1444-60.
92. Harris, T.L., et al., *Small molecule downregulation of PmrAB reverses lipid A modification and breaks colistin resistance.* ACS Chem Biol, 2014. **9**(1): p. 122-7.

93. Beceiro, A., et al., *Biological cost of different mechanisms of colistin resistance and their impact on virulence in Acinetobacter baumannii.* Antimicrob Agents Chemother, 2014. **58**(1): p. 518-26.
94. Hamad, M.A., et al., *Aminoarabinose is essential for lipopolysaccharide export and intrinsic antimicrobial peptide resistance in Burkholderia cenocepacia.* Mol Microbiol, 2012. **85**(5): p. 962-74.
95. Raetz, C.R., et al., *Lipid A modification systems in gram-negative bacteria.* Annu Rev Biochem, 2007. **76**: p. 295-329.
96. Nikaido, H., *Molecular basis of bacterial outer membrane permeability revisited.* Microbiol Mol Biol Rev, 2003. **67**(4): p. 593-656.
97. Moskowitz, S.M., R.K. Ernst, and S.I. Miller, *PmrAB, a two-component regulatory system of Pseudomonas aeruginosa that modulates resistance to cationic antimicrobial peptides and addition of aminoarabinose to lipid A.* J Bacteriol, 2004. **186**(2): p. 575-9.
98. Nummila, K., et al., *Lipopolysaccharides of polymyxin B-resistant mutants of Escherichia coli are extensively substituted by 2-aminoethyl pyrophosphate and contain aminoarabinose in lipid A.* Mol Microbiol, 1995. **16**(2): p. 271-8.
99. McCoy, A.J., et al., *Identification of Proteus mirabilis mutants with increased sensitivity to antimicrobial peptides.* Antimicrob Agents Chemother, 2001. **45**(7): p. 2030-7.
100. Cullen, T.W., et al., *Characterization of unique modification of flagellar rod protein FlgG by Campylobacter jejuni lipid A phosphoethanolamine transferase, linking bacterial locomotion and antimicrobial peptide resistance.* J Biol Chem, 2012. **287**(5): p. 3326-36.
101. Scott, N.E., et al., *Modification of the Campylobacter jejuni N-linked glycan by EptC protein-mediated addition of phosphoethanolamine.* J Biol Chem, 2012. **287**(35): p. 29384-96.
102. Cullen, T.W., et al., *EptC of Campylobacter jejuni mediates phenotypes involved in host interactions and virulence.* Infect Immun, 2013. **81**(2): p. 430-40.
103. Nairz, M., et al., *The struggle for iron - a metal at the host-pathogen interface.* Cell Microbiol, 2010. **12**(12): p. 1691-702.
104. Skaar, E.P., *The battle for iron between bacterial pathogens and their vertebrate hosts.* PLoS Pathog, 2010. **6**(8): p. e1000949.
105. Loomis L, R.K., *Solution Equilibria of Enterobactin and Metal Enterobactin Complexes.* Inorg Chem, 1991. **30**: p. 906-911.
106. Schaible, U.E. and S.H. Kaufmann, *Iron and microbial infection.* Nat Rev Microbiol, 2004. **2**(12): p. 946-53.
107. Braun, V., *Iron uptake mechanisms and their regulation in pathogenic bacteria.* Int J Med Microbiol, 2001. **291**(2): p. 67-79.
108. de Lorenzo, V., et al., *Operator sequences of the aerobactin operon of plasmid ColV-K30 binding the ferric uptake regulation (fur) repressor.* J Bacteriol, 1987. **169**(6): p. 2624-30.
109. Simpson, R.J. and T.J. Peters, *Forms of soluble iron in mouse stomach and duodenal lumen: significance for mucosal uptake.* Br J Nutr, 1990. **63**(1): p. 79-89.
110. Goddard, W.P., et al., *Iron uptake by isolated human enterocyte suspensions in vitro is dependent on body iron stores and inhibited by other metal cations.* J Nutr, 1997. **127**(1): p. 177-83.
111. Galley, H.F. and N.R. Webster, *Elevated serum bleomycin-detectable iron concentrations in patients with sepsis syndrome.* Intens Care Med, 1996. **22**(3): p. 226-9.

112. Ellis, T.N. and M.J. Kuehn, *Virulence and immunomodulatory roles of bacterial outer membrane vesicles.* Microbiol Mol Biol Rev, 2010. **74**(1): p. 81-94.
113. Avila-Calderon, E.D., et al., *Roles of bacterial membrane vesicles.* Arch Microbiol, 2015. **197**(1): p. 1-10.
114. Schwechheimer, C., C.J. Sullivan, and M.J. Kuehn, *Envelope control of outer membrane vesicle production in Gram-negative bacteria.* Biochemistry, 2013. **52**(18): p. 3031-40.
115. Guo, M.S., et al., *MicL, a new sigmaE-dependent sRNA, combats envelope stress by repressing synthesis of Lpp, the major outer membrane lipoprotein.* Gene Dev, 2014. **28**(14): p. 1620-34.
116. Mizuno, T., *A novel peptidoglycan-associated lipoprotein found in the cell envelope of Pseudomonas aeruginosa and Escherichia coli.* J Biochem, 1979. **86**(4): p. 991-1000.
117. Cascales, E., et al., *Proton motive force drives the interaction of the inner membrane TolA and outer membrane pal proteins in Escherichia coli.* Mol Microbiol, 2000. **38**(4): p. 904-15.
118. Cascales, E. and R. Lloubes, *Deletion analyses of the peptidoglycan-associated lipoprotein Pal reveals three independent binding sequences including a TolA box.* Mol Microbiol, 2004. **51**(3): p. 873-85.
119. Park, J.S., et al., *Mechanism of anchoring of OmpA protein to the cell wall peptidoglycan of the gram-negative bacterial outer membrane.* FASEB J, 2012. **26**(1): p. 219-28.
120. Sonntag, I., et al., *Cell envelope and shape of Escherichia coli: multiple mutants missing the outer membrane lipoprotein and other major outer membrane proteins.* J Bacteriol, 1978. **136**(1): p. 280-5.
121. Papenfort, K., et al., *SigmaE-dependent small RNAs of Salmonella respond to membrane stress by accelerating global omp mRNA decay.* Mol Microbiol, 2006. **62**(6): p. 1674-88.
122. Hayashi, J., N. Hamada, and H.K. Kuramitsu, *The autolysin of Porphyromonas gingivalis is involved in outer membrane vesicle release.* FEMS Microbiol Lett, 2002. **216**(2): p. 217-22.
123. Kaparakis, M., et al., *Bacterial membrane vesicles deliver peptidoglycan to NOD1 in epithelial cells.* Cell Microbiol, 2010. **12**(3): p. 372-85.
124. Nguyen, T.T., A. Saxena, and T.J. Beveridge, *Effect of surface lipopolysaccharide on the nature of membrane vesicles liberated from the Gram-negative bacterium Pseudomonas aeruginosa.* J Electron Microsc (Tokyo), 2003. **52**(5): p. 465-9.
125. McBroom, A.J. and M.J. Kuehn, *Release of outer membrane vesicles by Gram-negative bacteria is a novel envelope stress response.* Mol Microbiol, 2007. **63**(2): p. 545-58.
126. Hellman, J., et al., *Antiserum against Escherichia coli J5 contains antibodies reactive with outer membrane proteins of heterologous gram-negative bacteria.* J Infect Dis, 1997. **176**(5): p. 1260-8.
127. Namork, E. and P. Brandtzaeg, *Fatal meningococcal septicaemia with "blebbing" meningococcus.* Lancet, 2002. **360**(9347): p. 1741.
128. Li, Z., A.J. Clarke, and T.J. Beveridge, *Gram-negative bacteria produce membrane vesicles which are capable of killing other bacteria.* J Bacteriol, 1998. **180**(20): p. 5478-83.
129. Ciofu, O., et al., *Chromosomal beta-lactamase is packaged into membrane vesicles and secreted from Pseudomonas aeruginosa.* J Antimicrob Chemother, 2000. **45**(1): p. 9-13.

130. Forsberg, C.W., T.J. Beveridge, and A. Hellstrom, *Cellulase and Xylanase Release from Bacteroides succinogenes and Its Importance in the Rumen Environment.* Appl Environ Microbiol, 1981. **42**(5): p. 886-96.
131. Dorward, D.W., C.F. Garon, and R.C. Judd, *Export and intercellular transfer of DNA via membrane blebs of Neisseria gonorrhoeae.* J Bacteriol, 1989. **171**(5): p. 2499-505.
132. Haurat, M.F., W. Elhenawy, and M.F. Feldman, *Prokaryotic membrane vesicles: new insights on biogenesis and biological roles.* Biol Chem, 2014.
133. Horstman, A.L. and M.J. Kuehn, *Enterotoxigenic Escherichia coli secretes active heat-labile enterotoxin via outer membrane vesicles.* J Biol Chem, 2000. **275**(17): p. 12489-96.
134. Kolling, G.L. and K.R. Matthews, *Export of virulence genes and Shiga toxin by membrane vesicles of Escherichia coli O157:H7.* Appl Environ Microbiol, 1999. **65**(5): p. 1843-8.
135. Elhenawy, W., M.O. Debelyy, and M.F. Feldman, *Preferential packing of acidic glycosidases and proteases into Bacteroides outer membrane vesicles.* mBio, 2014. **5**(2): p. e00909-14.
136. Shen, Y., et al., *Outer membrane vesicles of a human commensal mediate immune regulation and disease protection.* Cell Host Microbe, 2012. **12**(4): p. 509-20.
137. Munford, R.S., et al., *Biological activity, lipoprotein-binding behavior, and in vivo disposition of extracted and native forms of Salmonella typhimurium lipopolysaccharides.* J Clin Invest, 1982. **70**(4): p. 877-88.
138. Huang, W., et al., *Immunization against multidrug-resistant Acinetobacter baumannii effectively protects mice in both pneumonia and sepsis models.* PLoS One, 2014. **9**(6): p. e100727.
139. Zhou, Z., et al., *Lipid A modifications in polymyxin-resistant Salmonella typhimurium: PmrA-dependent 4-amino-4-deoxy-L-arabinose, and phosphoethanolamine incorporation.* J Biol Chem, 2001. **276**(46): p. 43111-21.
140. Guo, L., et al., *Regulation of lipid A modifications by Salmonella typhimurium virulence genes phoP-phoQ.* Science, 1997. **276**(5310): p. 250-3.
141. Ernst, R.K., T. Guina, and S.I. Miller, *Salmonella typhimurium outer membrane remodeling: role in resistance to host innate immunity.* Microbes Infect, 2001. **3**(14-15): p. 1327-34.
142. Gunn, J.S., *The Salmonella PmrAB regulon: lipopolysaccharide modifications, antimicrobial peptide resistance and more.* Trends Microbiol, 2008. **16**(6): p. 284-90.
143. Frirdich, E. and C. Whitfield, *Lipopolysaccharide inner core oligosaccharide structure and outer membrane stability in human pathogens belonging to the Enterobacteriaceae.* J Endotoxin Res, 2005. **11**(3): p. 133-44.
144. Vaara, M. and T. Vaara, *Outer membrane permeability barrier disruption by polymyxin in polymyxin-susceptible and -resistant Salmonella typhimurium.* Antimicrob Agents Chemother, 1981. **19**(4): p. 578-83.
145. Vaara, M., T. Vaara, and M. Sarvas, *Decreased binding of polymyxin by polymyxin-resistant mutants of Salmonella typhimurium.* J Bacteriol, 1979. **139**(2): p. 664-7.
146. Chamnongpol, S., et al., *Fe(III)-mediated cellular toxicity.* Mol. Microbiol., 2002. **45**(3): p. 711-9.
147. Bijlsma, J.J. and E.A. Groisman, *Making informed decisions: regulatory interactions between two-component systems.* Trends Microbiol, 2003. **11**(8): p. 359-66.
148. Eguchi, Y. and R. Utsumi, *A novel mechanism for connecting bacterial two-component signal-transduction systems.* Trends Biochem Sci, 2005. **30**(2): p. 70-2.

149. Kato, A. and E.A. Groisman, *Connecting two-component regulatory systems by a protein that protects a response regulator from dephosphorylation by its cognate sensor.* Gene Dev, 2004. **18**(18): p. 2302-13.
150. Schauer, D.B. and S. Falkow, *The eae gene of Citrobacter freundii biotype 4280 is necessary for colonization in transmissible murine colonic hyperplasia.* Infect Immun, 1993. **61**(11): p. 4654-61.
151. Petty, N.K., et al., *The Citrobacter rodentium genome sequence reveals convergent evolution with human pathogenic Escherichia coli.* J Bacteriol, 2010. **192**(2): p. 525-38.
152. Winfield, M.D., T. Latifi, and E.A. Groisman, *Transcriptional regulation of the 4-amino-4-deoxy-L-arabinose biosynthetic genes in Yersinia pestis.* J Biol Chem, 2005. **280**(15): p. 14765-72.
153. Le Sage, V., et al., *An outer membrane protease of the omptin family prevents activation of the Citrobacter rodentium PhoPQ two-component system by antimicrobial peptides.* Mol Microbiol, 2009. **74**(1): p. 98-111.
154. Gibbons, H.S., et al., *Role of Mg^{2+} and pH in the modification of Salmonella lipid A after endocytosis by macrophage tumour cells.* Mol Microbiol, 2005. **55**(2): p. 425-40.
155. Tamayo, R., et al., *Identification of cptA, a PmrA-regulated locus required for phosphoethanolamine modification of the Salmonella enterica serovar Typhimurium lipopolysaccharide core.* J. Bacteriol., 2005. **187**(10): p. 3391-9.
156. Groisman, E.A., J. Kayser, and F.C. Soncini, *Regulation of polymyxin resistance and adaptation to low-Mg^{2+} environments.* J Bacteriol, 1997. **179**(22): p. 7040-5.
157. Cullen, T.W. and M.S. Trent, *A link between the assembly of flagella and lipooligosaccharide of the Gram-negative bacterium Campylobacter jejuni.* Proc Natl Acad Sci U. S. A., 2010. **107**(11): p. 5160-5.
158. Sambrook, J., E.F. Fritsch, and T. Maniatis, *Molecular Cloning: A Laboratory Manual*, ed. C.S. Harbor. 1989, NY: Cold Spring Harbor Laboratory Press.
159. Donnenberg, M.S. and J.B. Kaper, *Construction of an eae deletion mutant of enteropathogenic Escherichia coli by using a positive-selection suicide vector.* Infect Immun, 1991. **59**(12): p. 4310-7.
160. Soncini, F.C. and E.A. Groisman, *Two-component regulatory systems can interact to process multiple environmental signals.* J Bacteriol, 1996. **178**(23): p. 6796-801.
161. Baümler, A.J., et al., *Identification of a new iron regulated locus of Salmonella typhi.* Gene, 1996. **183**(1-2): p. 207-13.
162. Miller, J.H., *Experiments in Molelecular Genetics*. 1972: Cold Spring Harbor Laboratory, Cold Spring Harbor, NY.
163. Wiegand, I., K. Hilpert, and R.E. Hancock, *Agar and broth dilution methods to determine the minimal inhibitory concentration (MIC) of antimicrobial substances.* Nat Protoc, 2008. **3**(2): p. 163-75.
164. Roland, K., R. Curtiss, 3rd, and D. Sizemore, *Construction and evaluation of a Δcya Δcrp Salmonella typhimurium strain expressing avian pathogenic Escherichia coli O78 LPS as a vaccine to prevent airsacculitis in chickens.* Avian Dis, 1999. **43**(3): p. 429-41.
165. Edwards, R.A., L.H. Keller, and D.M. Schifferli, *Improved allelic exchange vectors and their use to analyze 987P fimbria gene expression.* Gene, 1998. **207**(2): p. 149-57.
166. Wang, R.F. and S.R. Kushner, *Construction of versatile low-copy-number vectors for cloning, sequencing and gene expression in Escherichia coli.* Gene, 1991. **100**: p. 195-9.

167. Murata, T., et al., *PhoPQ-mediated regulation produces a more robust permeability barrier in the outer membrane of Salmonella enterica serovar Typhimurium.* J Bacteriol, 2007. **189**(20): p. 7213-22.
168. Loh, B., C. Grant, and R.E. Hancock, *Use of the fluorescent probe 1-N-phenylnaphthylamine to study the interactions of aminoglycoside antibiotics with the outer membrane of Pseudomonas aeruginosa.* Antimicrob Agents Chemother, 1984. **26**(4): p. 546-51.
169. O'Callaghan, C.H., et al., *Novel method for detection of beta-lactamases by using a chromogenic cephalosporin substrate.* Antimicrob Agents Chemother., 1972. **1**(4): p. 283-8.
170. Aguirre, A., et al., *Phosphorylated PmrA interacts with the promoter region of ugd in Salmonella enterica serovar Typhimurium.* J Bacteriol, 2000. **182**(13): p. 3874-6.
171. Tamayo, R., A.M. Prouty, and J.S. Gunn, *Identification and functional analysis of Salmonella enterica serovar Typhimurium PmrA-regulated genes.* FEMS Immunol Med Mic, 2005. **43**(2): p. 249-58.
172. Mortimer, P.G. and L.J. Piddock, *The accumulation of five antibacterial agents in porin-deficient mutants of Escherichia coli.* J Antimicrob Chemother, 1993. **32**(2): p. 195-213.
173. Kawasaki, K. and T. Manabe, *Latency of the lipid A deacylase PagL is involved in producing a robust permeation barrier in the outer membrane of Salmonella enterica.* J Bacteriol, 2010. **192**(21): p. 5837-40.
174. Cascales, E., et al., *Pal lipoprotein of Escherichia coli plays a major role in outer membrane integrity.* J Bacteriol, 2002. **184**(3): p. 754-9.
175. Ruiz, N., D. Kahne, and T.J. Silhavy, *Transport of lipopolysaccharide across the cell envelope: the long road of discovery.* Nat Rev Microbiol, 2009. **7**(9): p. 677-83.
176. Miller, S.I., R.K. Ernst, and M.W. Bader, *LPS, TLR4 and infectious disease diversity.* Nat Rev Microbiol, 2005. **3**(1): p. 36-46.
177. Majdalani, N. and S. Gottesman, *The Rcs phosphorelay: a complex signal transduction system.* Annu Rev Microbiol, 2005. **59**: p. 379-405.
178. Naessan, C.L., et al., *Genetic and functional analyses of PptA, a phospho-form transferase targeting type IV pili in Neisseria gonorrhoeae.* J Bacteriol, 2008. **190**(1): p. 387-400.
179. John, C.M., et al., *Lack of lipid A pyrophosphorylation and functional lptA reduces inflammation by Neisseria commensals.* Infect Immun, 2012. **80**(11): p. 4014-26.
180. Chamnongpol, S., et al., *Fe(III)-mediated cellular toxicity.* Molecular microbiology, 2002. **45**(3): p. 711-9.
181. Westphal, O. and K. Jann, *Bacterial lipopolysaccharides: extraction with phenol water and further applications of the procedure*, in *Methods in Carbohydrate Chemistry*. 1965, Academic Press, Inc.: NY. p. 83-91.
182. Guzman, L.M., et al., *Tight regulation, modulation, and high-level expression by vectors containing the arabinose PBAD promoter.* J Bacteriol, 1995. **177**(14): p. 4121-30.
183. Fomsgaard, A., M.A. Freudenberg, and C. Galanos, *Modification of the silver staining technique to detect lipopolysaccharide in polyacrylamide gels.* J Clin Microbiol, 1990. **28**(12): p. 2627-31.
184. Erich, T., et al., *Binding characteristics and cross-reactivity of three different antilipid A monoclonal antibodies.* Journal of immunology, 1989. **143**(12): p. 4053-60.

185. Di Padova, F.E., et al., *A broadly cross-protective monoclonal antibody binding to Escherichia coli and Salmonella lipopolysaccharides.* Infect Immun, 1993. **61**(9): p. 3863-72.
186. Osborn, M.J., et al., *Mechanism of assembly of the outer membrane of Salmonella typhimurium. Isolation and characterization of cytoplasmic and outer membrane.* J Biol Chem, 1972. **247**(12): p. 3962-72.
187. Thomassin, J.L., et al., *OmpT outer membrane proteases of enterohemorrhagic and enteropathogenic Escherichia coli contribute differently to the degradation of human LL-37.* Infect Immun, 2012. **80**(2): p. 483-92.
188. Brade, L., et al., *A nonsubstituted primary hydroxyl group in position 6' of free lipid A is required for binding of lipid A monoclonal antibodies.* Infect Immun, 1997. **65**(9): p. 3961-5.
189. Young, K., et al., *The envA permeability/cell division gene of Escherichia coli encodes the second enzyme of lipid A biosynthesis. UDP-3-O-(R-3-hydroxymyristoyl)-N-acetylglucosamine deacetylase.* J Biol Chem, 1995. **270**(51): p. 30384-91.
190. Sorensen, P.G., et al., *Regulation of UDP-3-O-[R-3-hydroxymyristoyl]-N-acetylglucosamine deacetylase in Escherichia coli. The second enzymatic step of lipid a biosynthesis.* J Biol Chem, 1996. **271**(42): p. 25898-905.
191. Belunis, C.J., et al., *Inhibition of lipopolysaccharide biosynthesis and cell growth following inactivation of the kdtA gene in Escherichia coli.* J Biol Chem, 1995. **270**(46): p. 27646-52.
192. Chamnongpol, S., et al., *Fe(III)-mediated cellular toxicity.* Mol Microbiol, 2002. **45**(3): p. 711-9.
193. Braun, V. and V. Bosch, *Sequence of the murein-lipoprotein and the attachment site of the lipid.* Eur J Biochem, 1972. **28**(1): p. 51-69.
194. Schwechheimer, C. and M.J. Kuehn, *Synthetic effect between envelope stress and lack of outer membrane vesicle production in Escherichia coli.* J Bacteriol, 2013. **195**(18): p. 4161-73.
195. Bielaszewska, M., et al., *Enterohemorrhagic Escherichia coli hemolysin employs outer membrane vesicles to target mitochondria and cause endothelial and epithelial apoptosis.* PLoS Pathog, 2013. **9**(12): p. e1003797.
196. Stephens, D.S., et al., *Pili and outer membrane appendages on Neisseria meningitidis in the cerebrospinal fluid of an infant.* J Infect Dis, 1982. **146**(4): p. 568.
197. de Cock, H., et al., *Non-lamellar structure and negative charges of lipopolysaccharides required for efficient folding of outer membrane protein PhoE of Escherichia coli.* J Biol Chem, 1999. **274**(8): p. 5114-9.
198. Ferguson, A.D., et al., *Siderophore-mediated iron transport: crystal structure of FhuA with bound lipopolysaccharide.* Science, 1998. **282**(5397): p. 2215-20.
199. Lima, S., et al., *Dual molecular signals mediate the bacterial response to outer-membrane stress.* Science, 2013. **340**(6134): p. 837-41.
200. Ogura, T., et al., *Balanced biosynthesis of major membrane components through regulated degradation of the committed enzyme of lipid A biosynthesis by the AAA protease FtsH (HflB) in Escherichia coli.* Mol Microbiol, 1999. **31**(3): p. 833-44.
201. St Michael, F., et al., *Structural analysis of the lipopolysaccharide of Pasteurella multocida strain VP161: identification of both Kdo-P and Kdo-Kdo species in the lipopolysaccharide.* Carbohydr Res, 2005. **340**(1): p. 59-68.

202. Reynolds, C.M., et al., *A phosphoethanolamine transferase specific for the outer 3-deoxy-D-manno-octulosonic acid residue of Escherichia coli lipopolysaccharide. Identification of the eptB gene and Ca2+ hypersensitivity of an eptB deletion mutant.* J Biol Chem, 2005. **280**(22): p. 21202-11.
203. Perez-Cruz, C., et al., *New type of outer membrane vesicle produced by the Gram-negative bacterium Shewanella vesiculosa M7T: implications for DNA content.* Appl Environ Microbiol, 2013. **79**(6): p. 1874-81.
204. Caulfield, A.J., et al., *The Pla protease of Yersinia pestis degrades fas ligand to manipulate host cell death and inflammation.* Cell Host Microbe, 2014. **15**(4): p. 424-34.